ABSTRACT

Title of Document: MODELING THE MECHANICS OF
                            FREEZING CLAY

                            Sangjoon Han, Doctor of Philosophy, 2005

Directed By: Deborah J. Goodings, Professor
                            Department of Civil Engineering

This research was initiated to investigate the freezing mechanisms of clay, and to make a contribution to the development of a simple analytical model that can characterize frost heave in clay. It was also undertaken to examine the correctness of modeling full scale frost heave in small models cooled on the geotechnical centrifuge to simulate full scale stress conditions. To this end, twenty-three physical model tests were conducted including 1g freezing tests, centrifuge freezing test. Two soils were used; three freezing regimes were applied.

Centrifugal acceleration was found to influence the magnitude, and the development of frost heave, as well as depth of freezing, and changes in local water contents after freezing, when compared to freezing of similarly sized models frozen at 1g. Ratios of (heave/depth of freezing) were similar in 1g and centrifuge models. No difference in the size of ice lenses could be observed. Evidence of freezing consolidation was observed.

Prefreezing water content strongly affected development of heave in terms of both magnitude of heave, and depth of freezing. Migration of water was modest at best; the position of the phreatic surface did not appear to affect the development and magnitude of heave. Local permeability, however, appeared to have an important effect on development of heave, linked to the rate of cooling.

An analytical model that was developed from this research explained, rather than predicted, frost heave at this point. The analytical model was satisfactory in characterizing magnitudes of heave, both ultimate heave and during development of heave, when the model included the assumption that heave can and does occur even when soil is not saturated, and the soil may transition from a prefreezing saturated condition to an unsaturated frozen condition.

MODELING THE MECHANICS OF FREEZING CLAY

By

Sangjoon Han

Dissertation submitted to the Faculty of the Graduate School of the
University of Maryland, College Park, in partial fulfillment
of the requirements for the degree of
Doctor of Philosophy
2005

Advisory Committee:
Professor Deborah Goodings, Chair/Advisor
Professor M. Sherif Aggour
Associate Professor Charles W. Schwartz
Assistant Professor Ahmet H. Aydilek
Professor Marino di Marzo

ACKNOWLEDGMENTS

TABLE OF CONTENTS

LIST OF TABLES

LIST OF FIGURES

CHAPTER 1: INTRODUCTION

1.1 RESEARCH BACKGROUND

As technology develops, and population growth increases, the necessity of developing cold regions becomes inevitable and with it a demand for cold regions engineering. This knowledge of cold regions soil response is also relevant to temporary artificial soil freezing response which can be used both in construction to increase soil strength during excavation and to create an ice rich low permeability zone to limit the seepage of either water or other fluids, including contaminants.

Frost heave and subsequent thaw-induced settlement are significant engineering problems to be solved in seasonally or perennially frozen regions. Andersland, and Ladanyi (1994) defined cold regions as those in which the frost penetration into the ground is 300mm or greater at least once in every 10 years. With this definition, cold regions constitute approximately one-fourth of the land mass of the world. This includes all of Siberia, Greenland, and Antarctica; much of Canada and Alaska; and parts of China and northern Europe.

Several types of geotechnical engineering problems can arise in cold regions. More than any other engineered facility, roads, and railroads are the most at risk for damage due to frost heave and thaw settlement, because the unevenness caused by the cycles of heave and thaw is detrimental to their function. Damage can also occur to structures, and to utility lines, especially buried or even above ground pipelines, due to the heave pressure and subsequent uneven thaw settlement.

Frost heave requires sustained freezing temperatures, availability of soil moisture, and frost susceptible soil. With regard to soil type, the development of frost

heave is greatest in silts which pass the optimal combination of capillary rise, permeability, and void ratio. When silts heave, subsequent thaw settlement is generally equal to or somewhat less than the original heave. In clayey soils, however, the situation is different. Capillary rise is greater. And permeability is much less. Water content is typically much greater. Compressibility, and void ratio are greater. This means that these events leading to substantial heave in silt are not expected to be replicated in clays. Chamberlain (1981) identified over-consolidation effects on clay resulting from the freezing process. This means that subsequent thawing may lead to settlement. The freezing and thawing of clay has received substantially less attention than that of silt, and this is the focus of this research.

There will be two soils used in this research on heave and thaw settlement of clay. One is factory manufactured (EPK Kaolin), and the other is clay obtained by US Army Corps of Engineers Cold Regions Lab (CRREL) from Ft Edward, New Hampshire. As a means to understanding the heaving processes, specimens will be prepared to simulate freezing in 4m high column with different freezing indices; freezing modes (step, and ramp freezing); and location of the water table.

1.2 SCOPE OF WORK

The purposes of this research are two fold: to identify through experimentation the whole system response of clay when frozen under conditions that may occur naturally and from that, develop a simple predictive model that engineer can utilize easily with a reasonable accuracy for design, without requiring soil properties that can not be easily acquired or estimated, but which is scientifically valid. Such a predictive model does not exist at present for predicting the frost heave in clay. In addition to

above two purposes, centrifuge scaling laws are to be verified using clay in this research. This will be accomplished by utilizing "modeling of models" technique that researchers routinely adopt for checking the scaling relationship.

The effects of centrifugal acceleration on freezing behavior of clay are investigated by comparing the results from Ng tests to those from 1g tests in terms of frost heave, frost heave rate, water content profile, and ice lens characteristics. The same comparison will be conducted in a group of modeling of models, to check if all the models, constructed at different scales and tested for periods of time predicted by the scaling relationships appropriate for these scales, predicts the same frost heave within measurement error when they are scaled up to the prototype scale.

Between the groups of modeling of models, some variables such as initial water content, and freezing index for kaolin and Ft.Edwards clay were changed to investigate the effects on heave development from these factors.

CHAPTER 2: LITERATURE REVIEW

2.1 DEVELOPMENT OF HEAVE

There are three requirements for soil to undergo frost heave: water, sustained freezing temperature, and frost-susceptible soil. As the air temperature drops, heat is transmitted from the ground to the atmosphere mostly by conduction. When the temperature drops below freezing, the pore water in soil begins to freeze. When the water alone freezes, it expands its volume by approximately 9%. The volume of expansion during freezing period is frequently considerably greater than could be expected from expansion by freezing of the original pore water (O'Neill and Miller, 1982). This is because frost heave is a more complex process.

Freezing air temperature causes a temperature gradient in the soil, and a freezing front develops. At the uppermost elevations, where freezing occurs quickly, and water may not be plentiful, isolated needle ice develops. As the freezing air temperature persists, this 0°C isotherm or frost front advances into the soil, perpendicular to the soil surface. Figure 2.1 shows that the profile of freezing soil. Note that whereas the frost front is coincident with the 0°C isotherm, the freezing front is not. Between the two lies the frozen fringe (Miller, 1977). It could range from less than a millimeter in thickness to several centimeters, depending upon soil type, composition, temperature gradient and applied pressure.
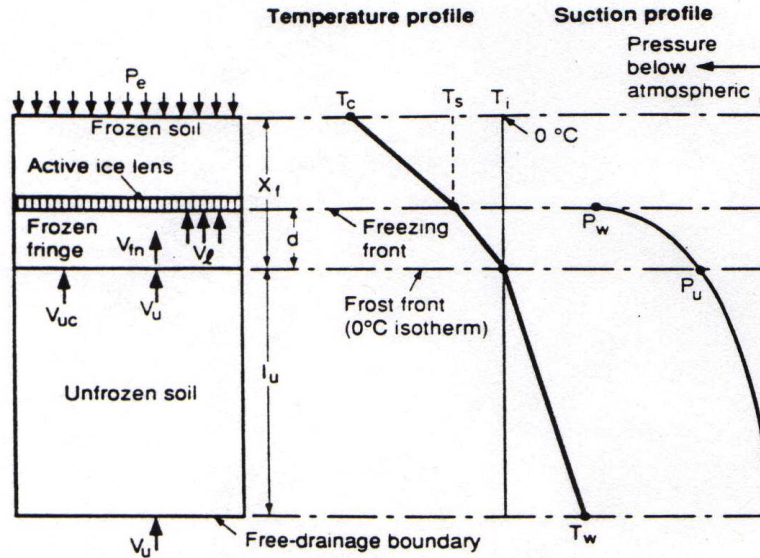
Figure 2. 1 Schematic description of the soil in frost heave process (after Konrad & Morgenstern, 1980)

Within the frozen fringe, there is a steep suction gradient caused by the thermal gradient. In addition, frozen and unfrozen pore-water co-exist. Water freezes first at the center of the pore, expelling salts that may exist in the pore water. This causes the unfrozen water closer to the particle surfaces to have a higher concentration of salts than previously existed, and a lower freezing point (Banin and Anderson, 1974). However, regardless of the salt concentration, the pore water closest to the particle surfaces remains unfrozen even well below 0°C. This percentage of unfrozen pore water depends on both the pore water composition, as well as the soil type. Finer grained soils, especially clays, maintain more unfrozen water as the temperature falls than coarse grained soils (see Figure 2.2).

The unfrozen water along the particle surfaces acts as a conduit for unfrozen groundwater to be drawn by the suction gradient through the frozen fringe and into the freezing soil above. The thickness of the frozen fringe depends upon the overall

temperature gradient in the soil, and the soil type. For a given soil, a larger temperature gradient means a smaller frozen fringe. This means that the temperature gradient, both at a particular moment as well as over time, strongly influences the frozen fringe and with it the development of ice in soil. As the pore water freezes, the permeability of the frozen fringe decreases, thereby slowing the flow of the water to the soil above, unless the suction gradient increases to compensate in whole or in part.

As the frost front penetrates into the soil, isolated needle ice no longer forms, because of the formation of the frozen fringe; a reduction in the rate of freezing; often increased availability of ground water; and increasing overburden pressure, which opposes upward heave. Below the needle ice, but still close to the soil surface, the rate of freezing remains relatively rapid, and small, closely spaced ice lenses form above the frozen fringe. Ice lenses in soil are distinct lenses, veins, or masses of ice. When a freezing front is penetrating vertically into the soil, the lenses are oriented horizontally, and are generally larger in one or both of the horizontal directions than the vertical. They are often formed in repeated layers. As the frost penetrates deeper into the soil, the temperature gradient is less and the overburden pressure is greater. This leads to larger and more widely spaced ice lenses (Konrad, and Morgenstern, 1980). The slowing of freezing at increasing depth means that more water can be conducted to the freezing front to feed the growing ice lenses.
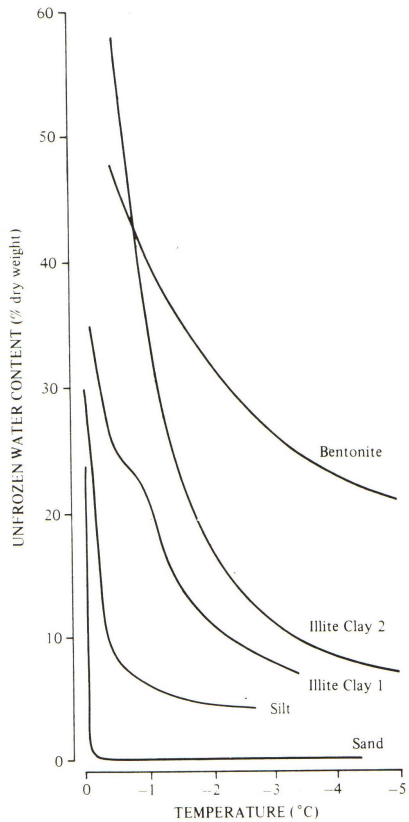
Figure 2. 2 Amount of water remaining unfrozen at temperatures below 0°C, various soils. (After Burt and William, 1976)

In clays, the result of this process is somewhat different than in silts. Chamberlain and Gow (1979) noted that in clays, a process of "freezing consolidation" occurs in the unfrozen zone below the freezing front owing to the negative pore-water pressures and high effective stresses generated at the frost front. Frost heave accompanied by this consolidation effect may result in little or no perceptible heave during freezing. Chamberlain (1981) noted that the amount of freezing-induced consolidation settlement is related to the plastic limit of the clay. By his laboratory testing, the plastic limit was found to be the minimum water content that can be obtained by freezing and thawing. This consolidation settlement actually

7

occurs during freezing, however it manifests during thaw. For example, upon thawing, the ice melts, and the water drains away rather than being reabsorbed into the clay, and there is net settlement. Other aspects specific to freezing and thawing of clays are described in the following section.

2.2 FROST HEAVE IN CLAYS

The magnitude of frost heave developing in clays is much less than in silts, primarily because of their smaller permeability and their much greater scope for consolidation. The greater problem in clays often develops after thawing, when substantial settlement and associated change in mechanical properties can occur. For example, Penner (1969), and Hamilton (1966) observed that clays shrink in size when first frozen. They identified that the amount of shrinkage is a function of the clay water content and its degree of saturation. Chamberlain (1981) observed that clays became over-consolidated when frozen and permeability increases because of shrinkage cracking.

Eigenbrod (1996) performed cyclic one-dimensional, open-system freezing and thawing tests on the soft, fine-grained soil, and found a linear relationship between the net volume changes subsequent to cyclic freezing and thawing and initial liquidity index (I_L) prior to freezing and thawing. According to his research, a maximum volume change of up to 30% occurred depending on the initial moisture content and plasticity of the clay as well as on the rate of freezing.

"Freeze-thaw consolidation" resulting from the volume changes in soft clays subsequent to cyclic freezing and thawing was observed in the laboratory by Chamberlain and Gow (1979). Konrad and Seto (1994) noted that Taber (1929), and

Tsytovich (1975) observed this also in the field. They also noted that an X-ray photography technique was used during freezing to measure the relative displacements of buried lead shot at different times during the freezing cycle, and Akagawa (1990), one of several researchers who utilized this technique, reported a maximum consolidation strain of 10% near the frost front during the freezing of natural, high water content clay.

R.N. Yong et.al (1984) conducted research on the clay under the cyclic freeze-thaw, and found that repetitive cyclic freezing and thawing can cause significant changes in soil characteristics, rearranging soil particles and regrouping them into larger stable fabric units. This brings about a change in the basic soil unit sizes and the corresponding micro-pores/macro-pores. In addition to the volume change, clays exposed to freezing and thawing were found to lose shear strength and increase compressibility (Graham and Au, 1985). This is accompanied by alterations in the soil permeability, because of the network of horizontal and vertical cracks formed in the soil during the freeze-thaw cycle (Wong and Haug (1991), and Benson and Othman (1993)). They also noted that the increase in the soil permeability was observed for the first few cycle of freeze and thaw for most clays and then ceased.

2.3 MECHANICS OF FROST HEAVE IN NON-COHESIVE SOIL

The majority of research on frost effects in soil has focused on the effects in silts, which undergo the greatest heave. Several theories have been developed to explain that heaving process. Along with development of theory, researchers also have developed predictive models of frost action and thaw weakening, applying empirical, numerical, and analytical approaches. Predictive models are generally developed for one of two purposes: either for the purpose of engineering design, or for the scientific study of the process itself.

The simplest approach in predicting frost heave is that the soil freezes from the surface down with in-situ pore water freezing and expanding 9%. However, this underestimated heave and failed to explain the development of ice lenses.

The first models developed were empirical formulas, based on purely empirical observations using a combination of field observations and frost heave tests in the laboratory (Arakawa 1966, Knutsson 1973).

Kujala (1997) refers briefly to some semi-empirical models, based partly on the physical nature of frost heave, and developed by Takaki (1978), Zhang, and Zhu (1983), Chen and Wang (1988). He notes that they have been used in design but he implies that their theoretical bases are not well developed.

The capillary theory developed to explain observation of ice lenses which were identified as the dominant cause of heave. Penner (1957), and Gold (1957) hypothesized that surface tension at the water-ice interface generates pore pressure which draws pore water to the developing ice lenses. This suction develops because the difference in the pressure potential between unfrozen pore water and the growing

ice crystal induces a suction pressure gradient. This process is assumed to be dominated by the porous matrix of the soil. It assumes that adsorption forces are negligible and the soil is an ideal granular material.

Everett (1961) developed equation 2.1 to predict pore water suction in the capillary theory, which is modeled on suction behavior of unfrozen partially saturated soil.

$$\Delta P_w = 2\frac{\sigma_{iw}}{r}$$ 2.1

where, ΔP_w = pore water suction in freezing soil
σ_{iw} = interfacial energy of ice-water interface ($\cong 0.0331$ Nm^{-1})
r = equivalent pore radius of the soil (m)

In this approach, small pore radius leads to maximum suction, and should also lead to maximum heave, and heaving pressure. The capillary theory could explain primary heaving due to the formation of needle ice in silt adjacent to a cooling surface prior to frost penetration (see Figure 2.3). However, Penner (1967) found the significant discrepancies between the measured and calculated values of frost heaving pressure in his laboratory testing. The computed values using the capillary theory were always too low.

The secondary heave theory was developed by Miller (1972). He observed that ice lenses formed some way behind the freezing front at temperature less than freezing point. Miller introduced the concept of the "frozen fringe" in which ice and liquid water coexist; this was also verified by several researchers; for example, Loch and Miller (1975), Penner and Goodrich (1980), and Phukan et al (1979).

11
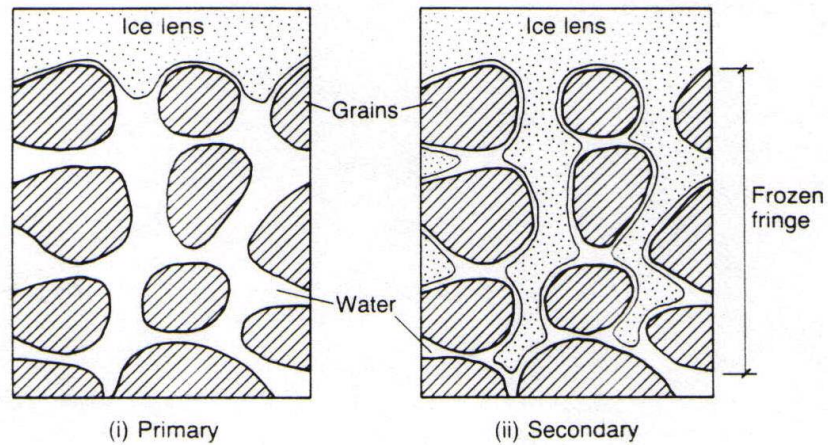
Figure 2. 3 Primary and secondary heaving (after J.S. Harris, 1995)

In Miller's secondary heave theory, ice is believed to develop on the warm side on the freezing front, then to melt, be drawn through the freezing front as water, and refrozen in lenses, as shown in Figure 2.4. He referred to this process of heat flow induced flow of water and the cycle of formation, melting, and reformation of ice as regelation. In order for new ice lenses to form, the effective stress must fall to zero, according to this theory. This will happen when the total stress equals the sum of the pore pressure in the unfrozen water (u_w) and the ice(u_i) combined as

$$u = \chi u_w + (1- \chi)u_i \dots\dots\dots\dots\dots\dots\dots\dots\dots\dots2\text{-}2$$

here χ is the stress partition factor which gives the proportions between ice and water pressure.

O'Neill and Miller (1982) later modified the secondary heave theory to become the rigid-ice model. Its main modification is that ice in the frozen fringe is assumed to be rigidly connected to the growing ice lens.
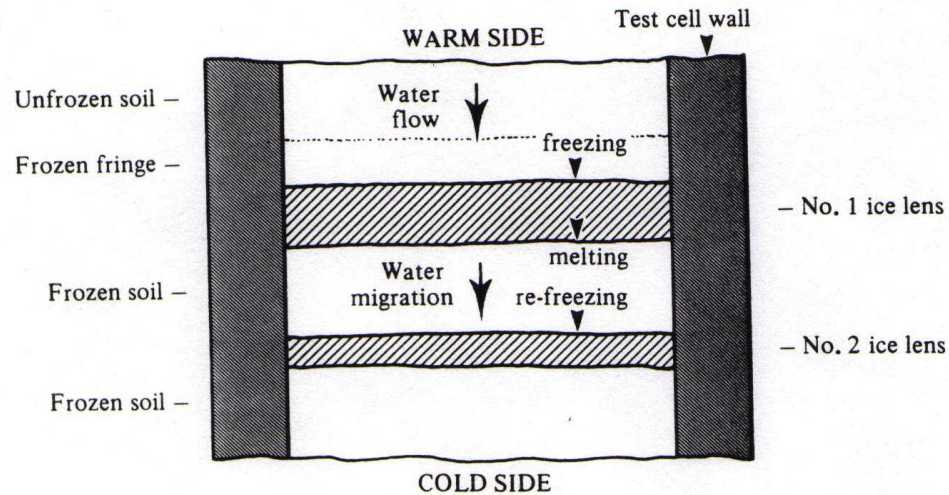
Figure 2. 4 Schematic diagram of moisture transfer through frozen soil (after Ohari & Yamamoto, 1985)

Several researchers simplified this theory for numerical application (Gilpin, 1980; O'Neill& Miller, 1985). Among them, Sheng (1994) further developed this rigid-ice model to handle field conditions such as stratified soils, unsaturated and insulation layers. His model correlated well with field data. Shen and Ladanyi (1987) included stress and strain characteristics in the model, and Hopke (1980) was first one who took external stresses such as foundation loads into consideration.

The first hydrodynamic model of soil freezing was developed by Halan (1973). He assumed that water transport in unsaturated unfrozen soils and water transport in partly frozen soil was similar. He developed a model for coupled heat and mass transfer in freezing soil based on the fact that movement of water in frozen soil involves heat flow because water releases latent heat as it freezes. He also assumed that pore ice is inherently immobile so that the mass transport involves only liquid flow. Several other models were developed based on the same concept (Sheppard

13

1978, Jansson and Haldin 1979, Fukuda 1982), however, a major drawback of these models is that they fail to predict formation of discrete ice lens. Nonetheless, Guymon, et.al. (1993) developed a numerical model of heave called Frost using a hydrodynamic mode; it is used in pavement design and for predicting frost heave and penetration.

A third theory, segregation potential (SP), was developed by Konrad and Morgenstern (1980, 1981) and was founded on Miller's concept of a frozen fringe (defined in section 2.1). They made a simple linear analysis of this frozen fringe based on the following propositions: 1) the Clausius-Clapeyron equation is valid at the base of the ice lens, 2) water flow is continuous across the frozen fringe, and accumulates at the base of a developing ice lens, 3) the frozen fringe can be characterized by an overall permeability K_f, and 4) the temperature varies linearly in the frozen fringe from "segregation" freezing temperature T_{so} at the lens to the freezing temperature of bulk water T_i. For coarse soil, T_i may be very close to the 0°C isotherm. For finer soils, T_i may be less than 0°C and slightly behind the 0°C isotherm. Figure 2.5 shows the characteristics of the frozen fringe proposed above in the simplified and actual configuration. As can be seen in the figure, the suction potential at the frozen-unfrozen interface, P_u to total suction potential at the freezing front, P_w also varies linearly. Permeability(K_f) is constant through the frost fringe.

From above propositions, when the temperature across a soil sample reaches steady state conditions, water intake flux to the final growing ice lens is proportional to the temperature gradient across the frozen fringe, and expressed in the following simple equation.

$$v = SP \text{ grad } T \quad \ldots\ldots\ldots\ldots\ldots\ldots\ldots\ldots\ldots\ldots\ldots.2\text{-}4$$

where v is the water velocity (Length/Time). grad T is the temperature gradient in the frozen fringe (Temperature/Length). SP is the segregation potential (Length^2 / (Time * Temperature)). This equation constitutes the coupling of the heat and mass flow.

SP i.e., the ratio of water intake flux to temperature gradient, is constant for a given soil, regardless of degrees of the cold end temperature as long as warm end temperature. The value of this suction can be affected only by warm end temperature, whereas, the cold end temperature decides the location of the final ice lens formation for the case of a uniform soil sample. Above fact was deduced by deriving an equation (beyond the scope of this paper) using two identical samples with different height under different cold side temperatures, and it was proved by a series of experiments (Konrad, Morgenstern, 1980).
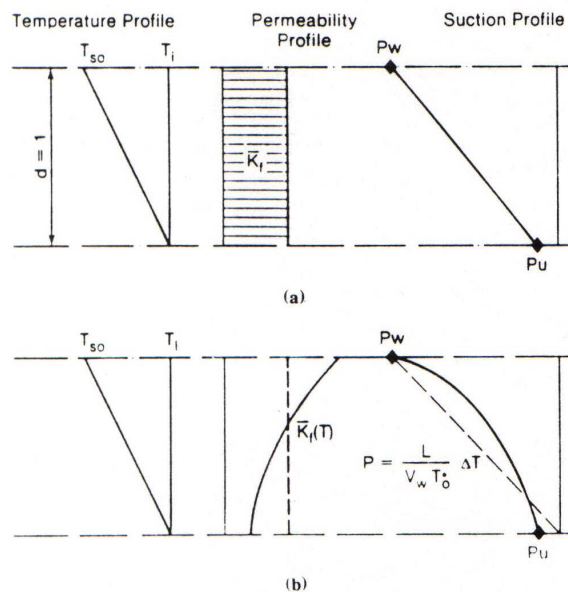
Figure 2. 5 Characteristics of the frozen fringe: (a) simplified; (b) actual shape. (After Konrad and Morgensten, 1981)

As briefly mentioned above, continuous research (Konrad, Morgenster, 1981) found that the segregation potential is a function of the suction at the frost front. In other words, even though average temperature in the fringe is same, different suction at the frost front, subsequently different average suction in the fringe, can result in different freezing characteristics of that given soil. Figure 2.6 shows that any soil freezing at the onset of the formation of the final ice lens is characterized by a set of straight lines (v_o versus grad T) passing through the origin lines. Each line represents the different suctions at the frost front. As can be seen in the figure, as the suction increases, the segregation potential decreases with concomitant decrease in the slope of the relationship v_o versus grad T. SP (Segregation potential) may be considered as a soil's index property that can represent its frost-heave susceptibility.

A segregation potential model was developed by Konrad and Morgenstern (1980, 1981), introducing the concept of Segregation Potential (SP). In this model, the frozen fringe is described by two basic parameters: the overall frozen fringe permeability K_f, and the segregation-freezing temperature T_{so}. Here the permeability is a function of the unfrozen water content of the fringe, and the suction generated at the ice lens according to the thermodynamics of phase equilibrium (Clausius-Clapeyron equation) is drawing the water the frost front. Several researchers have used the SP model to analyze frost heave data from field and laboratory tests (Nixon 1982, Knutson et al. 1985, Saarelainen 1992). They found that this model is accurate enough for the engineering needs.

More recently, a thermomechanical model was developed, taking into account mechanical properties of frozen soils along with heat and water transfer (Duquennoi

et al. 1985, Fremond and Mikkola 1991). This model adopted an approach is based on continuum mechanism and macroscopic thermodynamics e.g, the balance laws of mass, momentum and energy and the entropy inequality. This model deals with saturated soil which is considered to be a mixture of three constituents: the soil skeleton, liquid water, and ice. The constitutive equations of a porous medium are derived by applying the method of the accompanying local equilibrium state and choosing appropriate expressions for the free energy and the dissipation potential. The model can describe the suction resulting from freezing of pore water, the transfer of pore water and heat, and the frost heave but does not require lensing criterion. This model is still under development.
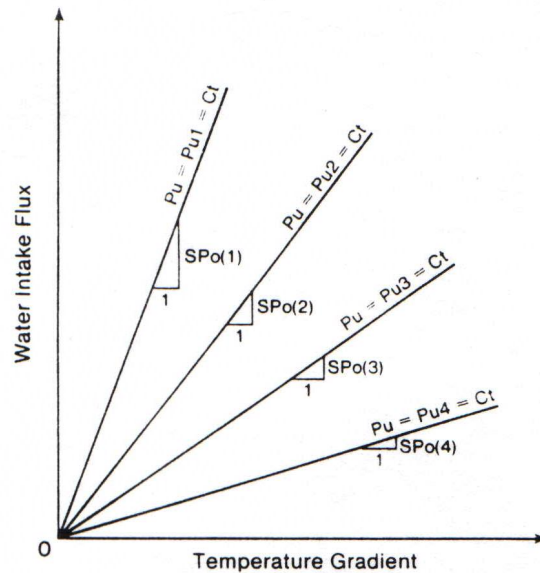
Figure 2. 6 Conceptual relationship between water intake flux and temperature gradient for different suctions at the frost front. (After Konrad and Morgenstern, 1981)

2.4 CENTRIFUGE MODELING OF FROST HEAVE

Centrifuge model testing provides a powerful tool to the geotechnical engineer since it enables the study and analysis of complete geotechnical systems of response. It is not a replacement for examination of micro mechanical behavior. Its purpose is to simulate a full scale geotechnical prototype behavior using a small-scale physical model. In general geotechnial applications, it is necessary to create a soil model with stress-strain behavior similar to that at full scale, and then to create a stress configuration in the model that is the same as the stresses at the corresponding points in the prototype. This is accomplished by placing the small model on a centrifuge and subjecting it to an increase in acceleration until the self weight stresses are equal to those at full scale. This means that a model built of prototype soil and constructed to a linear scale of 1/N compared to the full scale prototype, must be subjected N times earth's gravity for stresses to be equal in both.

Scaling laws involved in heat transfer by conduction and convection, density driven flow, solute migration due to concentration gradients and moisture transport in unsaturated soils have been discussed by Savvidou (1988) and Smith (1992). These scaling laws are summarized in Table 2.1. Diffusion processes (mainly heat transfer due to conduction and convection in this research) occur N^2 times faster in the centrifuge model. This is the combined effect of the gradients causing diffusion being N times greater in a model with the same boundary conditions as in the prototype, and the distances over which diffusion must occur being 1/N times that of the prototype. This means that a diffusion event requiring a year can be modeled at a scale of 1:35, in $1/35^2$ year, or 7 hrs 9 minutes.

This scaling relationship has been used to advantage in modeling seepage effects due to warm temperature gradients and concentration gradient (Arulanaandan, K. et.al 1988). However, few researchers working with the cold regions geotechnique have applied the centrifuge technique. Palmer, et.al. (1985) discussed the use of the centrifuge for both permafrost and ice engineering problems. Lovell and Schofield (1986) conducted a series of model tests to investigate the characteristics of ice grown on water in the centrifuge. They concluded that the crystal-structure of ice grown on the centrifuge was a much closer, but scaled down version of thick ice sheet formed at full scale, than ice grown at 1g intended to simulated full scale.

Jessberger (1989) performed centrifuge tests to study the frost penetration and heaving process in clay relevant to ground freezing for temporary stabilization of soil during construction, using a single vertical freeze pile to freeze clay and then investigating freezing and subsequent creep behavior of the frozen clay using LVDTs in flight.

The research of Yang (1996) at the University of Maryland is most directly relevant to this research. To examine the correctness of centrifuge scaling for frost heave, She tested using two soils, a silt and a clayey silt. She also examined the effects of different freezing regimes on behavior. Finally, she compared her results to predictions of heave and frost penetration using Guymon et. al's (1993) Frost numerical model. Straub (1999) used Yang's research effectively examine boulder jacking in silts.

Table 2. 1 Centrifuge Scaling Law (Smith, C.C. 1992)

Physical quantity	Prototype	Model
Defined		
Macroscopic Length	1	$1/N$
Microscopic Length	1	1
Gravitational acceleration	1	N
Temperature	1	1
Derived		
Strain	1	1
Pore-water Pressure	1	1
Stress	1	1
Time		
Diffusion process	1	$1/N^2$
Inertial event	1	$1/N$
Viscous processes	1	1
Total water potential	1	1
Interstitial water velocity	1	N
Moisture flux	1	N
Heat flux	1	N

In this research, an approach similar to Yang's will be used to examine the freezing and thawing behavior of clay, since its behavior is believed to differ significantly from that of the silts. Since relatively little research has been published on this, there will be three foci to the research. First, to characterize the freezing and thawing process of two clays as measured in centrifuge model testing under different temperature regimes, and with different phreatic surfaces; second, to identify the effects of freezing and thawing on soil properties, especially on soil strength or pre-consolidation effects. And third, to check on the validity of centrifuge modeling of

freezing in clays. If there is sufficient time, prediction using a numerical model of frost heave, presently under development by Fiorero and Ravonison (1998) will be compared to physical model results.

CHAPTER 3: TEST EQUIPMENT

3.1 THE GEOTECHNICAL CENTRIFUGE

The UMCP geotechnical centrifuge is a Genisco Model 1230-1 G-Accelerator. It is a manually controlled, hydraulically driven system. Its design capacity is 30,000 g-lbs. (13.6g-tons). Two swinging platforms are located at either end of the centrifuge arm, and they measure 54 cm wide by 56 cm deep. One platforms holds the model and the other is used for the counterweight for the static and dynamic balance. The distance from the center of rotation to the specimen platform is 1.5 m.

The electrical access to the centrifuge is provided by three 8 channel electrical slip rings that provide a total of 24 channels. Ten channels out of 24 are used for the Data Acquisition System, and the other 14 channels are used for the camera, lights, 120 volts electric power, and experimental control. In addition, there is a rotary union with two ports; one is for compressed air and the other is for passing fluid to the model. The port for the air is used to provide the compressed air for the cooling system. The port for the fluid is not being used in these tests. The air port can handle up to a maximum of 150 psi at the maximum speed of 500 rpm.

3.2 MODEL EQUIPMENT

The model and its accompanying apparatus are housed in a circular bucket made of aluminum. Its dimensions are 48 cm in diameter and 41 cm high. In order to improve cooling efficiency, the bucket is insulated using insulation materials manufactured for wrapping the air ducts of the air conditioner, attached to both the inside and the outside of the bucket. In addition to this, 6 mm thick polar fleece fabric

with thermal conductivity, 0.0356 W/m-°K (donated by Malden Mills) was wrapped twice around the outside of the bucket to improve insulation. To prevent heat loss through the bottom of the bucket, another length of polar fleece was also placed between the bottom plate and the centrifuge platform. In order to improve further the cooling efficiency, the empty spaces inside the bucket after the model testing apparatus is placed, was filled with styrofoam pieces, and spray type foam, as shown in Figure 3.1. The circular bucket is covered with a plywood lid after the testing setup is installed.

Figure 3. 1 Insulated model container before placement in circular bucket

3.2.1 MODEL CONTAINER

The model apparatus setup inside the circular bucket is shown in elevation in Figure 3.2. The soil is contained in a hollow Teflon cylinder with a 12.7 cm inside diameter, 15.2 cm outside diameter. It is 15.2 cm long. Teflon was chosen because of its small friction coefficient which allows the soil to heave and to settle with a minimum of boundary friction. WD-40 oil is sprayed on the inside wall of the Teflon cylinder to further reduce the side friction.

On the side of the Teflon cylinder, there are three holes to accommodate three thermistors. Swage lock fittings are used to make them water tight. These three thermistors were pushed through the holes, and into the soil in the cylinder by about 2.5 cm to measure the internal soil temperature. On the opposite side, using the same kind of fitting, one pore water pressure transducer is installed.

Since the experiments involve open system freezing, they require a continuous supply of water to the freezing front. The Teflon cylinder fits into an aluminum base designed to allow water to enter the soil from two temperature controlled water reservoirs. The connection is made water tight with a rubber gasket. The two rectangular aluminum water tanks which provide water to the specimen through the base plate have dimensions 5 cm by 20 cm with a height of 23 cm. The water table in the soil specimen is set by controlling the height of water in the two interconnected water tanks connected to the base plates. A water pressure transducer is located at the bottom of one of the two tanks to monitor the reservoir water levels during the experiment. The water tanks are capped with plexiglass to reduce evaporation of water during experiments.
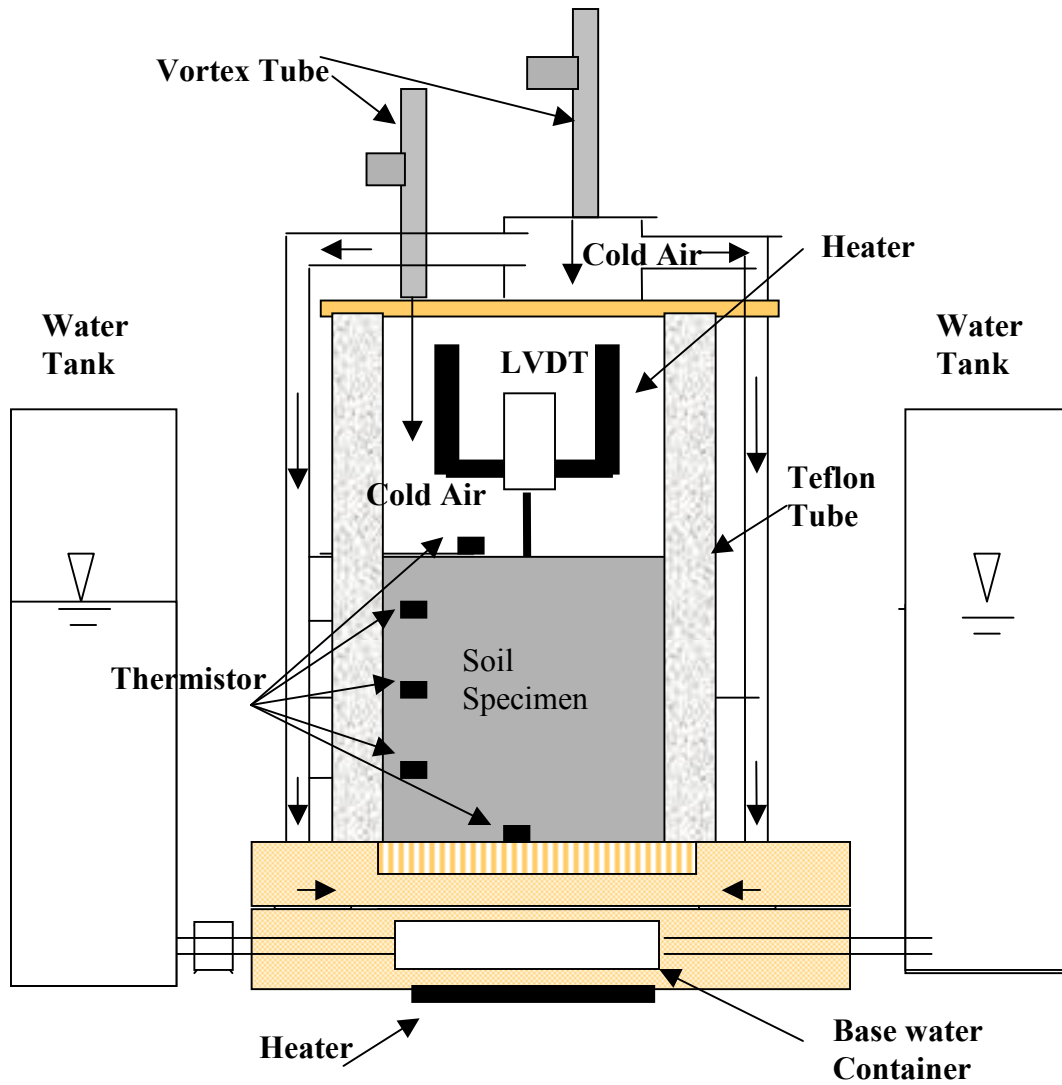
Figure 3. 2 Diagram of cold air route

3.2.2 COOLING FACILITY

Model cooling on the centrifuge is achieved using a Vortex tube 208-11-H, manufactured by the ITW Vortex Co, and schematically depicted in Figure 3.3. When compressed air is forced into the Vortex tube, a cylindrical generator inside the tube creates a vortex, rotating the compressed air like a tornado. The air rotating at high speed is hot and is forced to exit through a needle valve. The remaining cold air moving at slower speed is forced back through the center of the incoming air stream. The heat in the slower moving air is transferred to the faster moving incoming air. This cold air stream then exits from the other end through the center of the generator, and into the model box.

The temperature of the cold air blowing out of the vortex tube depends heavily on the pressure of the compressed air entering the vortex tube and its temperature. The cold fraction, which is the percentage of input compressed air that is released through the cold of the tube, can be controlled also by both the control knob and the generator. The control knob, which is a small needle valve, is attached on the hot air end. By adjusting the hot air volume coming from the hot end of the vortex tube, the temperature of cold air released from the cold end is also controlled.

There are several models of generators that can be installed to produce colder but less air to choose from.

Cold   Hot
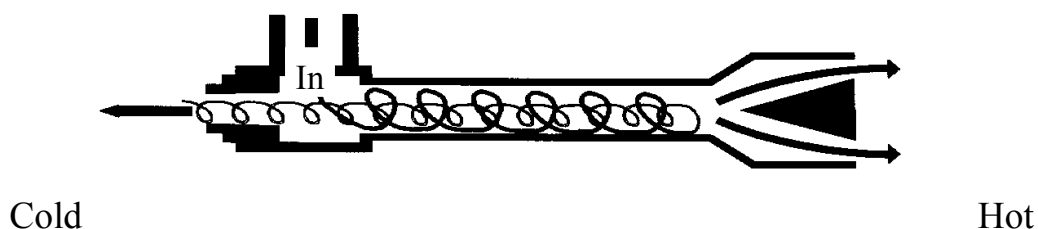
Figure 3. 3 Layout of a vortex tube

Compressed air is supplied by the house air compressor that has a maximum air pressure capacity of 120 psi and maximum flow rate of 45 cfm. The range of the cold air temperature obtained using this model with this compressed air source varies from -22°C to -28°C depending on the conditions described above.

The air fed to the vortex tube must be clean and dry, and preferably cool, to avoid frozen condensate clogging the cold exhaust of the vortex tube. The house compressed air hot in summer and colder in winter, but is very humid, even after it is filtered through the general laboratory mechanical dryer. Two different kinds of dryers are used in series to correct this problem: a refrigerated dryer, and a desiccant dryer as shown in Figure 3.4.

The air is routed first through a refrigerated dryer that cools the compressed air to just above freezing temperature, between +3°C and +10°C depending on the temperature of the incoming air, and in doing so, removes much of the moisture. After this pre-cooling, the air enters a disiccant dryer.

The desiccant dryer is a powerful moisture remover: a dewpoint as low as –73°C is achievable.

From House
Compressor

To

Regulator

Refrigerated
Dryer

Desiccant
Dryer
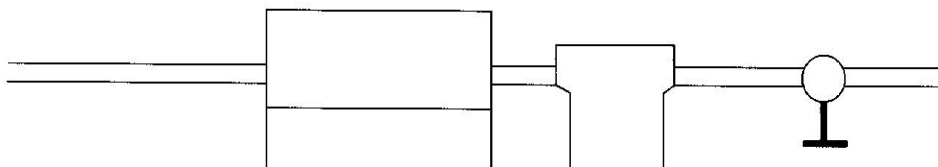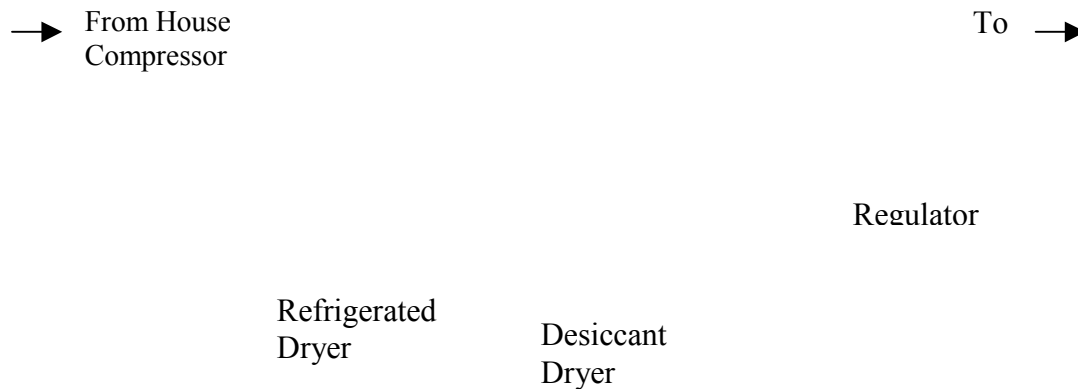
Figure 3. 4 Compressed air dryer setup diagram

3.3 SPECIMEN COOLING SYSTEM

Two vortex tubes are used for cooling the specimen. Cold air stream produced by one vortex tube is directed through a 22 mm-diameter hole on the plexiglass cover of the sample container, and then blows directly into the sample container to cool the top of the specimen. To prevent the desiccation of the soil surface by the cold dry air produced from the vortex tube, a plastic wrap with a sand layer (3 mm thick) on top of it covers the upper soil surface. The cold air produced by another vortex tube enters a circular plexiglass distribution chamber which is mounted on the Teflon sample cylinder over the soil as shown in Figure 3.2. The distribution chamber is 5 cm in diameter and 3.8 cm high. This cold air stream is directed through four 6 mm-diameter holes on the side of the distribution chamber, and enters a cold air belt. The cold air belt redirects this air stream into six lines leading to the bottom plates (see Figure 3.2) to provide a uniform cooling for the bottom of the specimen. In addition, the middle plate among the base plate assembly was machined to have a circular groove which is 1 inch wide and ¼ inch deep (see Figure 3.2). This groove is made to

shorten the heat loss distance between the bottom of the soil and the cold air circulating around it.

Finally, all cold air from both cooling routes vents out into the centrifuge model container to cool it and the water in the reservoir before it is released from the circular bucket.

3.4 BOUNDARY TEMPERATURE CONTROL

Since the cold air from the vortex tube varies between –22°C and –28°C, this requires additional control using heaters at the top and bottom of the soil specimen as shown in Figure 3.5. The top and bottom temperatures of the specimen must be controlled during the test to simulate realistic seasonal cooling and warming.

The upper air temperature control set up consists of two solid aluminum bars, 6 mm in diameter and 75 mm long, with a 4 inch-diameter aluminum disc is attached at the end of these bars. This aluminum disc has many small holes so that the cold air can pass through the holes down to the soil surface. A rope type heater, 5 mm in diameter, 1.8 m long with a maximum of 250 watt is wrapped around this set up. The rope heater turns on and off to maintain a particular upper soil temperature at a given time during the experiment. That control is achieved with a thermocouple set on the soil surface but below the thin rubber membrane that reduces soil water evaporation, and a PID (Proportional with Integral and Derivative) controller. This PID controller receives temperature data of both top and bottom of the specimen indirectly from LabVIEW in following manner; temperature data acquired by LabVIEW is converted

to voltage scaled accordingly by DAC (digital analogue converter), and this voltage is read into the controller via a digital channel (refer to 3.7 Data acquisition section), lastly, internal function built in PID controller converts it back to the temperature. PID controller acts to decrease the average power being supplied to the heater, as the temperature approaches a set-point temperature, using adjustments: integral, and derivative. SSR (Solid State Relay) was also used for controlling the power being supplied to the heaters. It is essential that the aluminum/rope heater set up be placed near the soil surface, so that the interaction between the heat source and the thermocouple on the surface of the specimen which controls the rope type heater, is rapid.

The bottom temperature of the soil was controlled indirectly by heating the water in the bottom plate reservoir using a 5 cm diameter, lightweight, flexible Kapton heater with a total wattage of 31.4 watt. That heater is also controlled by the PID controller. Temperature data from the thermocouple installed at the base of the soil column is fed to PID controller in same fashion as the top temperature via another digital channel. The bottom flexible heater was fixed on this bottom base plate, and then a thin aluminum disc was placed on top of it with the edge sealed by high thermally conductive-epoxy.
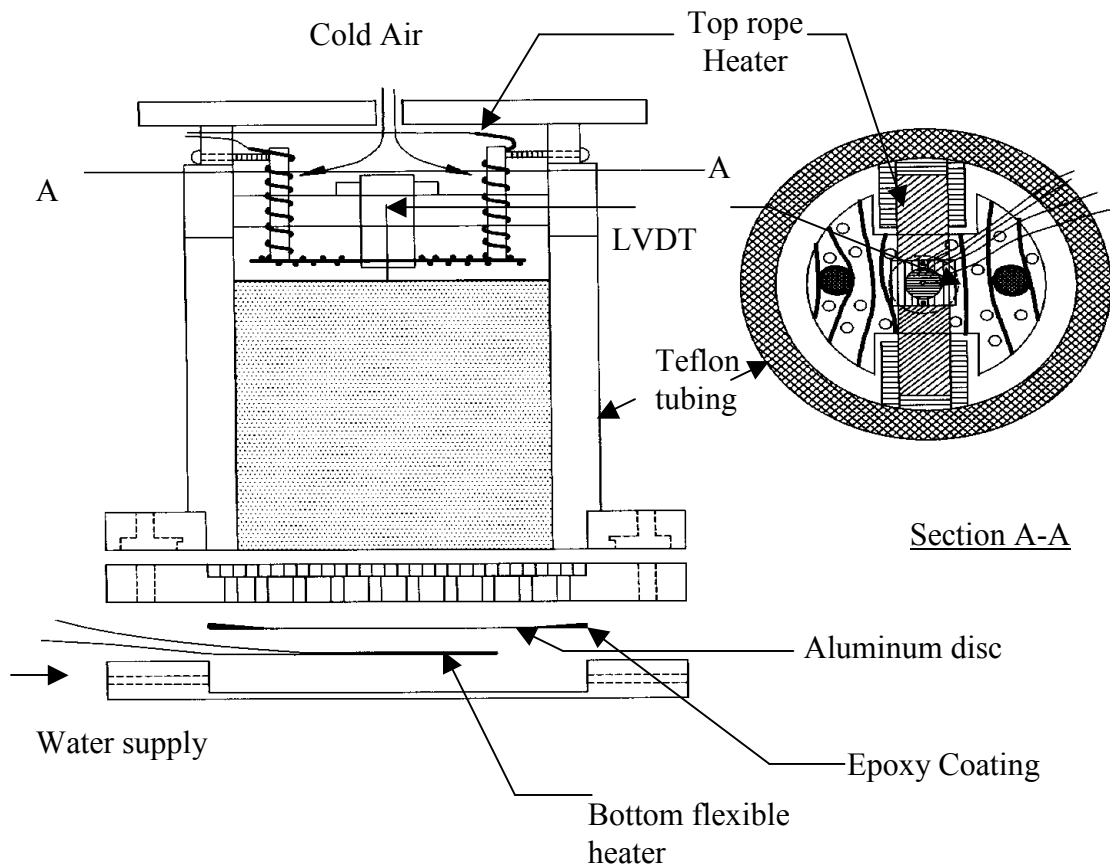
Figure 3. 5 Set-up for the top and bottom heater

3.5 TEMPERATURE SENSORS

Thermistors are used to measure the temperature of the soil specimen because they are more accurate temperature sensor than thermocouples. It registers a large change in resistance for a small change in temperature. Its resistance decreases with increasing temperature. The one used for this research is the Omega model # ON-401-PP having a resistance of 2,252 Ohms at 25°C. Its accuracy is ±0.1°C.

The calibration of the temperature sensors was performed using an ice bath, a cold bath and a high precision RTD that can read up to the resolution of 0.001°C was

used in the calibration. Calibration was done at 0.5°C interval from 0°C to 20°C. One more calibration point at less than 0°C will also be checked.

3.6 SOIL DISPLACEMENT MEASUREMENT

Soil displacement is anticipated due to specimen consolidation (down) and heave and thaw settlement (up and down). This is measured by LVDT's (Linear Variable Differential Transformer), which were manufactured by Trans-Tek Inc. A larger one with full 5 cm range (±2.5 cm) is used for measuring consolidation settlement of the soil specimen. A smaller one with a full 2.5-cm range (±1.25 cm) is used for measuring the frost heave and thaw settlement of the soil specimen during the testing. Each LVDT is mounted on a different platform as shown in Figure 3.6 since soil consolidation was achieved on the centrifuge before the freezing segment of tests began.

LVDT Platform

LVDT

Soil
Sample

(a)

(b)
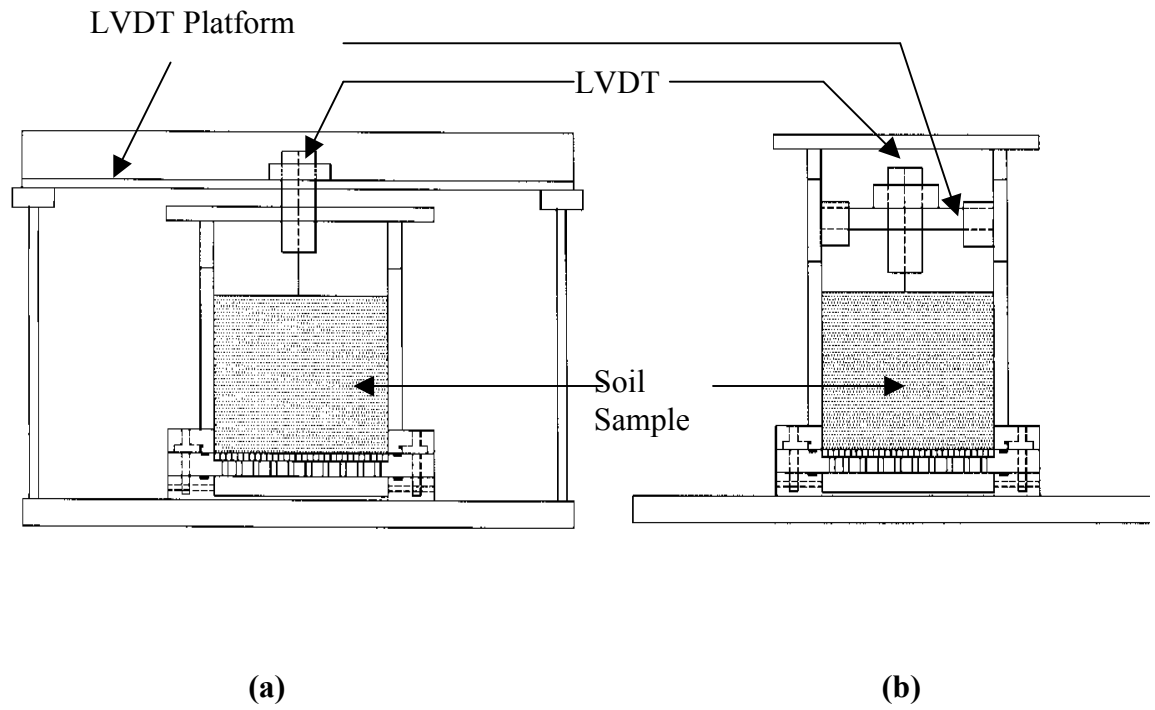
Figure 3. 6 Two different LVDT setup, a) for consolidation settlement, b) for frost heave measurement

3.7 DATA ACQUISTION SYSTEM

Getting the data acquisition system or DAQ installed and operational has been a major project in itself for this research. The DAQ is comprised of an SCXI Chassis (Model, SCXI 1001), six modules (SCXI 1121), six terminal blocks (SCXI 1321), and a data acquisition card (PCI-MIO-16E-4) as shown in Figure 3.7. These except DAQ card are mounted on the center of the centrifuge arm as assembled. Ten lines were singled out of a 68-pin cable from the SCXI chassis. These lines are comprised of two analog signal channels, several ground lines, and some lines for signal multiplexing purpose, which are essential minimum number of lines to transmit the signals from all sensors to a DAQ card installed in the computer outside centrifuge. To sort out these lines from a 68-pin cable, a connector block was used. Inside this connector block, 68 pins were broken down into 10 lines. These 10 lines from the connector blocks were connected to the terminal strip using 10 lines of wires. To eliminate the chance of picking up the noise from these wires during the rotation of the centrifuge arm, the connector block was placed as near the terminal strip as possible to minimize the wire length. A 2 m-long shield cable (68 pins) from the DAQ chassis is plugged into this 68-pin shielded connector block mounted at the edge of the centrifuge arm near the terminal strip.

Once outside the centrifuge enclosure, another connector block was located on top of the centrifuge enclosure near the slip-rings to have the identical setup as inside the centrifuge. Between the computer and this outside connector block, a 5 m-long shield cable was used for the transmitting the signal. From this connector block, two digital channels (each for top and bottom temperature control) are used for the

34

temperature controller. This cable is plugged into the data acquisition card installed at the back of the computer tower.

The DAQ uses the National instrument LabVIEW system to provide the following capabilities:

1. To record internal soil temperatures

2. To record soil surface displacement data during the initial phase of self-weight consolidation, during freezing.

Each terminal can accommodate 4 different sensors. They are plugged into each module enclosed by the chassis being used as housing. These terminals are held tightly in place using an aluminum mount to resist against the high level of g pushing them outward. Modules that do functions of filtering, amplifying, and multiplexing are also pre-programmed to match the specific sensors. The custom-made signal box is mounted on the centrifuge arm. This box acting as a bridge connecting the sensors from the sample container box to the terminal on the DAQ chassis provides secure signal connection and eliminates electric noise. The outline of a data acquisition system used in this research is shown in Figure 3.8.
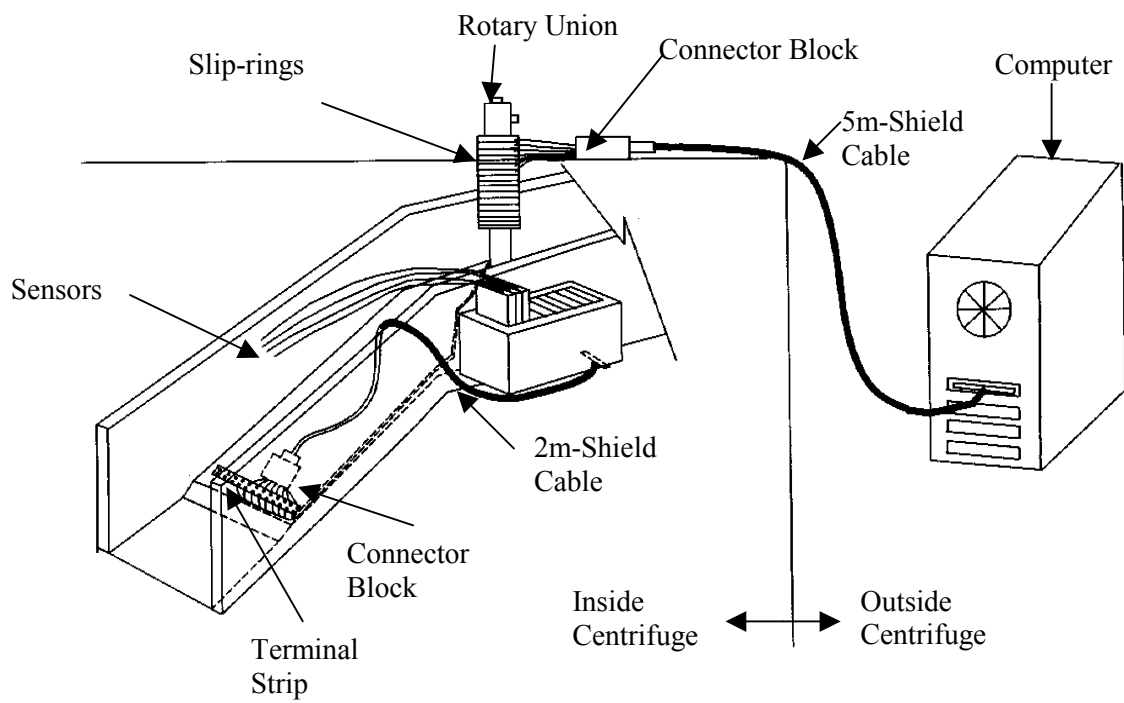
Figure 3. 7 The Diagram of Data Acquisition System set-up

```
                        ┌─────────────┐
                        │   Measure   │
                        └─────────────┘
                               │
                               ▼
                        ┌─────────────┐
      ┌────────────────▶│  Transducer │
      │                 └─────────────┘
┌───────────┐                  │
│  Power    │                  ▼
│  Supply   │           ┌─────────────┐          ┌─────────────┐
└───────────┘           │   Signal    │          │  Slip-rings │
                        │ Conditioning│          └─────────────┘
                        └─────────────┘
                               │
                               ▼
                        ┌─────────────┐
                        │ Transmission│
                        └─────────────┘
                               │
                               ▼
┌───────────┐           ┌─────────────┐
│  Control  │◀──────────│     ADC     │
└───────────┘           └─────────────┘
                               │
                               ▼
┌───────────┐           ┌─────────────┐
│ Software  │◀──────────│  Computer   │
│ (LabVIEW) │           └─────────────┘
└───────────┘            │          │
                         ▼          ▼
                  ┌───────────┐ ┌───────────┐
                  │  Display  │ │  Storage  │
                  └───────────┘ └───────────┘
```
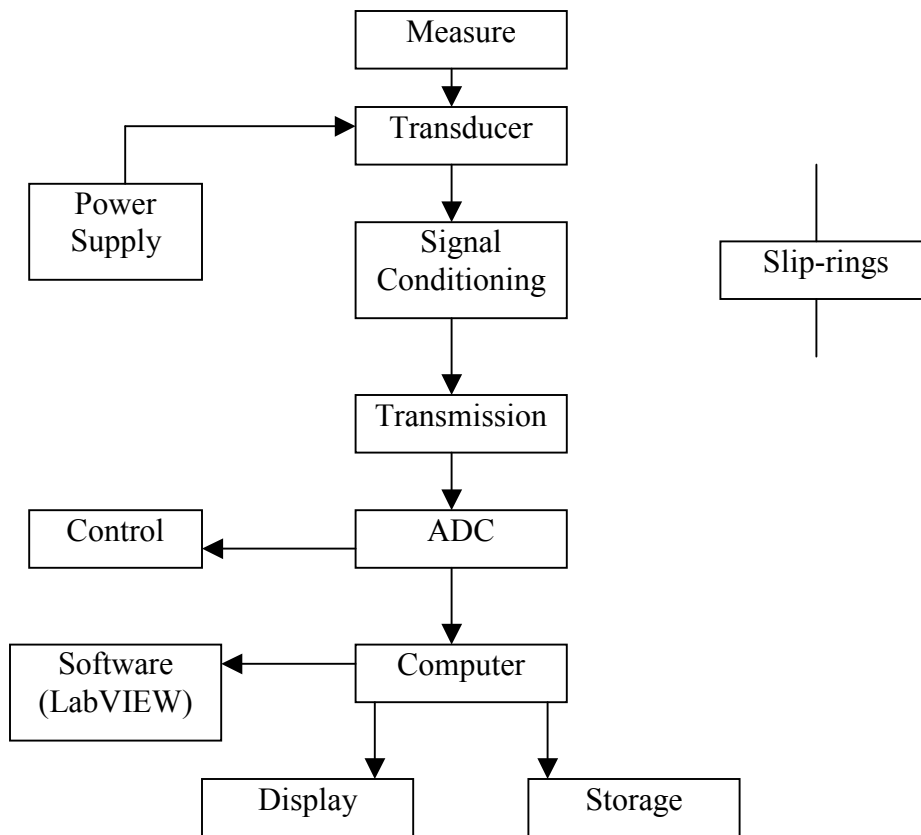
Figure 3. 8 Data Acquisition System Layout

CHAPTER 4: MATERIALS AND EXPERIMENTAL METHOD

4.1 FULL SCALE FREEZING CONDITIONS SIMULATED

The full-scale prototype soil layer simulated in this research is shown in Figure 4.1. The total prototype depth, H_p, modeled is 4 m that exceeds the maximum seasonal freezing depth of 1.8 m (Washburn, 1980) in the lower 48 United States. The soil surface is horizontal. Two depths have been chosen for the phreatic surfaces: one was set equal to 0.25 H_p, or 1 m and the other to 0.75 H_p or 3 m from the soil surface in order to assess influence of accessibility to water. Vertical, unidirectional geothermal heat flow is modeled.

Surface temperature variation can be idealized to undergo a sinusoidal variation on both a daily and an annual cycle as shown in Figure 4.2. In a homogeneous soil with no change of state, the temperature ($T_{z,t}$) at any depth and time can be idealized with the following equation (Andersland, and Ladanyi 1994)

$$T_{z,t} = T_m + A_s \exp\left(-z\sqrt{\frac{\pi}{\alpha_u p}}\right)\sin\left(\frac{2\pi t}{p} - z\sqrt{\frac{\pi}{\alpha_u p}}\right) \dots\dots\dots\dots\dots\dots.4.1$$

Where : α_u is the soil thermal diffusivity;

$\quad$ T_m is the mean annual temperature;

$\quad$ A_s is the surface temperature amplitude;

$\quad$ and p is the period, 24 hrs or 365 days.

Eq. 4.2, and 4.3 also show that change of temperature (Amplitude, A_z, Temperature T_z) decreases rapidly with increase in depth (z), and A_z , and T_z are given by
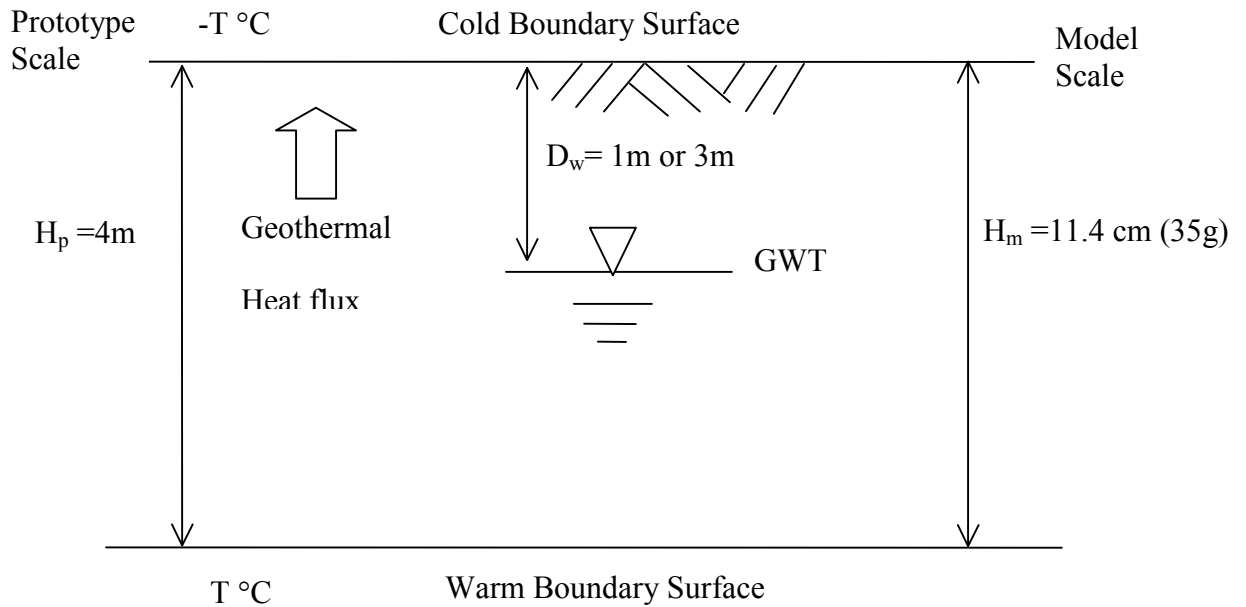
Figure 4. 1 Proposed prototype soil profile

$$A_z = A_s \exp\left(-z\sqrt{\frac{\pi}{\alpha_u p}}\right) \qquad (4.2)$$

$$T_z = T_m \pm A_s \exp\left(-z\sqrt{\frac{\pi}{\alpha_u p}}\right) \qquad (4.3)$$

Two types of freezing modes are used in frost heave research. One is referred to as "step-freezing", which means boundary temperatures are fixed for the duration of the experiment. The other mode is referred to as "ramp-freezing" which means boundary temperatures are varied with time to simulate seasonal cooling and warming. Konrad (1994) reported that these two different freezing schemes can have

quite different effects on the magnitude of both frost heave and heave rate and frost heave vs. time curve, even if the freezing indices, F (product of mean temperature below 0°C and duration of time) are the same. This was confirmed in the results of centrifuge modeling of frost heave in silt described in Yang and Goodings (1998), and Straub (1999). Whereas a few experiments in this research are conducted applying step freezing, the majority used ramp freezing. In ramp freezing test, both the top and bottom temperatures were varied to simulate annual cycles of freezing and thawing; daily cycles were not modeled.
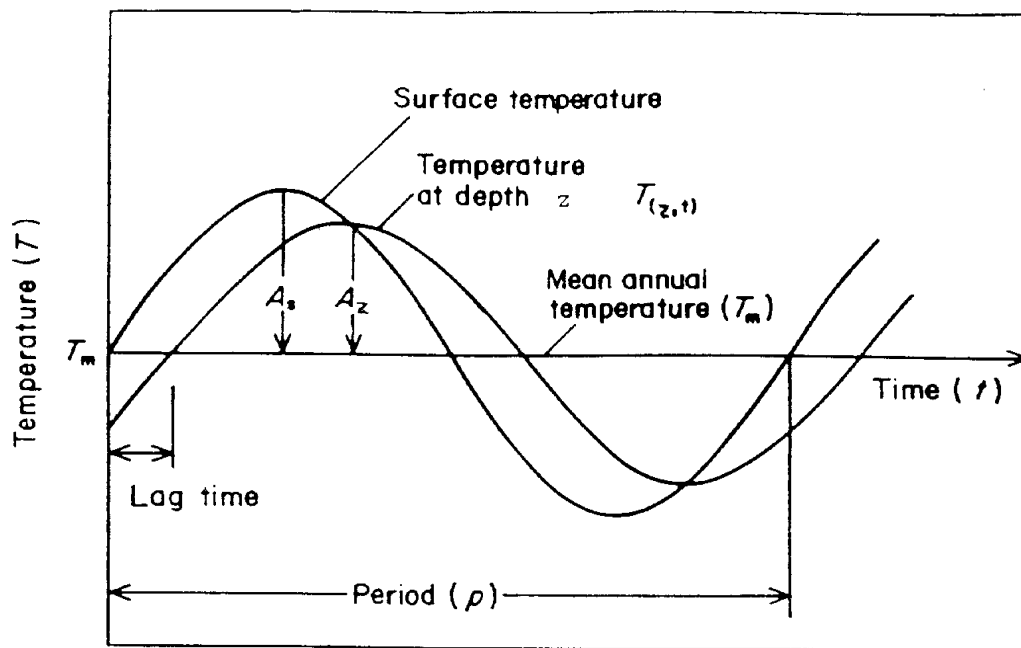
Figure 4. 2 Sinusoidal surface and ground temperature fluctuations

The temperature data for the following sites were considered in choosing the ramped boundary temperature regime for these tests: Happy Valley, Alaska; Delta junction, Alaska; and Nummi-Pusula, Finland. Their data are plotted in Figures 4.3,

40

4.4 and 4.5. The temperature data of Happy Valley, Alaska is plotted in Figure 4.3. It included 8449 hourly observations from 26 August 1994 to 18 August 1995. The data did not include depths below 100 cm, and the depth of freezing passed 100 cm after the frist 50 days of the record. Nonetheless, it is clear that ground temperature oscillates more or less sinusoidally. Note that surface temperature varies more than temperature at depth so that surface temperature becomes colder in fall ($\cong$30 days) than soil at depth, and then becomes warmer in spring ($\cong$250 days).

A second data set are plotted in Fig. 4.4. for Delta Junction, Alaska from Sharratt, (1993). Soil temperature data from this site were collected from September 1987 through May 1992 (temperature data are averaged from 5 years of data) at depths up to 320 cm. Again, there is a temperature reversal when shallow depths are more responsive to winter cooling and spring warming. Note also that when the surface temperature starts to warm in February, all temperature to a depth of 1.6 m also begin to rise. At a depth of 3.2 m, however, the temperature continues to decrease until May, and then it can be assumed to rise thereafter to return to the temperature in September at this depth. As in the Happy Valley data, the temperature gradient is less steep with increasinge depth.

The third data set from Nummi-Pusula, Finland is plotted in Figure 4.5. Here the greatest depth of freezing was 1.1 m and at a depth of 3 m the soil temperature never dropped below +2.5°C. This minimum temperature occurred after spring warming had begun, as was the case for Delta Junction, AK.

41

Figure 4. 3 Temperature Profile at Happy Valley

42

Figure 4. 4 Temperature Profile at Delta Jun
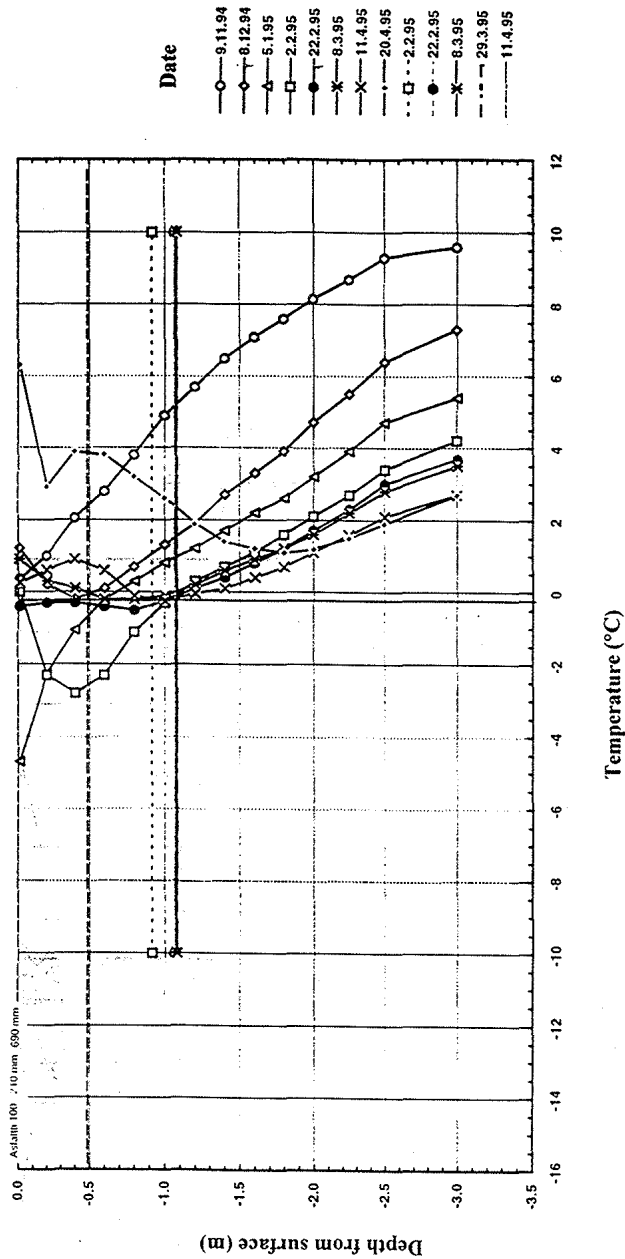
Figure 4. 5 Temperature Profile at Nummi-Pusula

Based on these site data, the following simplified temperature regime was adopted for the top and bottom boundary temperatures of the soil column in this research as shown in Figure 4.6. The year was divided into four quarters and the upper bundary temperature is allowed to fall over 0.25 year from $+3°C$ to $-3°C$. It was held constant for 0.25 year, and the ramped for 0.25 year resembling the temperature change pattern of Happy Valley AK, but the more temperate temperatures of Nummi-Pusula, Finland. The lower boundary model temperature resembles the general pattern of Delta Junction, AK at depth 320 cm, and the temperatures of Nummi-Pusula. Bottom surface temperatures were targeted to fall slowly over one fourth year from $+3°C$ to $+1°C$, and maintain $+1°C$ over another one fourth year.

A more sophiscated temperature regime was adopted in the latter part of this research as shown in Figure 4.7 to order to investigate the freezing mechanism in clay further. A distinctive characteristic of this regime is the two-tier ramping scheme for top temperature boundary. Top temperature was allowed, first, to fall from $+3°C$ to $-1°C$ over 63 days, maintained at $-1°C$ over 88 days, fall again from $-1°C$ to $-3°C$ over 63 days, and finally held constant at $-3°C$ over 126 days. Bottom temperature, on the contrary, was targeted to fall slowly from $+3°C$ to $+1°C$ over 88 days, and held constant for the rest of freezing period, namely, 252 days.

By adopting this sophicated temperature scheme, soil specimens were subjected to ramped freezing twice, and eventually, longer freezing than first simple temperature reigme.
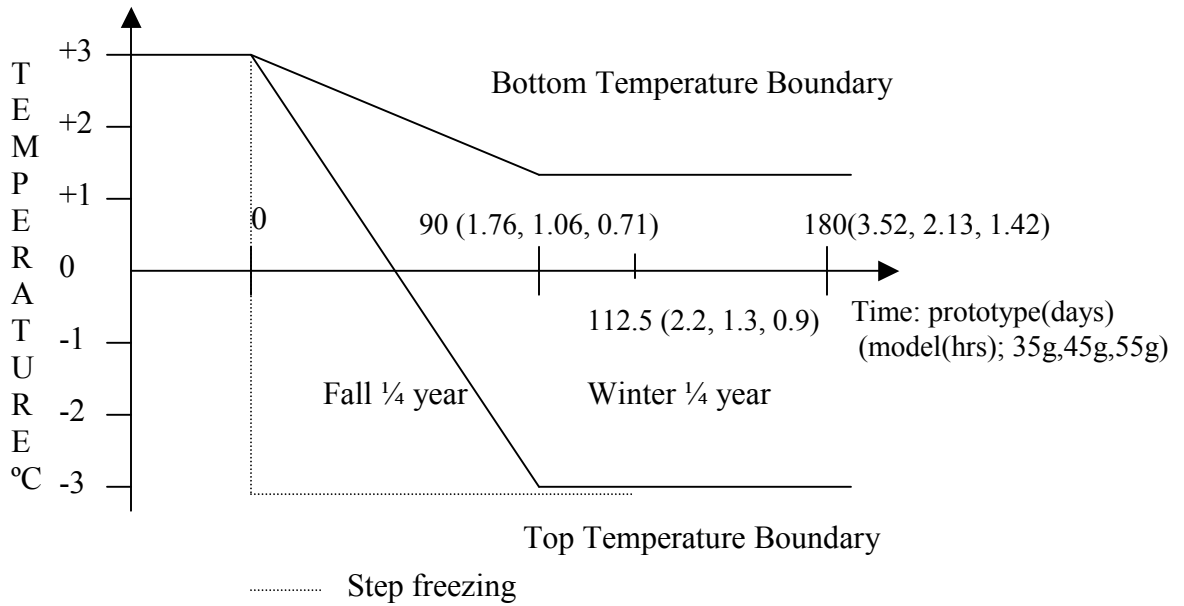
Figure 4. 6 Proposed Temperature Scheme 1 (not drawn to scale)
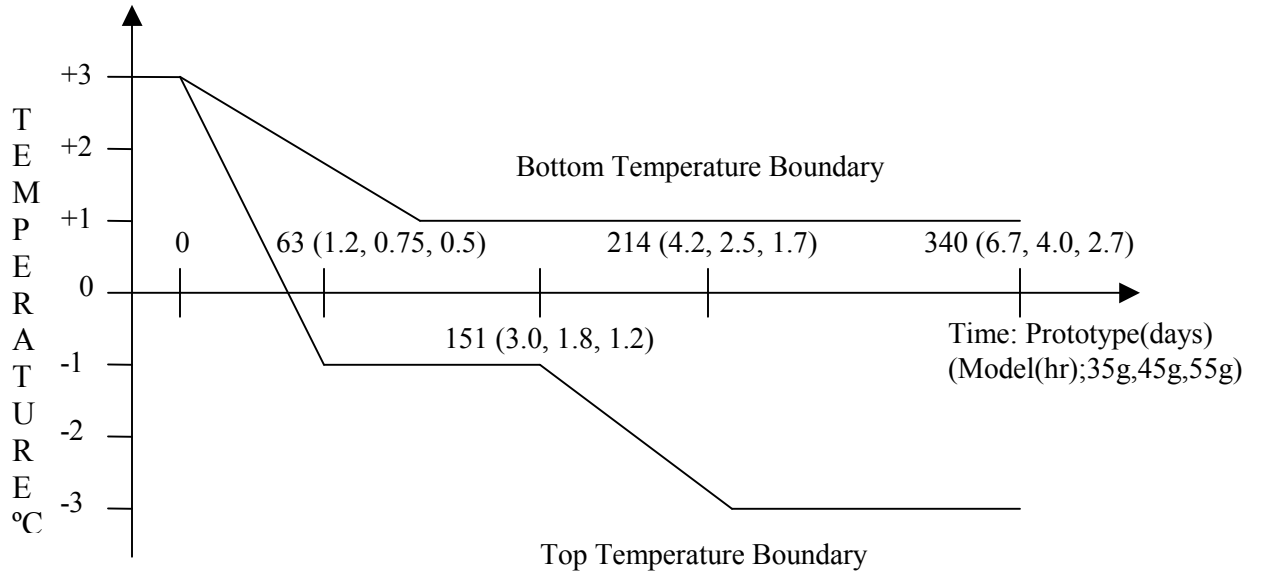
Figure 4. 7 Proposed Temperature Regime 2 (not drawn to scale)

4.2 SELECTION OF MODEL DIMENSION

"Modeling of model" is a technique that has been used by centrifuge researchers for verifying scaling laws. In this technique, a single hypothetical full scale prototype is selected. Models at different scales are then built and tested in compliance with theoreically based modeling laws, to check if all models predict the same hypotheical full scale prototype.

$$H_m = H_p/N = 4m/N$$

Savvidou (1988) established that the scaling relationship for the rate of heat loss in two bodies, identical in geometry, material, and boundary condition, but different absolute size, is $t_m = t_p/N^2$, where N is the scale of the dimensions of the model. Her models involved temperatures well above freezing. Yang and Goodings (1998) established the same in soil freezing, judging indirectly from rate of development of heave in columns of silt.

In these models, a full scale freeizng indices or freezing-degree days (the sum of days times their negative temperatures) were calculated to be equal to − 337.5 °C-days for the first temperature regime, and − 600°C-days for second temperature regime. For example, − 337.5 °C-days can be be applied to the specimen by varying upper boundary temperatur from + 3°C to − 3°C over 180 days. Based on the $t_m = t_p/N^2$ time scaling, 180 days or 4320 hours at prototype scale should be modeled correctly in $t_m = 4320/N^2$ hours to simulate freezing effects of − 337.5 °C-days at full scale with the same upper boundary temperature variation. Including − 600°C-days of second temperature regime, which is more sophiscated one, all model test time are summarized in Table 4.1. Test duration was a key consideration in choice of model

scale. The objective was to select the largest scale model that could be tested in a single measurable test day. In case of – 600°C-days, models at 1:35 sclae required 6.6 hours to simulate 340 days of cooling; models at 1:45 and 1:55 scales required 4.1 hours and 2.7 hours, respectively. In this research, the model sample heights were calculated for 1:35, 1:45, and 1:55 scale models to be those shown in Table 4.1.

Table 4. 1 Experiment Variables

Ng	Temperature Scheme 1 (-337.5 ºC-days)				Temperature Scheme 2 (-600 ºC-days)		Sample Height	
	Ramp		Step		Ramp		Prototype (m)	Model (cm)
	T_p (days)	T_m (hours)	T_p (days)	T_m (hours)	T_p (days)	T_m (hours)		
35	180	3.5	112.5	2.2	340	6.7	4	11.4
45	180	2.1	112.5	1.3	340	4.0	4	8.9
55	180	1.4	112.5	0.9	340	2.7	4	7.3

Theoretically based modeling laws are captured indirectly through Buckingham π ratios that allow models at different scales to be related to each other, and models to be related to full scale. If all parameters of significance to the phenomenon being studied are not included in the π's developed, so that similarity is not strictly achieved between models, then modelling of models will indicate that some feature of importance in behavior has not beeen adqueately accounted for. Buckingham π ratios for frost heave lead to the scaling relationships set out by Smith (1995) for cold region engineering, and summarized in Table 4.2.

In the absence of full scale data against which to compare models are full scale results, modelers must look for internal consistency using modeling of model. If the results of two models at different scales with equal values of controling Buckingham π ratios predict the same hypothetical full scale behavior, then models are assumed to

be self-confirming, and are also assumed to be satisfactorily representative of full scale behavior. This is used as indirect proof of the validity of the modeling relationships.

Table 4. 2 Centrifuge Scaling Law (R.N Taylor, 1995)

Physical quantity	Prototype	Model
Defined		
Macroscopic Length	1	1/N
Microscopic Length	1	1
Gravitational acceleration	1	N
Temperature	1	1
Derived		
Strain	1	1
Pore-water Pressure	1	1
Stress	1	1
Time		
$\quad$ Diffusion process	1	$1/N^2$
$\quad$ Inertial event	1	1/N
$\quad$ Viscous processes	1	1
Total water potential	1	1
Interstitial water velocity	1	N
Moisture flux	1	N
Heat flux	1	N

Table 4.2 indicates that all model linear dimension, L_m, including model height, depth of phreatic surface, magnitude of frost heave, and depth of freezing, are related to full sclae prototype dimesions, L_p, as $L_m = L_p/N$, where N equals both model scale and model acceleration expressed as multiples of earth gravity. Duration of periods of cooling and warming in a model, t_m, are predicted to related to the duration a full

sclae tp as $t_m = t_p/N^2$. The same is true for times for consolidation and times for flow of water, $t_m = t_p/N^2$.

4.3 ENGINEERING PROPERTIES OF SOILS

Two types of clays are being used for this research. One is EPK Kaolin manufactured by the Feldspar Corporation, and the other is a natural clay obtained by the US Army Corps of Engineers Cold Regions Lab (CRREL) from Ft Edwards, NH. This latter soil was selected because CRREL has done extensive soil freezing testing on it themselves.

The standard soil identification tests were conducted on both the kaolin and Ft.Edwards clay. The results are summarized in Table 4.3.

According to the Unified Soil Classification System (USCS), the soils are classified as CH, clay with high plasticity for kaolin, and CL, silty clay with medium plasticity for Ft.Edwards clay. Figure 4.8 shows the grain size distribution of these two soils. Falling head permeability tests were performed on the kaolin, and Ft.Edwards specimens after consolidation complete to determine the saturated, unfrozen permeability of the soils using a Flexible Wall Permeameter according to ASTM D 5084 (refer to Table 4.1). Its saturated permeability for kaolin and Ft.Edwards clay were measured to be $5.3*10^{-8}$ cm/s, and $1.3*10^{-8}$ cm/s, respectively. As soil freezes, permeability decreases as shown in Figure 4.9, as open pores became progressively smaller with the formation of ice. The absorbed water layer remains open to flow at temperatures below 0°C, and is more important in finer grained soils.

It was not possible to measure the thermal properties of the soils with the apparatus in the UMCP laboratory. Phase changes, however, dominate the thermal conditions in the system, and the thermal properties of the soil minerals do not influence these significantly. As a result, the thermal properties of the soils were estimated from data provided by Farouki (1986), and are listed in Table 4.1. Other thermal properties such as thermal diffusivity, specific heat, and latent heat, etc are also a function of the temperature, soil type, water and/or ice content, degree of saturation, and soil density.

Table 4. 3 Engineering Properties of Soils

Engineering Index	Kaolin	Ft. Edwards
Liquid Limit, w_L %	56	47
Plastic Limit, w_p %	34	29
Plasticity Index, I_p	22	18
Specific Gravity, Gs	2.63	2.77
USCS symbol	CH	CL
Optimum water content, w_o %	34	26
Maximum dry density, γ_{dmax}, g/cm^3	1.33	1.54
Permeability, k_{20}, cm/s	$5.3*10^{-8}$	$1.3*10^{-8}$
Latent heat of soil (kJ/m^3)	203,500	178,200
Unfrozen heat capacity, C_u (kJ/Mg ° C)	2060	1800
Frozen heat capacity, C_f (kJ/Mg ° C)	1260	1160
Unfrozen thermal conductivity, k_u, (kJ/m day° C)	210	213
Frozen thermal conductivity, k_f, (kJ/m day ° C)	422	370
Frost group based on US Army Corps of Engineers frost design soil classification system	F3	F3

The U.S. Army Corps of Engineers defines a frost graph designation based on 1) the percentage of particles smaller than 0.02 mm, 2) soil type based on the Unified Soil Classification System, and 3) a laboratory freezing test. Their classification system is given in Table 4.4 and shown in Figure 4.10. The frost group designation for the two soils used in these tests is F3, which indicate very low to very high potential for frost heave.
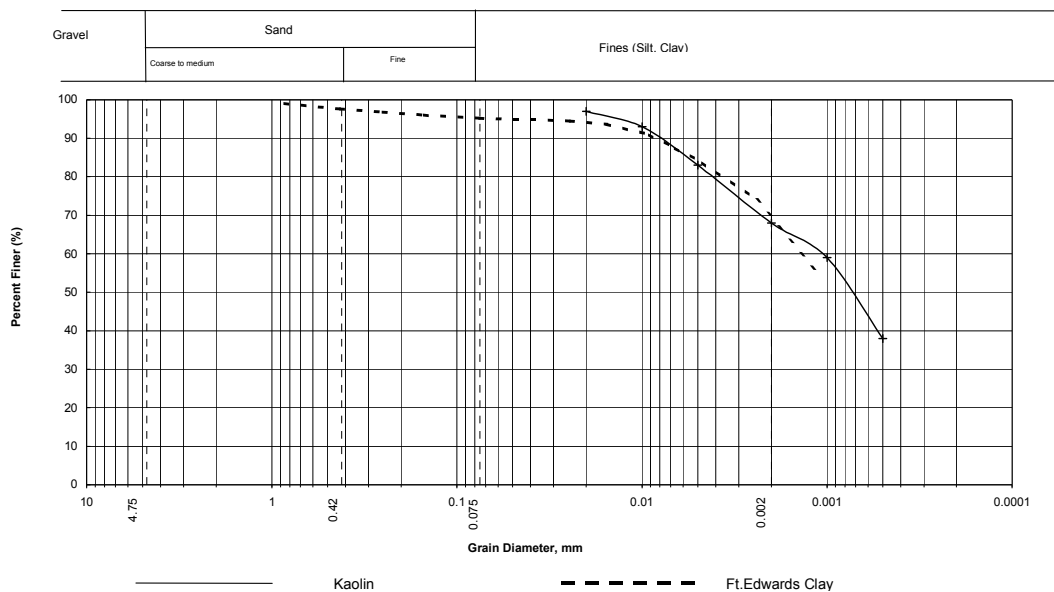
Figure 4. 8 Grain size distribution curve
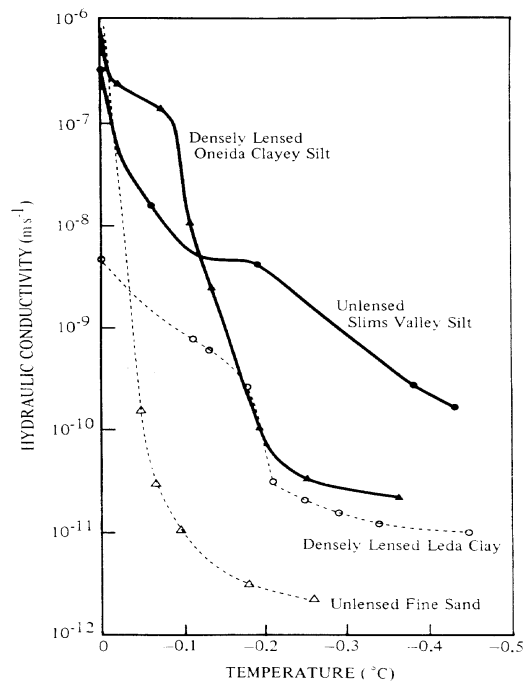
Figure 4. 9 Hydraulic conductivity as a function of subfreezing temperature (after Burt and Williams, 1976)

Table 4. 4 US Army Corps of Engineers frost design soil classification system (1965)

Frost Susceptibility*	Frost Group	Kind of soil	Percent finer Than 0.02mm	Typical soil type Under USC system**
Negligible to low	NFS	a) Gravels b) Sands	0-1.5 0-3	GW, GP SW, SP
Possibly***	PFS	a) Gravels b) Sands	1.5-3 3-10	GW, GP SW, SP
Low to Medium	S1	Gravels	3-6	GW, GP, GW-GM, GP-GM
Very low to high	S2	Sands	3-6	SW, SP, SW-SM, SP-SM
Very low to high	F1	Gravels	6-10	GM, GW-GM, GP-GM
Medium to high Negligible to high	F2	a) Gravels b) Sands	10-20 6-15	GM, GM-GC, GW-GM, GP-GM, SM, SW-SM, SP-SM
Medium to high Low to high Very low to very high	F3	a) Gravels b) sands, except very find silty sands c) clays, PI>12	>20 >15	GM, SC SM, SC CL, CH
Low to very high Very low to high Low to very high Very low to very high	F4	a) all silts b) very fine silty sands c) clays, PI<12 d) varved clays and other fine-grained banded sediments	- >15 - -	ML, MH SM CL, CL-ML CL and ML; CL, ML, and SM; CL, CH, and ML; CL, CH, ML and SM

* Based on laboratory frost heave tests
** G-gravel, S-sand, M-silt, C-clay, W-well-graded, P-poorly-graded,
   H-high plasticity, L-low plasticity
*** Requires laboratory frost heave test to determine frost susceptibility
NFS- non frost susceptible
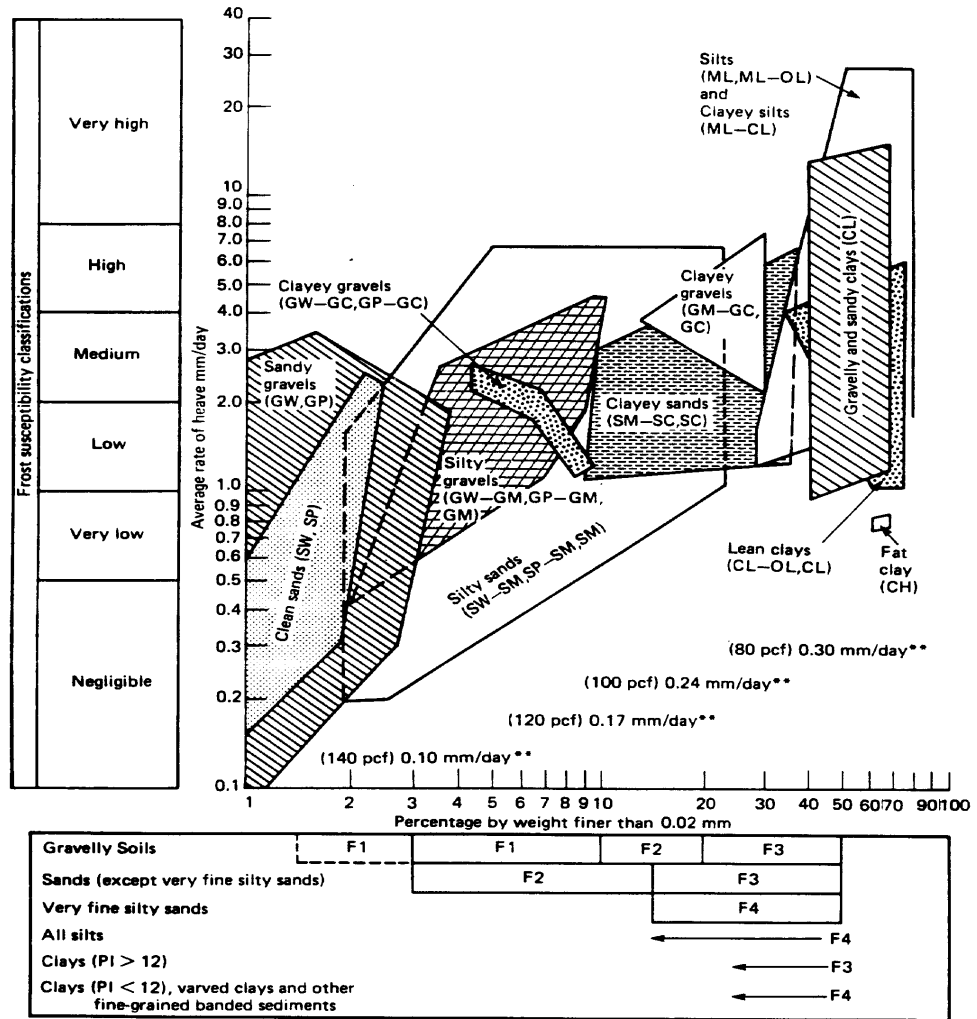
Figure 4. 10 Frost susceptibility of soils

There is no clear distinction between kaolin and the Ft. Edwards clay made in this classification. A laboratory freezing test is recommended to obtain more precise assessment of frost susceptibility, but was not conducted here.

One-dimensional oedometer tests were performed on the unfrozen kaolin and Ft.Edwards clay prepared from slurries to determine the compression index (C_c) of the normal consolidation line and consolidation coefficient (C_v). The test results are provided in Table 4.5, and Figure 4.11. The compression index (C_c) was back calculated from the actual consolidation data, and was found to be in good agreement with the value from the oedometer test mentioned above well. The coefficients of consolidation (C_v) are plotted in Figure 4.11. These were used to estimate the time required to complete above 90% of consolidation. For specimens 25.4 mm in thickness with one-dimensional consolidation and two-way drainage, t_{90} is predicted to range from10 hours to 23 hours for kaolin, and in the range of 14 hours to 22 hours for the Ft.Edwards clay depending on the magnitude of the surcharge. The smaller the surcharge, the smaller the value of C_v, the longer the time required for 90% consolidation completed.

Table 4. 5 Compression Coefficient

Soil Type	Coefficient of Compression (Cc)	Coefficient of Recompression (Cr)
Kaolin	0.3835	0.0127
Ft. Edwards	0.6910	0.0333
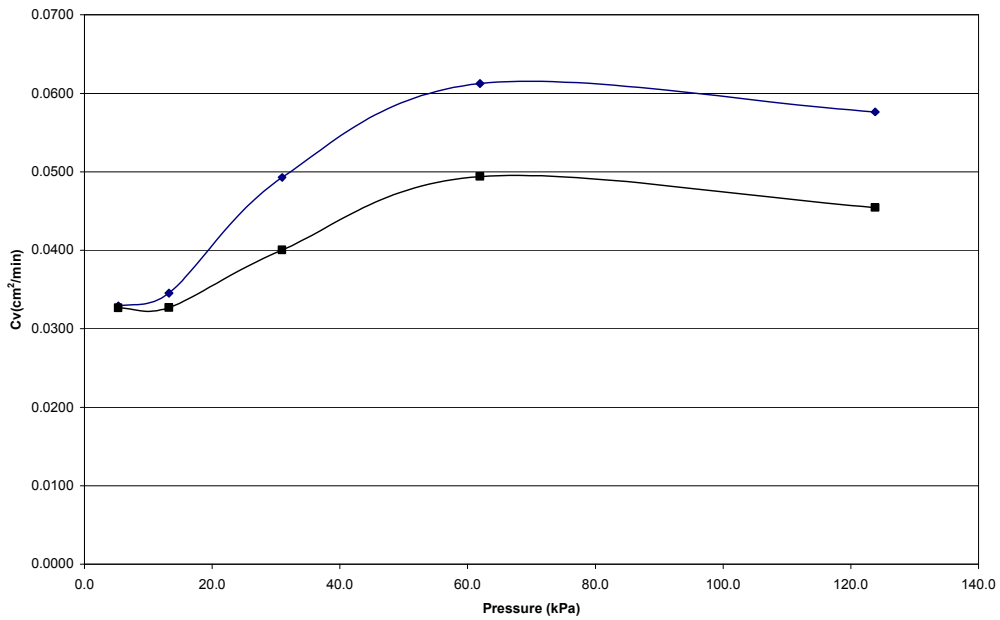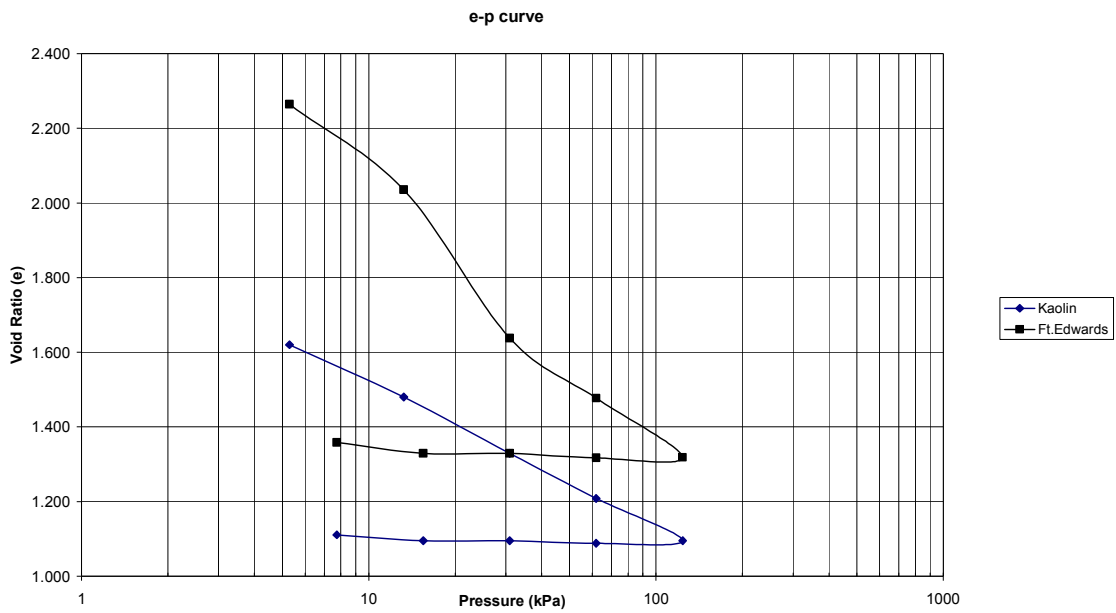
Figure 4. 11 Plot of void ratio(e) vs. Pressure and consolidation coefficient(Cv) vs. Pressure

4.4 TEST PROCEDURE

4.4.1 SAMPLE PREPERATION

Soil specimens are prepared beginning with clay slurry. The kaolin was mixed one hour to achieve w = 90%, which is 1.6 times of its liquid limit (LL $\cong$ 56%), and Ft.Edwards clay was mixed to achieve w = 60%, which is 1.3 times of its liquid limit (LL $\cong$ 47%). This gave both clays similar consistency. In the latter part of this research, the water content of slurry was even lowered to w = 70%, which was the lowest value for kaolin to be workable for preparing specimens. These models were used to investigate the initial water content effects on freezing behavior in clay

WD-40 light lubricating oil was sprayed on the inside wall of a sample container to minimize the friction along the vertical boundary of the soil sample, and filter paper was placed on top of the perforated bottom base plate to prevent the loss of the soil through it. A thermister was placed on the paper filter; this thermistor can be used to control the bottom soil temperature. The clay slurry was then transferred into the sample container.

Samples were prepared to achieve an over-consolidated state for the upper half of the specimen, and normally consolidated state for bottom half of the specimen when the model was being tested on the centrifuge. Consolidation scheme involved the following steps: First, filter paper and then an aluminum disc with many small drainage holes were placed on the top surface of the clay. The water table in the soil was set to be a little higher than the top of the soil surface by adjusting the height of water in the water tanks. Consolidation was performed in 5 stages in order to avoid the generation of high pore pressure that may cause piping through the initially very

soft clay mass, and leading to preferential drainage path. For example, first 3 stages are conducted at 1g, and last 2 stages are conducted on the centrifuge. This also involves transferring the specimen to the centrifuge cooling apparatus for self-weight centrifuge consolidation. This scheme is set out in Table 4.6. Figure 4.12 shows the soil stress history of kaolin prepared with w = 90% of slurry for 35g model test schematically, although the soil stress histories differ slightly depending on the soil type, centrifugal accelerations, and water content of slurry.

Table 4. 6 Consolidation Stages

Stage	Number g	Surcharge (kg)	†Soil Stress (kN/m²)		Duration (hr)
			Top	Bottom	
1	1	8.69	6.7	8.7	24
2	1	17.15	13.3	15.1	24
3	1	2.7	26.8	28.1	24
4	¹N	0	0	67.8	5~6
5	N	0	0	67.8	1~2

Note: N = Centrifugal accelerations (35g, 45g, and 55g).
$\quad$ †= These values vary slightly depending on the soil type, and centrifugal accelerations.

When specimens were transferred to the centrifuge apparatus, the soil surface was covered by kitchen quality plastic wrap and thin layer (2 mm) of fine, uniform sand to limit evaporation which can be very substantial during freezing. Lastly, thin copper disc was placed on top of this sand layer to provide a uniform heat flow over the top soil surface. Connection of all sensors (thermistors, LVDT, etc) was also completed at that time.

Specimens of each clay were consolidated and dissected after consolidation was completed in order to measure the final unit weights and water content without freezing.

Saturated unit weights of kaolin samples prepared from slurry water contents 90% narrowly ranged from 15.9 kN/m^3 to 16.2 kN/m^3. And water contents were from w = 60% to w = 62%. Saturated unit weights of kaolin samples prepared from slurry water contents 70% narrowly ranged from 17.0 kN/m^3 to 17.3 kN/m^3. And water contents were from w = 50% to w = 51%. Saturated unit weight of Ft.Edwards clay prepared from slurry water content 60% narrowly ranged from 17.6 kN/m^3 to 18.5 kN/m^3. And water content was from 45% to 46% through the depths tested at 35g, 45g, and 55g. Saturation degree (S_r) was calculated to be 100% using relationship ($S_r e = wGs$).

Soil Stress History Profile of kaolin sample (35g, Hp=4m)
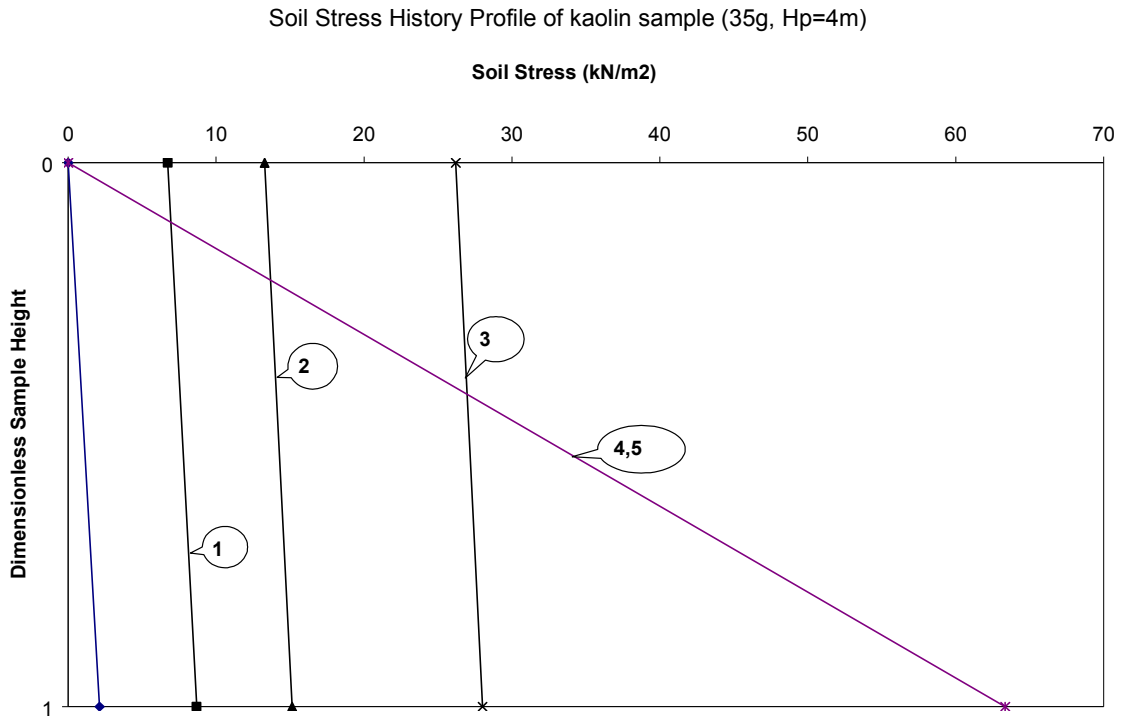
Figure 4. 12 Soil Stress Profile at Each Stage of Consolidation

4.4.2 CENTRIFUGE TESTING PROCEDURE

After consolidation on the centrifuge, each specimen was cooled overnight in an environmental chamber to bring the specimen to 3.3°C throughout. The next morning, the sample was returned to the centrifuge and accelerated to the desired acceleration: 35g, 45, or 55g. This second cooling phase on the centrifuge lasted 1 to 2 hours. During this period, the soil sample resettled and cooled further to 3.0°C throughout the sample length. The water table was set at the intended level of the phreatic surface using two reservoirs.

After resettlement was complete, the specimen cooling test was initiated as shown in Figure 4.3, and Figure 4.4.

During this period, internal thermisotrs registered soil temperatures during the test, and an LVDT located on the sand surface registered surface elevation changes. All data were transmitted directly to the computer using the on board data acquisition system described previously in Section 3.7.

After the test, the specimen was dissected immediately to observe ice lens formation and collect samples for the water content profile. A portion of the frozen specimen was also used for a consolidation test.

4.4.3 RADIAL WATER CONTENT DISTRIBUTION

As described earlier in section 4.4.1, soil specimens were made from slurries by the static compression of 1g and centrifuge consolidations, and ensuing water content reduction is checked to obtain the initial water content of a soil specimen before freezing. This water reduction should also be uniform in all directions in a soil column because this confirms that a soil column has been subject to the same soil stresses and uniform pore water flow throughout consolidation phases, consequently provides the reliability, reproducibility of test results.

In this research, water contents at three different horizontal locations along an uniform lengthwise interval for each specimen were examined. The three horizontal locations were selected from two edges (across each other), and a center, which can represent the whole surface of a specimen. The phreatic surface in all models was set to be $D_w = 0.25H_m$, where D_w is depth of phreatic surface in soil columns, and H_m is the height of model.

Figure 4.13 shows the water contents of three kaolin specimens at the end of centrifuge consolidation prepared from the slurry of 90%. These three specimens with different sample heights prepared for 35g, 45g, and 55g were consolidated on the centrifuge at corresponding centrifugal forces. The variations of the water contents obtained from each dissected specimen across the horizontal planes are within a small range, with the coefficient of variation (CV) of 1.5% or less. Strong similarity in the water contents results is shown within this group, and through each horizontal cross section.

Figure 4.14 shows the water contents of additional two specimens: a kaolin specimen prepared from 70% water content of slurry; and a Ft. Edwards clay prepared from 60% water content of slurry. The sample heights of these specimens were 11.4 cm (35g model). The variations of the water contents obtained from each dissected specimen across the horizontal planes are also within a small range, with the coefficient of variation (CV) of 1.0% or less.

Kaolin, Dw=0.25Hm
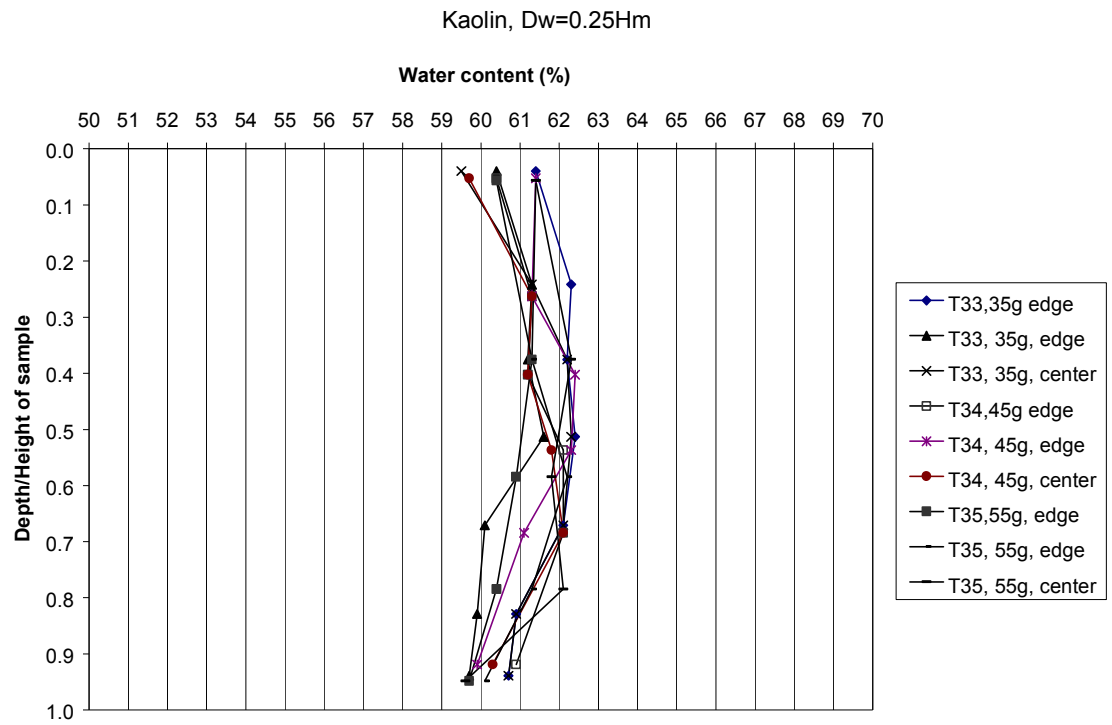
Figure 4. 13 Water content profile after self-weight consolidation

Kaolin, Dw=0.25 Hm

Water Content (%)

Ft.Edwards, Dw=0.25 Hm
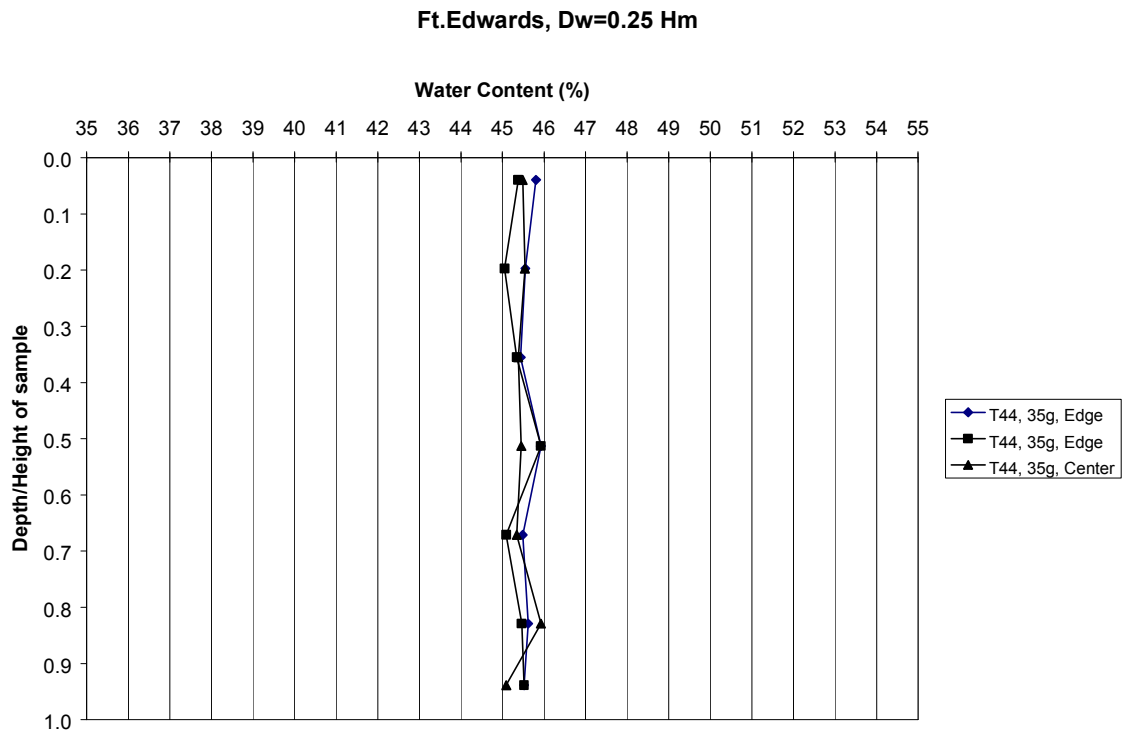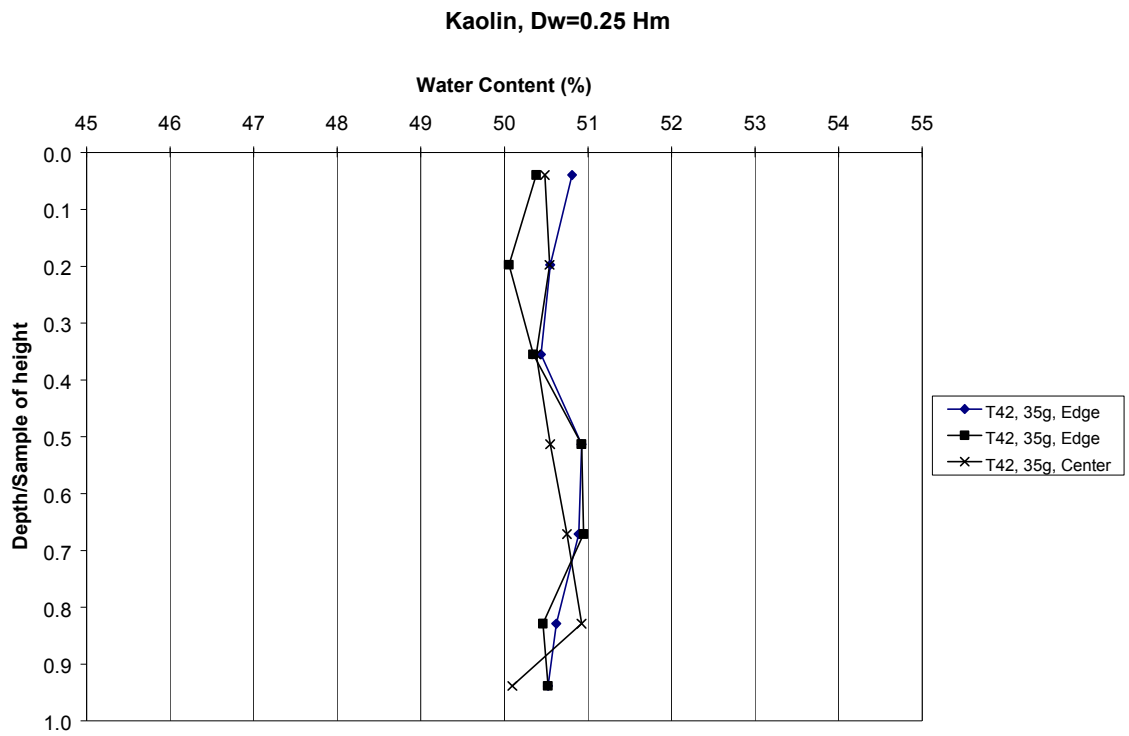
Water Content (%)

Figure 4. 14 Water content profile after self-weight consolidation

CHAPTER 5: RESULTS AND DISCUSSION

5.1 GENERAL DESCRIPTION OF THE EXPERIMENTAL PROGRAM

The experimental program involved twenty-three model tests, including: three 1g freezing tests, and twenty geotechnical centrifuge freezing tests. All the specimens underwent 1g and self-weight centrifuge consolidations. After self-weight centrifuge consolidation, the radial and vertical water contents of the specimens were examined, and those results are presented in Section 4.4.3. Specimens were then frozen under different conditions. These results were the basis both for understanding the mechanics of the freezing response of clay, and for development in Chapter 6 of a simple model that characterizes heaving response, with the intention of providing engineers with a tool they can utilize easily with a reasonable accuracy for design. Experimental results and discussions are presented in following sections.

Three 1g freezing tests were used as reference data to examine the influence of self-weight effects on the development of frost heave; these test results are discussed in Section 5.3, comparing those results to soil response in otherwise similar centrifuge models. The remaining soil freezing tests were conducted on the centrifuge to identify through experimentation the whole system response of clay when frozen under conditions that may occur naturally. The comparison of soil response to different freezing regimes -- step freezing and ramp freezing-- is provided in Section 5.4. The role in freezing response of the availability of water was investigated and is discussed in Section 5.5. And finally, modeling of models evidence to examine the validity of the method of centrifuge modeling and its associated scaling laws, as well as issues of

model repeatability are discussed in Sections 5.6 and 5.7. Table 5.1 shows the summary of all tests conducted for this research.

Table 5. 1 Summary of Tests

Target	Soil	Ng	Test No	Freezing Scheme	Freezing Model	H_m cm	w_i %
Effect of gravitational acceleration	[1]K	1	T11	1	Ramp	11.4	61
		35	T13	1	Ramp	11.4	61
		1	T39	1	Ramp	8.9	61
		45	T37	1	Ramp	8.9	61
	[1]E	1	T54	1	Ramp	11.4	45
		35	T38	1	Ramp	11.4	45
Freezing mode effects	K	35	T22	1	Step	11.4	61
		45	T27	1	Step	8.9	61
GWT effects†	K	35	T41	1	Ramp	11.4	61
Model Repeatability	K	35	T14	1	Ramp	11.4	61
		35	T31	1	Ramp	11.4	61
		45	T17	1	Ramp	8.9	61
		55	T52	2	Ramp	7.3	61
Modeling of model: One-step ramp	K	35	(T13)	1	Ramp	11.4	61
		45	(T37)	1	Ramp	8.9	61
		55	T55	1	Ramp	7.3	61
	E	35	(T38)	1	Ramp	11.4	45
		45	T43	1	Ramp	8.9	45
		55	T48	1	Ramp	7.3	45
Modeling of model: Two-step ramp Longer freezing Milder freezing rate	K	35	T47	2	Ramp	11.4	50
		45	T46	2	Ramp	8.9	50
		55	T45	2	Ramp	7.3	50
	E	35	T51	2	Ramp	11.4	45
		45	T50	2	Ramp	8.9	45
		55	T49	2	Ramp	7.3	45

Note: 1 = K stands for Kaolin, and E stands for Ft.Edwards clay

w_i = Average water content before freezing

† := Water table for T41 was set to be $D_w = 0.75H_m$, all other models were set to be $D_w = 0.25H_m$.

5.2 SELF-WEIGHT CONSOLIDATION AT Ng

All models tested on the centrifuge required a period of further consolidation on the centrifuge after the completion of the 1g consolidation sequence in order to make the under-consolidated bottom half of the specimens normally consolidated before cooling was initiated (refer to Section 4.4.1). This final consolidation on the centrifuge lasted for 5 to 6 hours. The self-weight consolidation data of the nine models are shown in Figure 5.1. This includes: three kaolin specimens prepared from slurry with initial water content 90% for the 35g, 45g, and 55g models and three Ft.Edwards specimens prepared from slurry with initial water content 60% for the 35g, 45g, and 55g models; and another three kaolin specimens prepared from slurry with initial water content 70% for the 35g, 45g, and 55g models. All models were tested with high water tables, $D_w = 0.25H_m$, where D_w is depth of the phreatic surface in the soil columns measuring from the soil surface, and H_m is the height of model. The final heights of the soil columns were: 11.4 cm high tested at 35g; 8.9 cm high tested at 45g; and 7.3 cm high tested at 55g. All model soil columns simulated columns of soil with final height equal to 4 m high, but since they are of different scales, their data are all shown in prototype equivalent times and prototype equivalent settlements for more direct comparison of their behavior. The conventional scaling relationships for time ($t_p = N^2 \times t_m$, where t_p = prototype time; t_m = model time; and N = centrifugal acceleration expressed in multiple of earth's gravity), and settlement ($l_p = N \times l_m$, where l = settlement) were applied in these plots to make comparison possible between the consolidation settlements of the different soil columns. This self-weight centrifuge consolidation sequence caused both sets of kaolin specimens to

69

achieve more than 90% of full consolidation, and the Ft.Edwards clay specimens to achieve more than 85% of full consolidation based on plots of time vs. surface displacement. After centrifuge consolidation, some specimens were dissected to evaluate post-consolidation water contents throughout column depth, checking also the radial uniformity of water content on the horizontal plane (discussed also in section 4.4.3). The plot also indicates that Ft.Edwards clay specimens ($w_i = 60\%$) developed larger settlement than kaolin specimens ($w_i = 70\%$, and $w_i = 90\%$), which is in agreement with expectations based on the odeometer test results reported in section 4.3. Those tests showed Ft.Edwards clay to have a compression index (C_c) almost twice that of kaolin.

Additional tests were conducted to assess settlement associated with close to 100% consolidation. Two kaolin specimens ($w_i = 70\%$, and $w_i = 90\%$), and one Ft.Edwards specimen ($w_i = 60\%$) were consolidated for further 6 to 7 hours on the centrifuge, over and above the 4 days of 1g consolidation and 5 to 6 hours of centrifuge consolidation already completed. The magnitudes of additional settlement at model scale from this subsequent self-weight consolidation were 0.034 cm for kaolin ($w_i = 90\%$), 0.026 cm for kaolin ($w_i = 70\%$), and 0.044 cm for Ft.Edwards clay ($w_i = 50\%$), which are all very small, as expected. These values are less than 13% of the smallest measured ultimate heave for kaolin and equal to a maximum of 14% of the previous consolidation settlement in kaolin for models prepared with either initial water content; and 22% of the smallest measured ultimate heave for Ft Edwards clay and 13% of its previous consolidation settlement.

Because full, 100% consolidation, strictly speaking, was unachievable in the models, even after 6 to 7 hours of additional consolidation, and this further consolidation on the centrifuge lengthened an already long pre-cooling consolidation sequence, this final centrifuge consolidation phase was not applied to the freezing test specimens. So, all model freezing tests on the centrifuge were performed after the first self-weight centrifuge consolidation sequence that led to 85% or greater consolidation. In reporting frost heave in centrifuge models, the decision was made to add back to measurements of frost heave expansion the anticipated self-weight settlement occurring during freezing period. There was no further self-weight settlement in 1g models, and, accordingly, no correction was made to the magnitude of heave in those models.
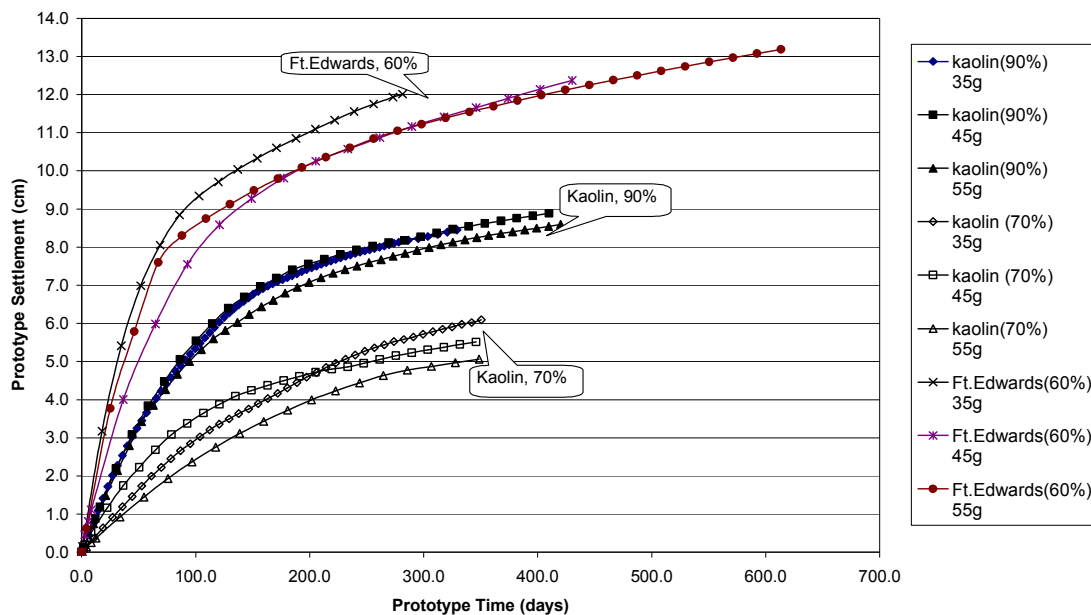
Figure 5. 1 Self-weight consolidation at Ng

71

5.3 SELF-WEIGHT EFFECT ON FREEZING BEHAVIOR

Three pairs of models tests were conducted to identify self-weight effects on the development of frost heave in small soil columns cooled at 1g compared to identical soil columns frozen at greater than 1g. These included two pairs of kaolin specimens: one frozen at 1g and the other frozen at 35g with w = 61% after consolidation; and one frozen at 1g, and the other frozen at 45g, again with w = 61% after consolidation. Two Ft.Edwards clay specimens were also examined: one frozen at 1g and the other frozen at 35g, with w = 45% after consolidation. The phreatic surface in all models was held constant at $D_w = 0.25H_m$, where D_w is the depth of the phreatic surface in soil columns, and H_m is the height of the model columns. All models were frozen under temperature scheme 1 (see section 4.1), under which all Ng models were frozen over a period simulating 180 days in prototype scale time, t_p (= t_m x N^2): all 1g models were frozen for the same duration. This meant that the first and third pairs of models (scale 1:35) were frozen for 3.52 hours, and the second pair of models (scale 1:45) was frozen for 2.13 hours. Values of ultimate heave and model heave rate are made only within a pair.

As mentioned in the previous section, testing at 1g and Ng also put the models in different pre-consolidation states: all 1g specimens were over-consolidated throughout their full heights, whereas the Ng specimens were over-consolidated in their upper halves and normally consolidated in their lower halves. Test results of these tests are summarized in Table 5.2.

Table 5. 2 Ng heave compared to 1g heave

Soil	Test No	Ng	Ultimate model heave cm	Model frozen depth cm	Maximum model heave rate cm/hr	[1]DOF	Heave/ DOF
Kaolin	T11	1	0.42	2.0	0.50	1.58	0.27
	T13	35	0.29	1.5	0.20	1.21	0.24
	T39	1	0.33	1.5	0.40	1.18	0.27
	T37	45	0.26	1.3	0.26	1.06	0.23
Ft.Edwards	T54	1	0.24	1.6	0.25	1.37	0.17
	T38	35	0.19	1.4	0.19	1.21	0.16

Note: 1. DOF stands for depth of freezing (frozen depth minus heave)

5.3.1 HEAVE DEVELOPMENT AT 1g AND Ng
5.3.1.1 KAOLIN CLAY

Exploring first the effects of increased self-weight on the magnitudes of ultimate heave within kaolin models, Figure 5.2 and Figure 5.3 show heave developing in models of kaolin with high water table. The time axis is for real model time, and heave measurements are also shown in model scale dimensions. In Figure 5.2 and Figure 5.3, the internal temperature profiles are shown for the 35g kaolin model (T13) and the 45g kaolin model (T37), although the 1g kaolin models (T11, and T39) had similar temperature profiles. Note in these figures that even though temperature in the models reached equilibrium, heave did not reach equilibrium in any model. This is a result of the ongoing flow of water to the freezing zone and subsequent freezing. Heave will ultimately reach equilibrium for constant boundary conditions, and heaving will cease but that point had not been reached by the end of these tests, which, applying $t_p = t_m$ x N^2 had simulated 180 days of cooling and freezing. This decision to terminate tests before the cessation of heave is repeated in the work of other leading researchers: see, for example, the laboratory results of

Konrad and Morgenstern (1980). It is also a situation that occurs naturally in the field.

A first observation is that these magnitudes of frost heaves developed are not insignificant when depths of freezing and model column heights are considered. This is contrary to the typical expectation in the field that heave in clay should be negligible because its low permeability is expected to choke off essential delivery of water to the freezing front. Two aspects of these specimens account for this difference. First, Konrad and Seto (1994) noted that soil that has never been frozen before or has been reconstituted or remolded will behave differently from soil in situ that has undergone many cycles of freezing and thawing, because repeated freezing changes the microstructure of clay to make it more heave resistant and to give it higher permeability. The soil in these tests had not been frozen before and was remolded – this would be the case in situ for soil newly exposed by a slope failure, an excavation, or a newly constructed embankment. And second, unlike clay deposits typical in the field, these soil specimens were saturated to the soil surface, and pre-freezing water content in the clay – 61% for kaolin-- was high. Consistent with this, very substantial heave was measured by Konrad and Seto (1994) in remolded Champlain Sea Clay with initial water content of 85%.

A second observation is that the onset of surface heave in all the kaolin models, including both the 1g and the centrifuge models, was first recorded when the temperature of the soil surface reached –0.5°C. However, rate of heave, and therefore magnitude of ultimate heave for pairs of models cooled for identical periods at 1g and in the centrifuge, were both far greater in the 1g columns than in the corresponding

74

centrifuge columns. This can be explained by the fact that in centrifuge models, the significant overburden pressure developed by the increase in self-weight will oppose heave, but the effect appears to be more complex.

An end result of increased rate of heave in the 1g models was that the magnitude of heave in those models exceeded heave in the Ng models at all corresponding times including the ultimate magnitude. The ultimate magnitudes of heave (relative to the elevation of the initial, pre-cooling soil surface) were 0.42 cm (1g) vs. 0.29 cm (35g) in the first pair of kaolin models, or 45% greater in the 1g model; and 0.33 cm (1g) vs. 0.26 cm (45g) in the second kaolin pair or 27% greater in the 1g model. However, while the increase in self-weight of the water in a centrifuge tested model column is expected to reduce both the rate of flow of water to the freezing zone, and the depth of soil below the freezing front from which water can be drawn to the freezing zone, water contents in the 1g models in the frozen zone were less than those in the frozen zone in centrifuge models with less heave.

As noted below, there was a difference in the depths of freezing between centrifuge and 1g models, however this may also be explained in part by the findings of Nixon (1991). He found in his 1g freezing tests on silty clay in which he changed surcharge alone, that the effect on heave of an increase in surcharge was "dramatic". Among other observations, he confirmed that the rate of heave decreased with increased surcharge, but he also reported that freezing saturated soil under a surcharge decreased the temperature of freezing. The latter effect means that water will cease flowing to a freezing zone with lower surcharge or at a shallower depth, before it ceases flowing to a freezing zone with greater surcharge. This will have the

effect that ice lenses and water contents can be less at shallower depths/lower surcharges, which supports the observation that ice lenses are greater at greater depths at full scale.

Since heave at 1g was greater than heave in the centrifuge models, but water contents were measured to be less, the degree of saturation in the frozen zones of 1g models, adding frozen and unfrozen water together, may fall below 100%. Degree of saturation, which could not be measured with sufficient accuracy in these tests, is likely, at a minimum, to be less at 1g than in the centrifuge models, with greater overburden stresses. Shoop and Bigl (1997) hypothesized that although heave has typically been assumed to occur only in the absence of air voids, the degree of saturation appeared to fall below 100% in their full scale freezing tests. Correct overburden gradient, then, is clearly a significant factor in the details of development of heave.

A third observation is that depths of freezing (DOF) (= thickness of frozen soil minus heave) differed in the 1g models from their corresponding centrifuge models: in the first kaolin pair (scale 1:35), DOF was 1.58 cm at 1g vs. 1.21 cm at 35g or 30% greater in the 1g model, and in the second kaolin pair (scale 1:45), DOF was 1.18 cm at 1g vs. 1.06 cm at 45g, or 11% greater. This occurrence also is supported by Nixon's (1991) experience. When increased surcharge decreases the temperature at which ice lenses form, the freezing front in the centrifuge models will not penetrate as deeply into the soil as in a 1g model, even if internal temperature profiles were identical. An effect of this freezing point depression will also be that water can continue to flow toward and through freezing soil at lower temperatures.

Yang (1996)'s experiments on columns of silt also indicated that 1g models developed greater depth of freezing than Ng models.

A fourth, rather unexpected, observation regards the ratios of (heave/DOF). For the first kaolin pair (heave/DOF) was 0.27 at 1g vs. 0.24 at 35g, and for the second pair (heave/DOF) was 0.27 at 1g vs. 0.23 at 45g. Therefore, while there was some pattern of an effect associated with self-weight effects, the differences in these ratios were smaller than expected -- < 20% -- given the marked differences in magnitudes of heave recorded. Yang (1996) found similarly small differences; calculations of these ratios from her results showed that heave/DOF was 0.028 at 1g, and 0.020 at 30g. Therefore, while both heave and DOF were markedly greater in the 1g models, which points to self-weight effects on heave related to soil overburden stress, these effects seem to be more or less self-balancing when the ratio (heave/DOF) is calculated for a soil with a given water content and low permeability.
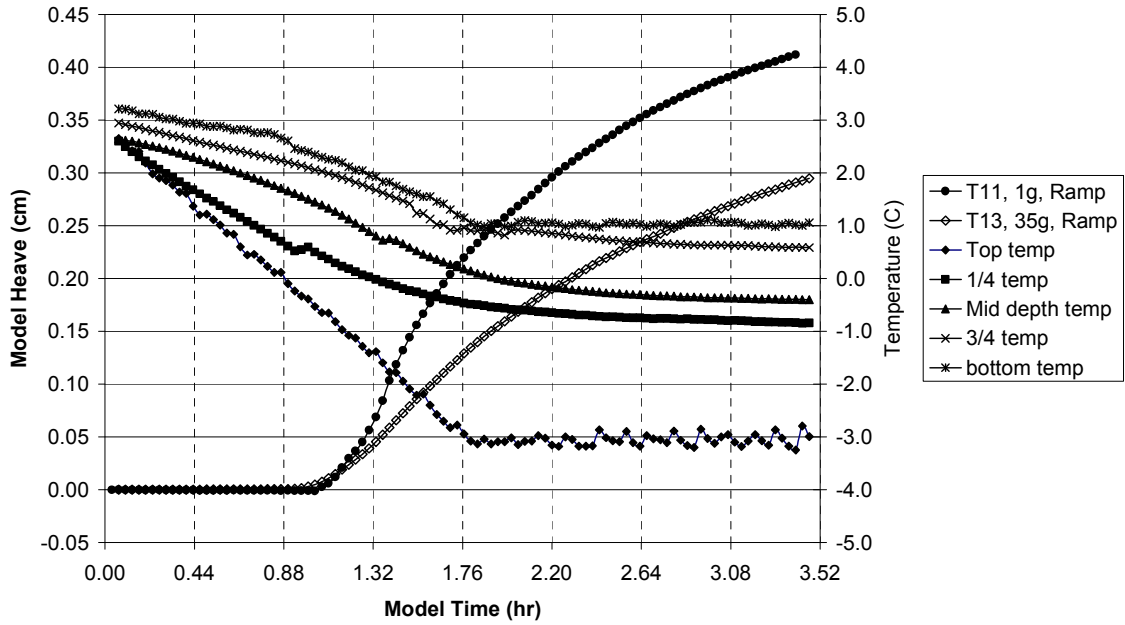
Figure 5. 2 Freezing Response of kaolin at 1g and 35g (displacements are unscaled)
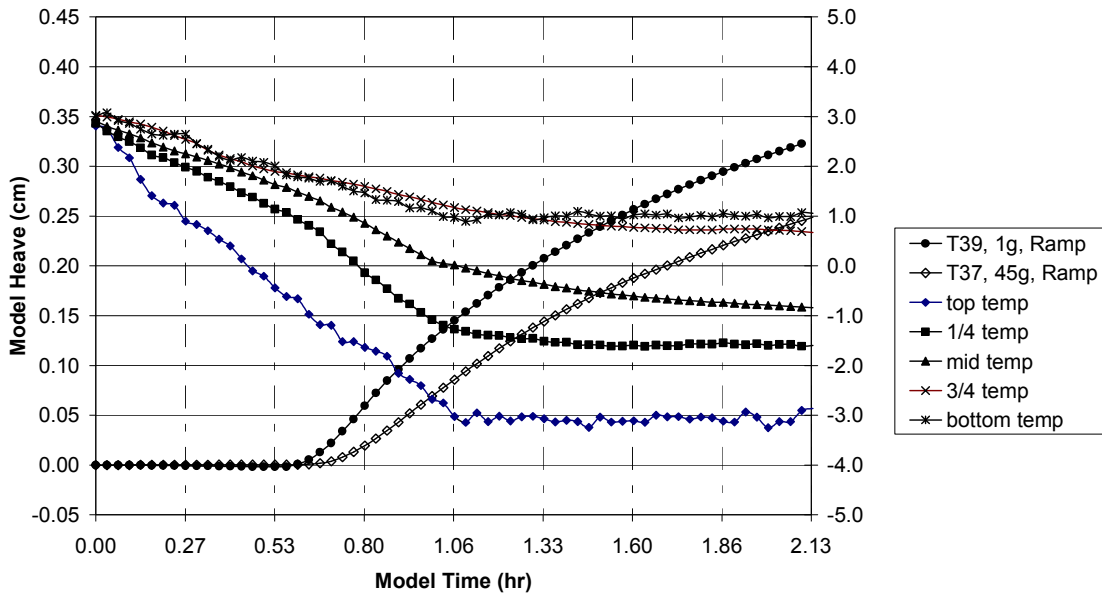
Figure 5. 3 Freezing Response of kaolin at 1g and 45g (displacements are unscaled)

Frost heave rates are replotted as heave rate curves in Figures 5.4, and 5.5. In Figure 5.4, the 1g and the 35g kaolin specimens responded to cooling with steadily increasing frost heave rate, and reached the maximum frost heave rate at the same time, which is t = 1.32 hrs (model scale). This was before the coldest surface temperature was achieved: at this time, soil surface temperature reached –1.5°C. The maximum frost heave rate for the 1g model was 0.50 cm/hr, which is 2.6 times larger than 0.20 cm/hr (full scale[1] = 0.14 cm/ day) of the 35g model. Nixon (1991) noted that thickness of the frozen fringe increases when surcharge is increased. Such an increase is accompanied by a reduction in suction gradient drawing the water to the freezing zone (Konrad and Morgenstern, 1980). After the peak, the rate for both specimens decreased to roughly the same rate of 0.05 cm/hr, which indicates continuing, if decreasing, heave at a much reduced rate due to ongoing freezing of pore water. Fig. 5.5 shows a similar pattern of the frost heave rate during freezing for the 1g and the 45g pair of kaolin columns. Again, both specimens reached the maximum frost heave rate at the same time, which is t = 0.80 hrs (model scale). At this time, the same boundary temperature for the soil surface existed in these models as in the case of the 1g and 35g model pair. The maximum frost heave rates of the 1g model and the 45g model were 0.40 cm/hr, and 0.26 cm/hr (full scale = 0.14 cm/day), respectively. After the peak, the rate for both specimens converged to roughly the same rate of 0.10 cm/hr, but they may not have reached an asymptotic value, yet, as was the case for the 1g:35g pair.

---

[1] 0.20 cm/hr at 1:35 model scale at 35 g = (0.20 x 35/35^2) x 24 hours/day = 0.14cm/day.
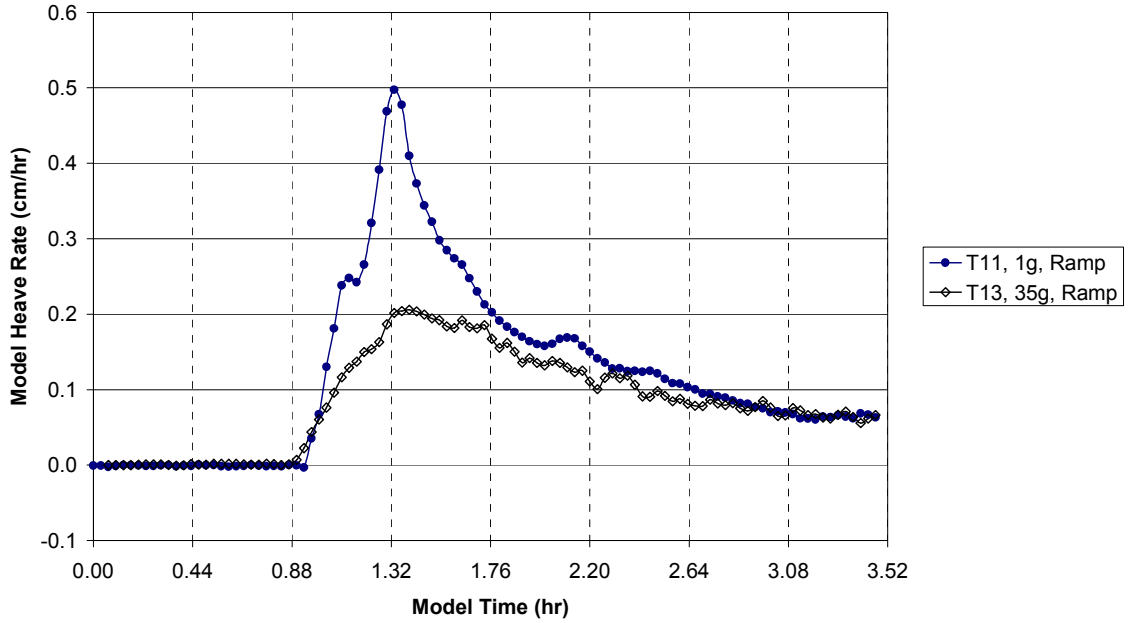
Figure 5. 4 Frost heave rate curve of kaolin at 1g and 35g
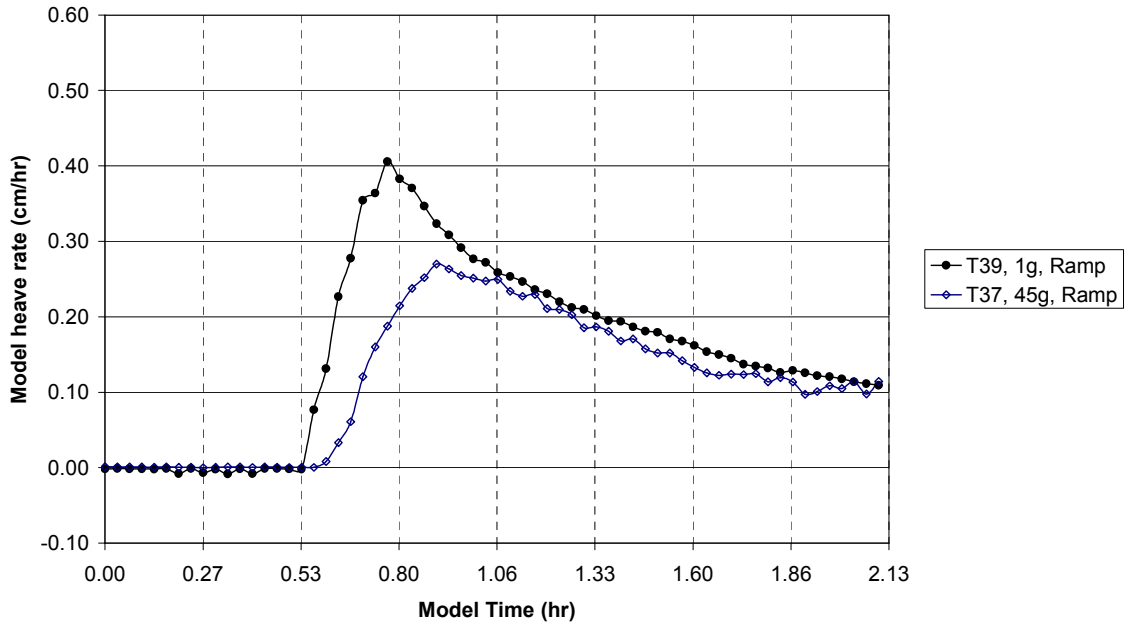
Figure 5. 5 Frost heave rate curve of kaolin at 1g and 45g

5.3.1.2 FT. EDWARDS CLAY

The self-weight effect on heave development was also investigated using Ft.Edwards clay which has different engineering properties compared to kaolin: permeability is less than kaolin by a factor of 4; Atterberg limits (liquid and plastic limits) are both less than those of kaolin, as well as plasticity index; and maximum dry density was greater than that of kaolin. Initial, prefreezing water content was also markedly less, at 45%. The freezing response of this pair of models is shown in Figure 5.6.

The ultimate heave of the models was not insignificant, but was less than that recorded in the corresponding kaolin models. Ultimate heave in the 1g model was 0.24 cm, which is, again, greater than the ultimate heave of 0.19 cm in the 35g model, this time by 26%. Initiation of detectable net heave began, as in the kaolin models, when the surface temperature reached – 0.5°C, and while heave continued developing after internal temperature equilibrium had been reached, it did not last long after, and heave was almost complete by the end of these tests, even in the 1g model. This characteristic is consistent with lower permeability.

The depth of freezing for the 1g model was 1.37 cm, which, again, is greater than 1.21 cm for the 35g model by 20%. The ratios of heave/DOF for both models are 0.17 and 0.16, respectively, which differ little from each other. In this clay, then, trends in behavior noted in the kaolin models tested at 1g and in the 35g model were repeated, although absolute values were not the same (refer to Table 5.2). The patterns of rates of heave and magnitudes of heave are consistent with the lower permeability and the lower water content of this Ft. Edwards clay compared to those

of the kaolin models. Although water content of the Ft.Edwards Clay is less than the kaolin, which leads one to expect that depth of freezing should be greater, the maximum depth of ice lens formation is less in Ft.Edwards Clay. This is attributed to the lower permeability of the Ft.Edwards clay, which limits formation of ice lenses and makes them thinner.

The frost heave rates of these models during freezing were shown in Figure 5.7. It shows a pattern again similar to that in kaolin with a few differences. The ratio of the maximum heave rate at 1g (= 0.25 cm/hr) is 1.3 times greater than the maximum heave rate at Ng (= 0.19 cm/hr). This is a smaller ratio than noted in kaolin, however, these maximum occurred at close to t =1.32 hours, as they had in the kaolin models subjected to the same freezing regime. Heave rates for both specimens reached near zero by the end of the test. Again, these differences in behavior are attributed to the smaller initial water content and lower permeability of the Ft.Edwards clay.
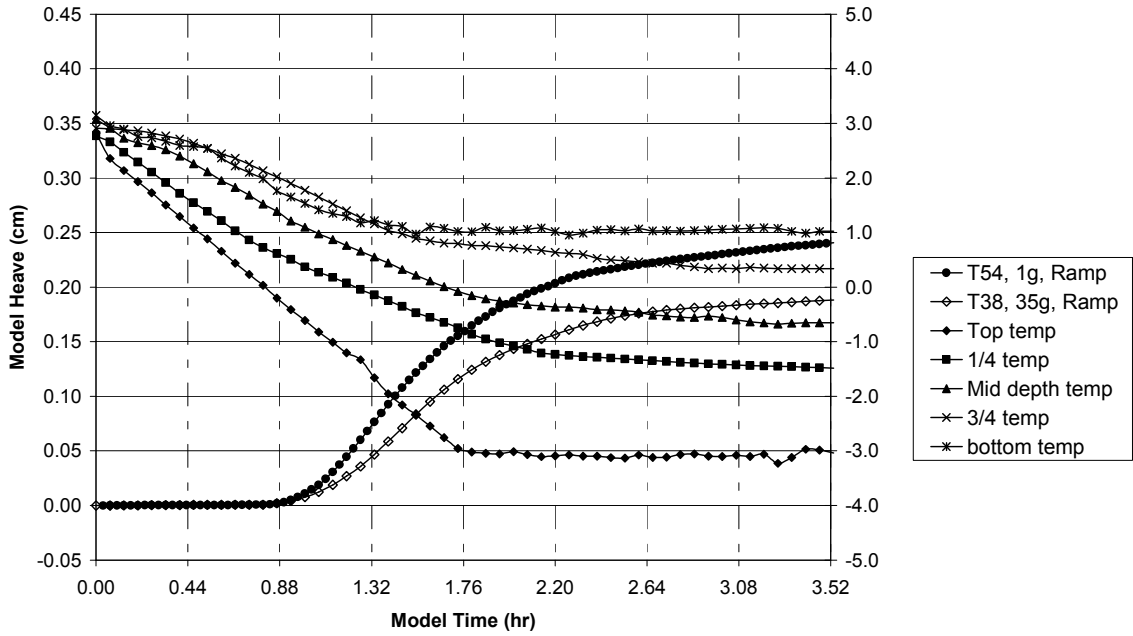
Figure 5. 6 Freezing Response of Ft. Edwards clay at 1g and 35g (displacements are unscaled)
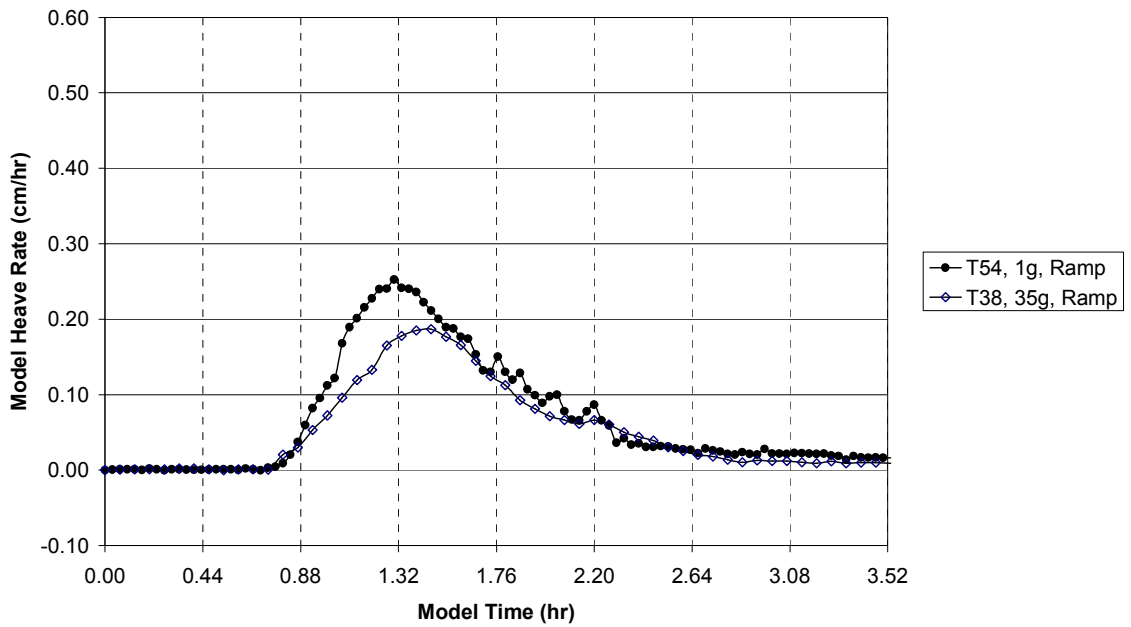
Figure 5. 7 Frost heave rate curve of Ft.Edwards at 1g and 35g

83

5.3.2 WATER CONTENT EFFECTS AND PROFILES AT 1g AND AT Ng

As mentioned previously, water contents of these soils were important to freezing behavior. The initially high water contents, in particular, played a critical role in the freezing response in two respects. On the one hand, the high water content slowed the penetration of the freezing front into the clay, so that the depth of freezing measured here was shallow compared to the depths Yang and Goodings (1998) reported in their columns of saturated (w_i = 22% to 24%) silt subjected to similar freezing conditions. Depths of freezing in their silt models of similar dimensions and subjected to similar freezing regimes was 58mm, or 290% larger than in these clay columns. The heat capacity of water is about 2 times larger than that of clay, and the thermal conductivity of water is about one fifth of dry clay. These two factors combine to make clay with high water content cool much more slowly than soils with lower water content. But, on the other hand, even in this shallow depth of freezing, there was far more immediately local pore water in the clay available to freeze and expand. The net result was that notwithstanding the shallower depth of freezing, the ultimate magnitude of heave in this saturated clay was found to be at least two times greater than that of Yang and Goodings (1998) silt and clayey silt soil columns, and ratios of (heave/depth of freezing) were about one tenth in those silt models compared to these clay models.

Degree of saturation – 100% or close to 100% starting at the soil surface, even separate from the high water content -- also played a two part role in development of significant frost heave. First, heave developing near the soil surface in the presence of only minor overburden pressures will be proportionally larger than at greater

84

depth, where overburden opposes heave to a greater degree. And second, full saturation allows for more effective movement of water through the soil skeleton to the freezing front, unimpeded by air bubbles that block channels.

Water contents after freezing provide important information also on the freezing process. In Figures 5.8 to 5.10, water content profiles for the two pairs of kaolin models (1g:35g pair, and 1g:45g pair), and the one pair of Ft.Edwards clay models (1g:35g pair) are shown after freezing. The average water contents before freezing are also shown; these prefreezing water contents were measured by dissecting specimens after all consolidation phases were complete, but without freezing.
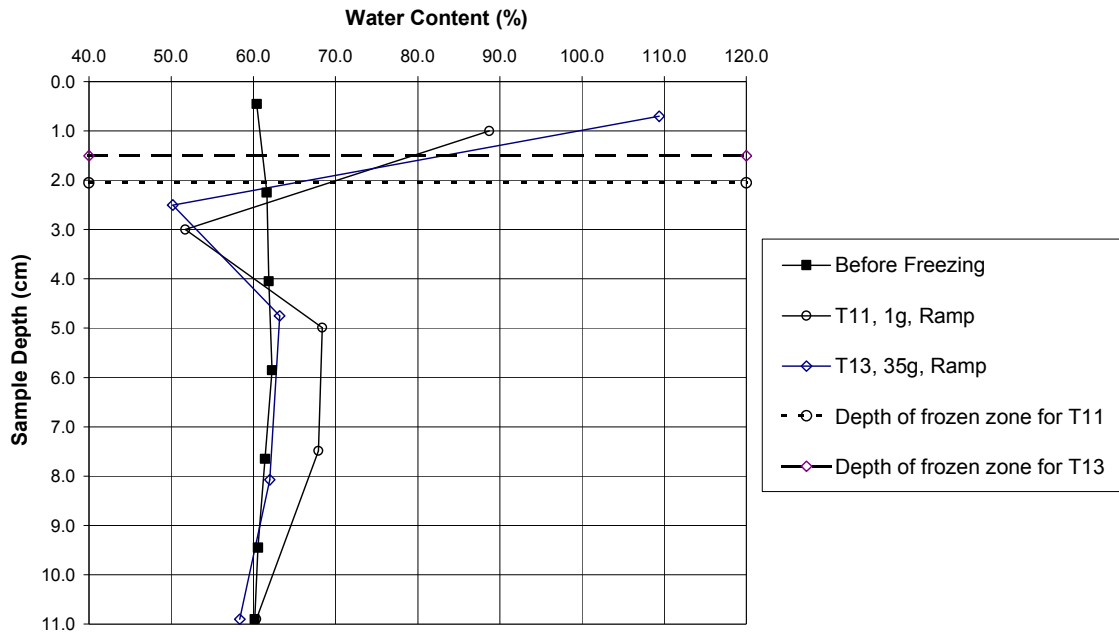
Figure 5. 8 Water content profile before and after freezing (1g:35g, kaolin)
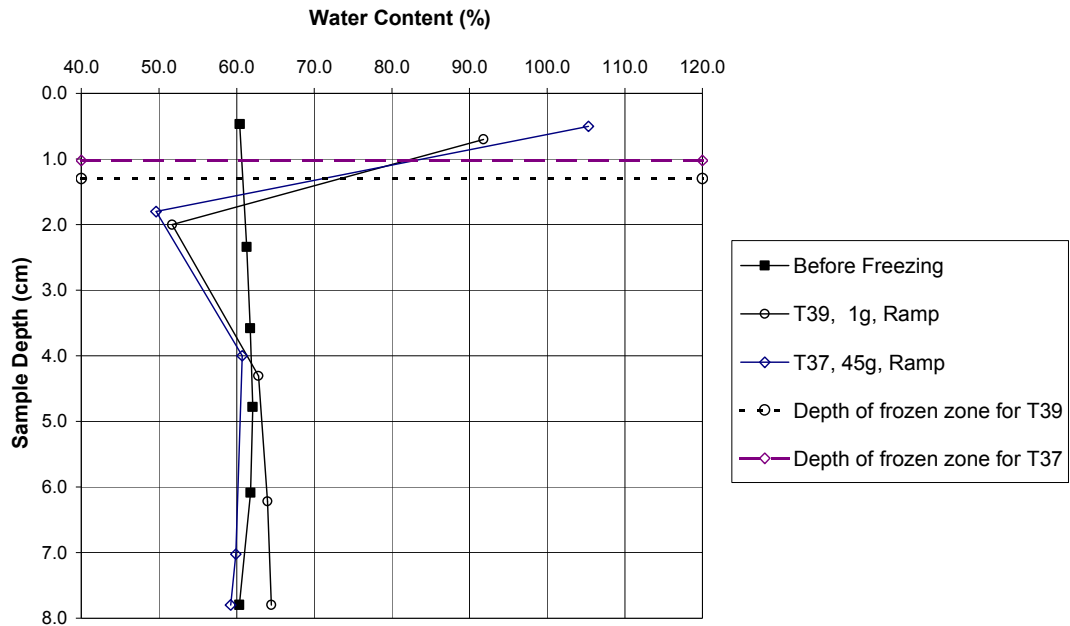
Figure 5. 9 Water content profile before and after freezing (1g:45g, kaolin)
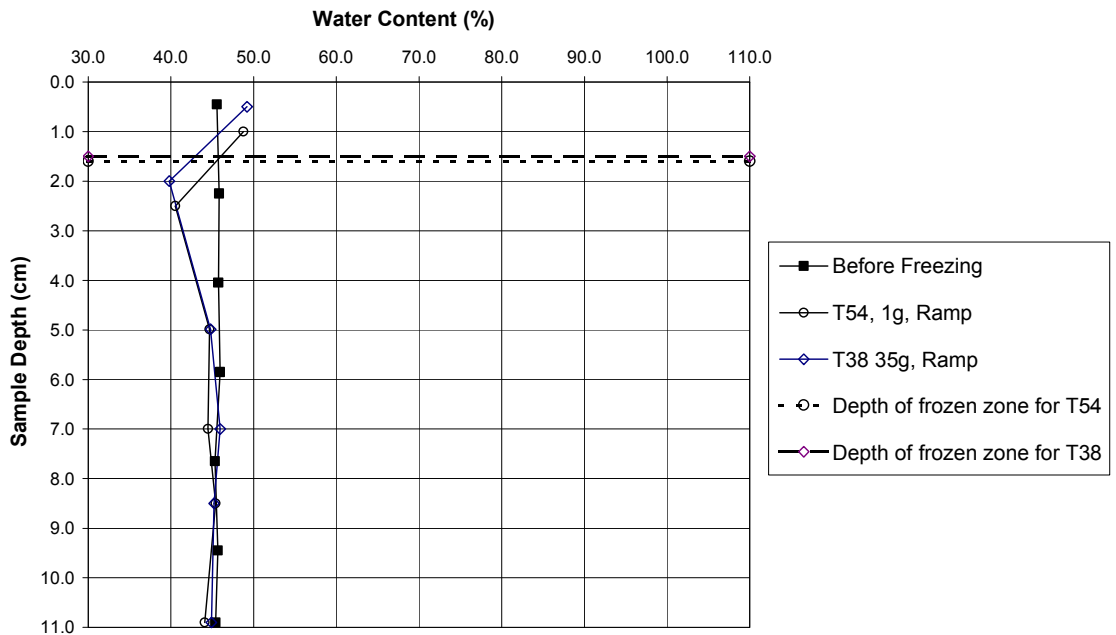
Figure 5. 10 Water content profile before and after freezing (1g:35g, Ft.Edwards)

Figure 5.8 and 5.9 show that water contents in kaolin specimens were largely unaffected by freezing in the soil columns at depths below 5 cm in models of 1g:35g pair, and below 4 cm in models of 1g:45g pair. At shallower depths, in contrast, water contents were strongly affected by freezing. Immediately below the depth of freezing, average water contents in the 1g models were 51% (1g:35g pair), and 52% (1g:45g pair), indicating a depression of 10%, and 9% compared to the pre-freezing condition of w = 61% at the end of consolidation. A similar trend was noted in the Ng models: the average water contents immediately below the depth of freezing were 49% (1g:35g pair), and 50% (1g:45g pair). This reduction in water content is symptomatic of the freezing/suction induced compression expected in compressible soil immediately below the freezing front in the frozen fringe. It is deeper in 1g models than in Ng models because DOF is greater in 1g models than in Ng models. Nixon (1991) concluded that thickness of the frozen fringe was greater when surcharge was greater, however in these small models, changes in water content are difficult to pinpoint accurately from conventional water content sampling.

Chamberlain (1981) observed in his 1g soil freezing columns of saturated clay that the minimum water content that could be achieved in the frozen fringe was equal to the plastic limit, although it makes sense that this would be influenced by both the freezing regime and the initial water content. Konrad and Seto (1994) worked with 10 cm high specimens of a back-pressured, remolded, saturated Champlain Sea clay – which is not mineralogically a clay – with an initial water content of 85%. They measured an abrupt reduction in water content in a 4cm frozen fringe in a step frozen model, to about 43%, a reduction of roughly 40%; and in their ramp frozen model, the

87

reduction was less abrupt, but somewhat less in value, reducing to 50%. These values were greater than the plastic limit for that clay, which they reported to be 21% on average. The permeability of that clay was about 4 times that of the kaolin, so that between that and the test back-pressured that ensured 100% saturation and access to ample water, greater redistribution of water in the specimens is to be expected. Although there was a marked reduction in water content in the tests in this research which simulated water and overburden conditions more likely to exist in situ, the layers of depressed water content here remained well above the plastic limit of 34% of kaolin.

The depression in water content in that layer, identified as the frozen fringe, is associated with suction induced consolidation that advances ahead of the development of ice lenses. That soil was noticeably stiffer, although it contained no visible ice lenses. As freezing penetrates into the soil, this layer also advances. Its thickness is not believed to be constant, but depends on the local thermal gradient (see Konrad and Morgenstern, 1980) and the overburden surcharge at that depth (Nixon, 1991). This consolidation response is expected to be pronounced in the freezing response of high water content, compressible clay that has not been frozen before or has not been subjected to preconsolidation pressures that exceed the freezing suction pressures (Konrad and Seto, 1994). In a soil column with an advancing cooling front, this frozen fringe layer travels immediately ahead of the penetrating freezing front. The freezing front may be contracting at the same time that the freezing soil – previously consolidated by suction effects -- is expanding with the formation of ice lenses. Net heave measured at the soil surface, then, will be the sum

of expansion associated with the formation of ice lenses in the depth of freezing (DOF) minus the suction induced consolidation traveling ahead of the DOF.

The suction pressures thus developed are expected to be substantial. Chamberlain (1981) indicated that the suction pressures developing in freezing clay often exceed 100 kN/m^2, although he could not measure values directly with his simple tensiometers. He reasoned, however, that because clay retains a memory of its maximum past effective stress, a suction force can be measured indirectly by performing a consolidation test on the portion of soil that have been through the freezing consolidation. By conducting consolidometer tests on specimens, he measured preconsolidation pressures due to freezing as large as 500 kN/m^2 or more. Konrad and Seto (1994) reported that Tavenas and Leroueil (1977) concluded that the isotropic consolidation brought about by freezing is roughly one half the preconsolidation pressure measured from a conventional one-dimensional oedometer test. Even with this correction, Chamberlain's suction pressures were large. Eigenbrod et al. (1996) developed special apparatus, and measured negative pore water pressures directly as negative as -22 kN/m^2 in small columns of remolded, saturated clayey silt, with and without surcharging, although they speculated that that value was probably an underestimate. Their tensiometers were not available for this research, so Chamberlain's approach using the consolidometer test results was adopted here.

Figure 5.11 shows two consolidometer test results plotted for samples retrieved using consolidometer rings from the 35g kaolin model after freezing on the centrifuge. One test was conducted on a sample retrieved from the bottom of the soil

column, 9 cm from the original soil surface, and well below the depth of influence of the freezing. The other sample was taken from a depth of 1.5 cm, in the depressed water content frozen fringe, immediately below the depth of freezing. They were both tested after thawing.

The semi-log slopes of the normal consolidation lines were measured to be roughly equal: in the deep, never frozen sample, C_c = 0.35, and in the specimen retrieved from the freezing fringe, C_c = 0.29. The results from the sample taken from the deeper, never frozen zone showed a preconsolidation pressure of 40 kN/m^2. This value is somewhat less than expected, because this zone is calculated to have experienced a normal vertical effective stress of 40 kN/m^2 to 60 kN/m^2 due to its consolidation history alone. If freezing had had no effect on consolidation, then the second, shallower sample would show a preconsolidation pressure less than 40 kN/m^2. The results from the sample taken from the shallower, freezing fringe shows, instead, a preconsolidation pressure of 95 kN/m^2. This is about 3 times the vertical effective stress it is calculated to have experienced during initial, non-freezing related consolidation at this depth or about 60 kN/m^2 greater. Even if the Tavenas and Leroueil correction from consolidometer readings of simple vertical preconsolidation pressure to isotropic freezing induced consolidation pressures is applied, it is clear that cooling induced consolidation occurred in this zone, as Chamberlain indicated.
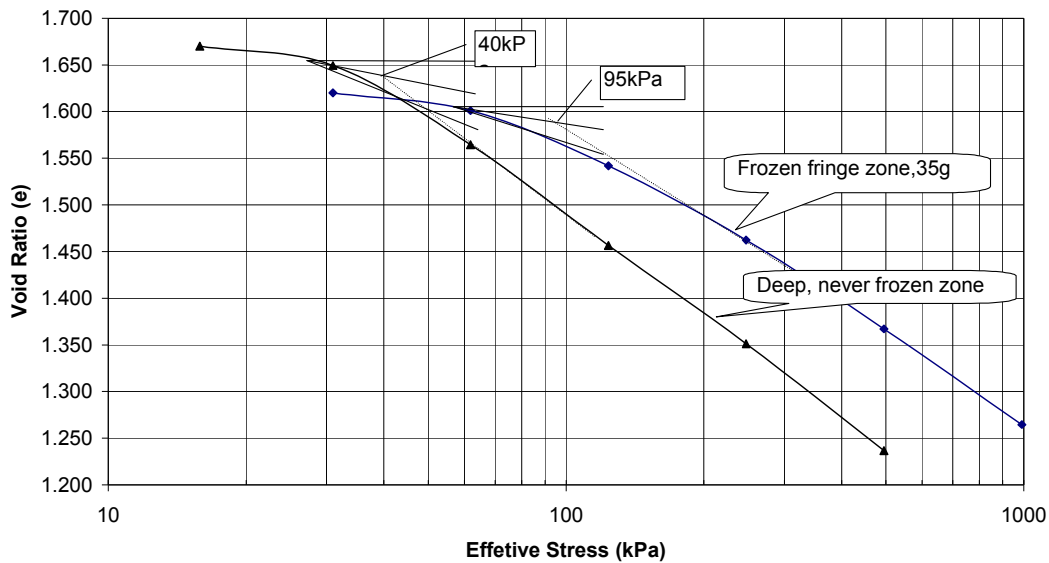
Figure 5. 11 Plot of log σ' vs. Void Ratio (e)

In the zone of frozen soil above that depressed zone, the average water contents (frozen + unfrozen water together) increased in all models by greater than 27%. Increases in total water content were somewhat less in the 1g models – 27% and 31% -- compared to 48% and 44% in the centrifuge models. At 1g, final water contents were 90% and 92%. In the centrifuge models: the average water contents were 110% and 105%. Turning again to Konrad and Seto's (1994) tests on small samples of Champlain Sea clay for general comparison, water contents in the frozen depths of their specimens increased from 90% to an average of 140%. In the pair of Ft.Edwards columns, plotted in Figure 5.10, behaviors are much more muted. Water

content before freezing averaged 45%. Immediately below the depth of freezing, average water content in the 1g model, and the 35g model were only slightly less, at 40% and 41%, respectively, indicating a small depression of 5% and 4%, respectively. The layers of depressed water content here, again, remained well above the plastic limit of 29% for Ft.Edwards clay. In the zone of frozen soil above that depressed zone, the average water content in the 1g model and the 35g model were 49%, and 48%, which increased modestly by only 4% and 3%, respectively. These smaller changes in water content are attributed to the combination of smaller permeability and smaller initial water content. Consolidation tests were not conducted in these specimens

5.3.3 ICE LENSES CHARACTERISTICS IN FROZEN CLAY

Ice lenses characteristics can be an additional lens through which to understand the freezing response of the soil. Needle ice may develop in soil at shallow depths in which freezing has occurred quickly, water has not migrated to the freezing zones, and overburden is small. This is commonly noted in unsaturated shallow depths. At greater depth, where freezing is slower and overburden is greater, thicker, more horizontally aligned lenses, more widely spaced, are typical. Nixon (1991) found that increasing surcharge alone was sufficient to cause this to occur. Yang and Goodings (1996) prepared thin sections from their centrifuge models of frozen columns of silt. They reported stratification of ice, beginning with needle ice at shallow depths, underlain by larger ice lenses at greater depth. Ice lenses were reported to tend to be

somewhat larger in their small 1g silt models than in otherwise identical centrifuge models.

In these kaolin models, the onset of cooling led to an initially steep local thermal gradient, which is expected to draw water quickly from the soil. Because the water content of the clay was large and saturation was 100% to the soil surface, there was sufficient pore water available to result in formation of a thin ice cake on the soil surface in all these kaolin models. The ice cake was 2 mm to 3 mm in thickness, varying across the now slightly irregular soil surface. The irregularity of the thickness and its small magnitude made it impossible to identify a reliable estimate of any differences in thickness between 1g and Ng models.

Below that ice cake, ice lenses were observed in the soil to a depth of 2.0 cm in the 1g model of the 1g:35g pair, and 1.5 cm in the 1g model of the 1g:45g pair. In the centrifuge models, depths of freezing were less, and ice lenses were observed to a depth of 1.5 cm in the 35g model of the 1g:35g pair in the 35g model, and to a depth of 1.3 cm in the 45g model of the 1g:45g pair. Lenses were horizontal and did not resemble needle ice. Ice lens thicknesses varied, but ranged up to 3 mm in the 1g models and up to 2 mm in the centrifuge models.

There were also distinct, vertical, ice filled cracks in both 1g and centrifuge models. The cracks are attributed to desiccation developing during the freezing process, and are reported by other researchers; see for example, Chamberlain (1981). Again, it was not possible to comment on possible effects of increased self weight on the sizes of either the horizontal ice lenses, or the vertical ice filled cracks, because of the variation in thicknesses. Certainly there were no clear cut differences apparent.

Below the deepest ice lenses, which was also considered to mark the maximum depth of freezing (DOF) in each model, a thin layer of markedly stiffer soil was clearly identifiable. The thickness of a frozen fringe itself is somewhat difficult to measure because the transition from the frozen fringe to the unfrozen layer is not clearly marked. These layers were directly associated with distinctly depressed water contents, discussed in Section 5.3.2. And while these layers are identified as the "frozen fringes" in each model, there was no observable evidence of ice lenses in these layers.

Ft.Edwards clay also developed an ice cake covering the soil surface at the end of the test, although it was very thin (≤1 mm). Below the ice cake, the thicknesses of individual ice lenses within the frozen layer were much smaller than in the kaolin models. Typically, ice lenses were horizontal and had thicknesses less than 1 mm. There were also vertical cracks developed in a pattern similar to that observed in kaolin clay. As for the kaolin column tests, there was a thin, stiff layer of soil below the deepest ice lens, identified as the frozen fringe, but in which no ice was observed. The thinner surface ice cake, and thinner ice lenses in Ft.Edwards clay are both attributed principally to a combination of its lower initial moisture content, and its lower permeability, which limited water migration from the water table. No patterns in thickness of lenses as a consequence of increased self-weight could be identified.

5.3.4 EFFECTS OF FREEZING UNDER FULL SCALE, IN SITU STRESS CONDTIONS

It is clear from these test results that the trends observed in these models, when examined by observation, are completely consistent with freezing behavior reported

by other researchers. However, these tests in which all self-weight effects in a model soil column are brought into similarity with full scale conditions, are capable of simulating the complete system of freezing response. In these columns, all interactions of self-weight and water flow freely developed through the soil column depth, in a way that researchers working with small elements of clayey soil either surcharged or not surcharged, back pressured or not back pressured, have not been able to achieve. In particular, when thermally generated suctions develop in the frozen fringe of a soil column, the ability of the soil to quench those suctions, and to pass or partially obstruct water to the freezing zone beyond that freezing fringe is key to soil heaving response. Self-weight overburden which increases with depth, in situ water content, permeability, accessibility to soil water, and local thermal conditions are essential parameters controlling soil freezing and heaving response. These are changing as the frost front penetrates the soil, and they are correctly simulated in the soil columns frozen on the centrifuge, but not in the experiments of other researchers.

The differences between 1g soil column freezing and centrifuged (Ng) soil column freezing for saturated, remolded clays include the following:

1. The temperatures that bring about the initiation of heave seem independent of the self-weight conditions of saturated columns of clay soil.

2. Rates of heave showed broadly similar patterns of development, independent of self-weight, however, magnitudes of those rates were distinctly greater in the 1g columns than in their corresponding Ng model columns when rates of heave were greatest. Magnitudes of ultimate heave were, as a result, much greater in 1g columns than in corresponding Ng tested models.

3. Depths of freezing were greater in 1g model columns than in corresponding Ng model columns.

4. The ratios of surface measured frost heave: depth of freezing was only slightly different similar in Ng and 1g model columns, being somewhat greater in 1g models.

   Water contents in the frozen zone, that is through the depth of freezing (DOF) where ice lenses are observable, were greater in Ng models than in corresponding 1g models. The fact that magnitude of heave at 1g was greater than in corresponding Ng models suggests degree of saturation falls below 100%, and is less than in Ng models. This is attributed to two effects. First, the decrease in freezing temperature that occurs at higher stress, permits water to continue to flow to the freezing zone longer and at cooler temperatures. Second, the fact that magnitude of heave at 1g was greater than in corresponding Ng models, even though water contents were similar or less, suggests degree of saturation falls below 100%, and is less in 1g models than in Ng models. When degree of saturation falls below 100%, water drawn up to the freezing zone through water channels, may be stopped by pockets of air. Thus higher saturation in the Ng models may permit more water migration.

5. Water contents measured at greater depths (after freezing) seem unaffected by self-weight, when consolidation histories before freezing are identical.

6. Ice lenses developed in all models, but were too small and too variable in size to identify differences between 1g and Ng models.

7. These effects were noted in both the kaolin models and the Ft Edwards clay models, and were more pronounced in the kaolin models in which permeability and water contents were larger.

5.4 TEMPERATURE REGIME EFFECTS

5.4.1 STEP FREEZING VS RAMP FREEZING

5.4.1.1 EFFECTS ON DEVELOPMENT OF FROST HEAVE

It is well established now that total heave and heave rate are sensitive to the freezing mode, because the balance between the rate of penetration of the freezing front into the soil, and the rate of delivery of water to that freezing front are essential to the development of heave. Several researchers, see, for example, Nixon (1991), and Konrad and Seto (1994) working with isolated, saturated 1g specimens, and Yang and Goodings (1998) working with centrifuge models of columns of silt, have confirmed that slower freezing leads to greater heave.

In this research, ramped freezing was adopted because it represents the temperature profile developing in the field from seasonal cooling more closely than step freezing, even though these tests were conducted much faster, following the relationship: $t_p = t_m/N^2$. Step-freezing, however, has been used by many researchers because temperature control is easier and rate effects were not initially understood. Step freezing tests are also often conducted at very cold temperatures -- $-10°C$ -- to speed the freezing process. This may simulate the construction stabilization technique of ground freezing, but it does not simulate gradual cooling more typical in nature.

To identify the difference in development of heave arising from the two freezing modes, two step freezing tests at 35g, and 45g were conducted, and compared to the results from two ramp freezing tests conducted at the same centrifuge accelerations. The prototype equivalent freezing degree-days of −337.5 degree-days, which is equal to that applied to ramp freezing tests, was also applied to the step freezing tests (refer to Table 4.1). The step freezing was applied by varying the upper boundary temperature from +3°C to −3°C abruptly and maintaining it at −3°C over 112.5 prototype days, or 2 hrs 12 min for the 35g model, and 1 hr 20 min for the 45g model on the centrifuge, in contrast to gradual cooling in the ramp freezing test. The ultimate boundary temperature gradient, however, was the same in all models. Since cooling was measured in this research by surface soil temperature, rather than by air temperature, sudden changes in air temperature are somewhat delayed by the time necessary to cool a soil to a given temperature. Thus temperature changes in step freezing are as abrupt as possible, but not instantaneous. The results of these four tests are tabulated in Table 5.3.

Table 5. 3 Results of Step vs. Ramp models

Soil	Test No	F.M	Ng	Ultimate model heave cm	Model frozen depth Cm	Maximum model heave rate cm/hr	DOF	Heave/ DOF
	T13	Ramp	35	0.29	1.5	0.20	1.21	0.24
Kaolin	T22	Step	35	0.10	1.5	0.20	1.40	0.08
	T37	Ramp	45	0.26	1.3	0.27	1.06	0.24
	T27	Step	45	0.09	1.3	0.25	1.21	0.08

Figures 5.12, and 5.13 show heave vs. time curves of step and ramp frozen models tested at 35g, and 45g. In Figure 5.12, the internal temperature profile of the step freezing test T22 is also shown. In both figures, the models subjected to step freezing show steep and early development of heave, but with heave quickly tapering off. The faster cooling of step freezing led to faster formation of ice, causing the permeability to decrease rapidly in the frozen fringe as the pores became clogged with ice. In contrast, the ramp frozen models showed steady increase of heave.

There were also differences in the depths of freezing. In the ramp frozen models, depths of freezing (DOF) were 1.21 cm for the 35g model (42 cm at full scale), and 1.06 cm for the 45g model (48 cm at full scale). Magnitudes of ultimate heave were 0.29 cm (10 cm full scale) for the 35g model, and 0.27 cm (12 cm full scale) for the 45g model; and for both ramp frozen models, heave/DOF = 0.24 for both models. In the step frozen model, magnitudes of ultimate heave were 0.10 cm (3.5 cm full scale) for the 35g model, and 0.09 cm (4.1 cm full scale) for the 45g model. The ratios of heave/DOF were somewhat less: 0.08 for the 35g model, and 0.12 for the 45g model, which were much less than the value of 0.24 for the ramp frozen. Slower cooling, then, leads to slower initial development of heave on the one hand, but allows more time for freezing and movement of water to the freezing front to occur, and slower decrease in permeability due to clogging of pores with ice, allowing more water to pass to the freezing front, even in soil with low permeability.

The data are replotted in Figure 5.14 in terms of freezing degree days vs. heave to account for differences in cooling rates. This plot shows an even stronger influence on heave when rate of cooling is slowed: the ramp-frozen model developed more

99

rapid initial heave than step-frozen model at all times in this plot. There is some speculation that rapid step freezing also leads to development of more cooling induced settlement, as larger temperature gradients are applied to the soil; this was unmeasurable in these tests.
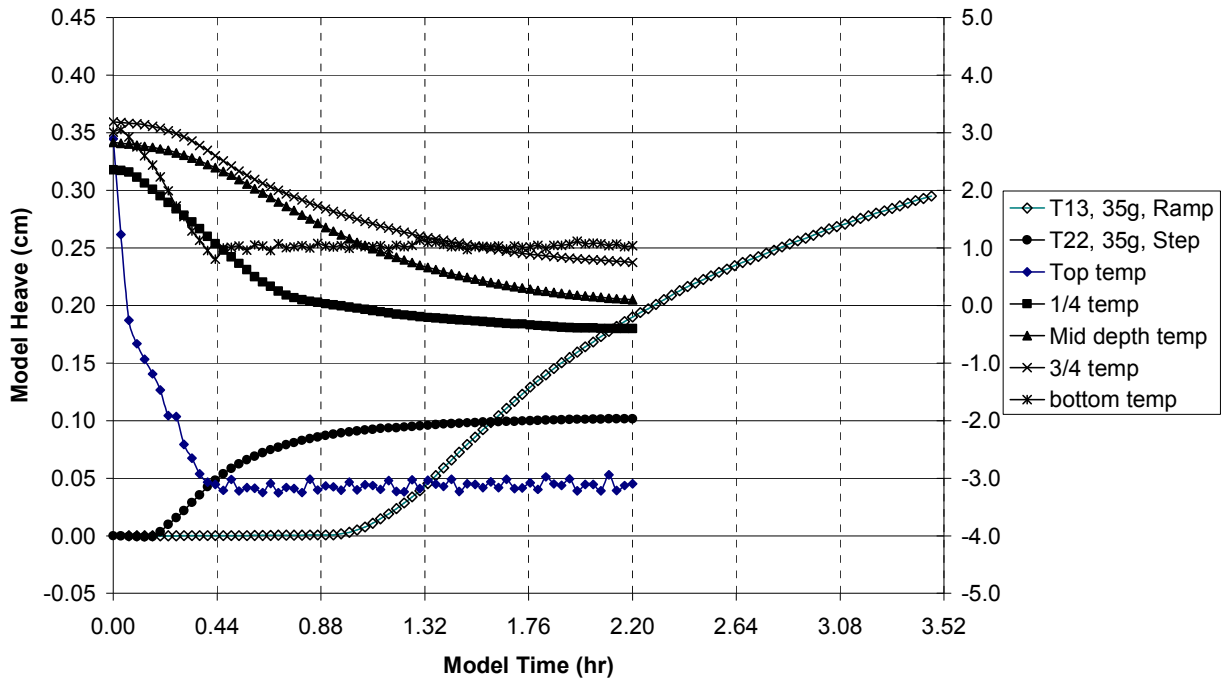
Figure 5. 12 Frost heave vs. Time for 35g Kaolin Columns (ramp vs step)
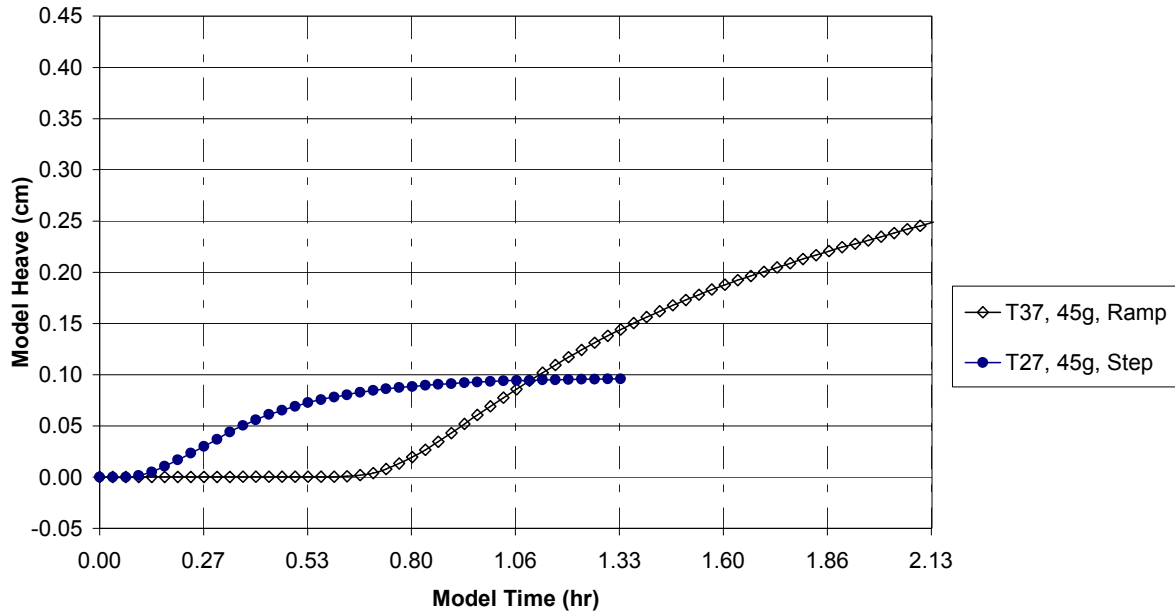
Figure 5. 13 Frost heave vs. Time for 45g Kaolin Columns (ramp vs step)
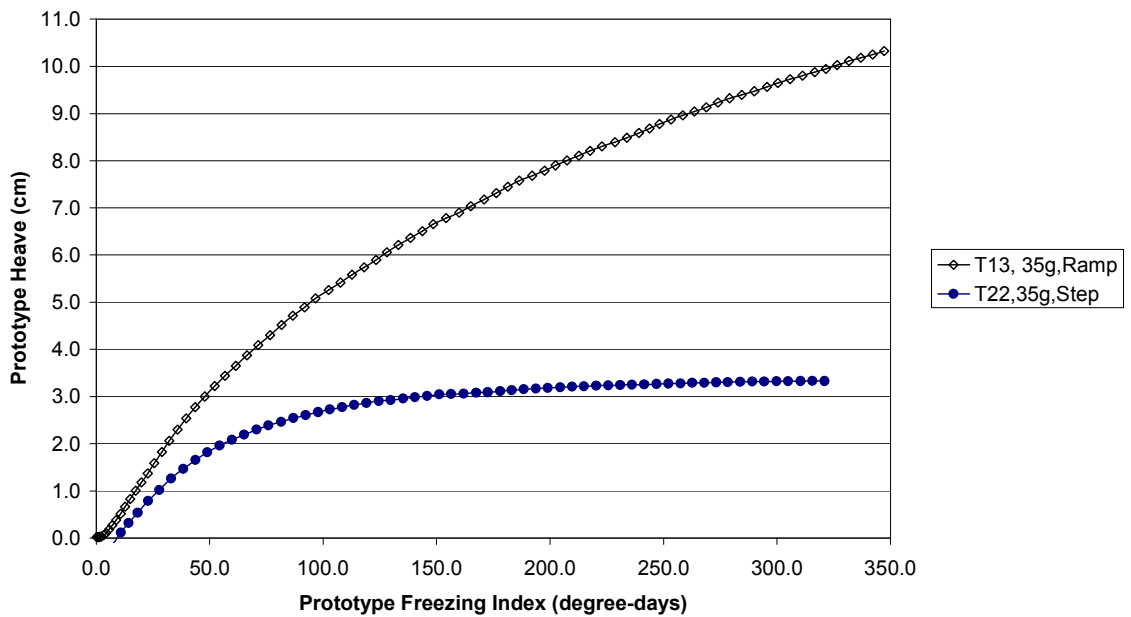
Figure 5. 14 Frost heave vs. Freezing Index for 35g Kaolin Columns (ramp vs step)

Figures 5.15 and 5.16 show another picture of the development of heave by examining the frost heave rate throughout the freezing period of ramp frozen and step frozen models at 35g, and 45g. In Figure 5.15, both models had approximately the same maximum frost heave rate of 0.20 cm/hr, but the step frozen model developed the maximum heave rate much earlier (t = 0.30 hrs) than the ramp frozen model (t = 1.32hrs) due to the faster cooling rate applied. In the step frozen models the maximum heave occurred before the coldest surface temperature was achieved. As for the ramp frozen models, this seemed to occur when the soil surface temperature reached − 1.5°C. After the maximum frost heave rate was reached, the frost heave rate of the step frozen model abruptly decreased, in contrast to both the more gradual rise and the more gradual decrease observed in the rate for the ramp frozen model. The heave rate dropped close to zero at t = 1.5 hr approximately, and remained essentially zero to the end of the freezing period. This is again due to the faster cooling, which caused the frozen permeability to decrease abruptly, leading to much faster clogging of the soil pores. In contrast, ramp frozen models continued to develop heave even after internal temperatures had reached equilibrium.

Figure 5.16 shows a repeat of the same trend in behavior for the 1:45 scale models tested under step frozen and ramp frozen conditions. The one exception was that the 45g ramp frozen model had a somewhat larger maximum heave rate than the 45g step model.
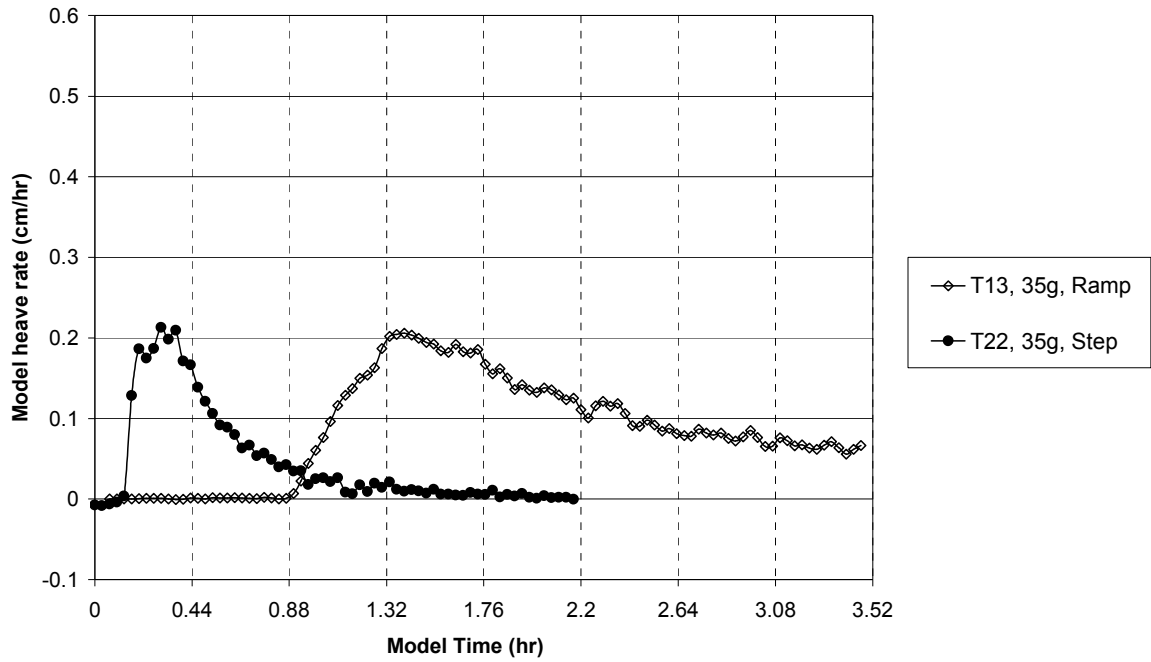
Figure 5. 15 Frost heave rate vs. Time for 35g Kaolin Columns (ramp vs step)
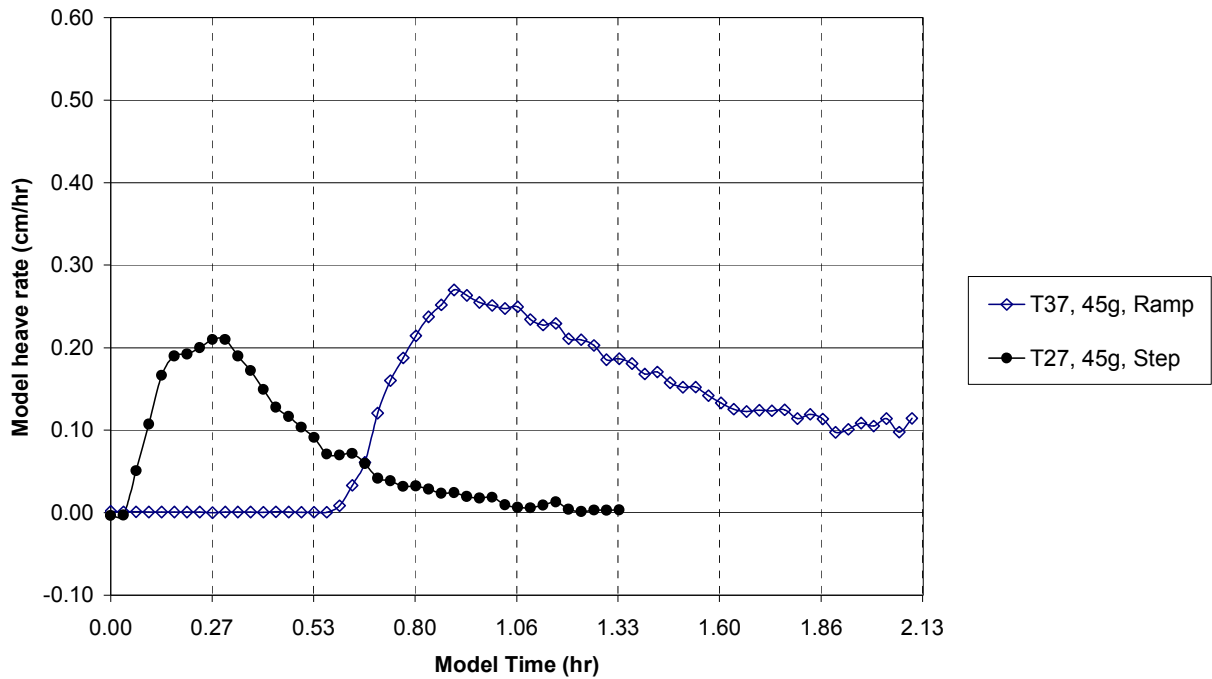
Figure 5. 16 Frost heave rate vs. Time for 45g Kaolin Columns (ramp:step)

5.4.1.2 EFFECTS ON ICE LENS CHARACTERISTICS

The ice formation in the ramp and step frozen models differed. In the step-frozen model, an ice cake 2 mm to 3 mm in thickness formed on the soil surface again. Below that cake, the ice lenses in the soil observed were very closely spaced and needle type. Lenses below the needle ice were horizontal and very thin, increasing noticeably with depth to a maximum thickness of 0.4 mm.

In the ramp frozen model, an ice cake 2 mm to 3 mm in thickness had formed, but, in contrast, ice lenses, rather than needle ice, was observed in the soil beneath the cake. Thicknesses of the ice lenses were larger than in the step frozen models close to the soil surface, and there was no discernible pattern of increasing thickness of the lenses with increasing depth. The ice lenses varied from 0.3 mm to 2 mm in thickness through the frozen depth without correlation between thickness and depth.

104

This difference in ice lens formation is, once again, an expected result of the different cooling rates and their effect on degree of migration of water to the freezing front. When temperature drops rapidly, ice forms predominantly from immediately available water, leading to needle ice, rather than more slowly forming ice lenses.

The relationship between water contents and ice lens sizes was also reflected to some degree in the water content profile after freezing between ramp frozen and step frozen soil columns as shown in Figure 5.17 and 5.18. Step frozen models showed more pronounced depression in water content in the frozen fringe and less increase in total water content in the depth of freezing.
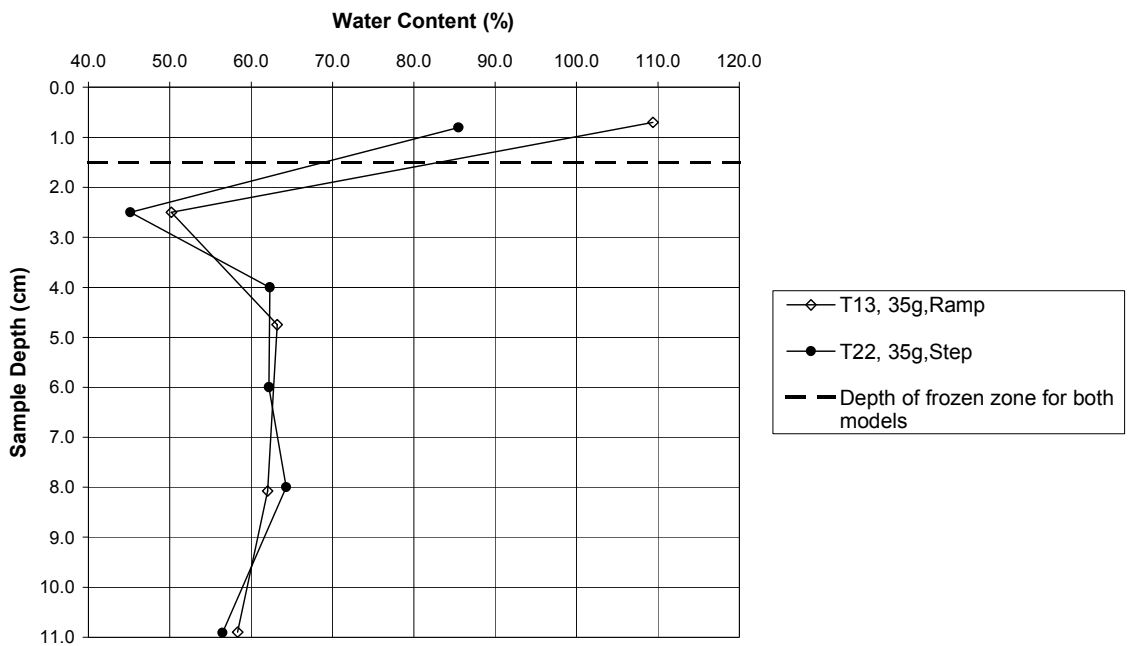
Figure 5. 17 Water content profile before and after freezing for 35g ramp and step
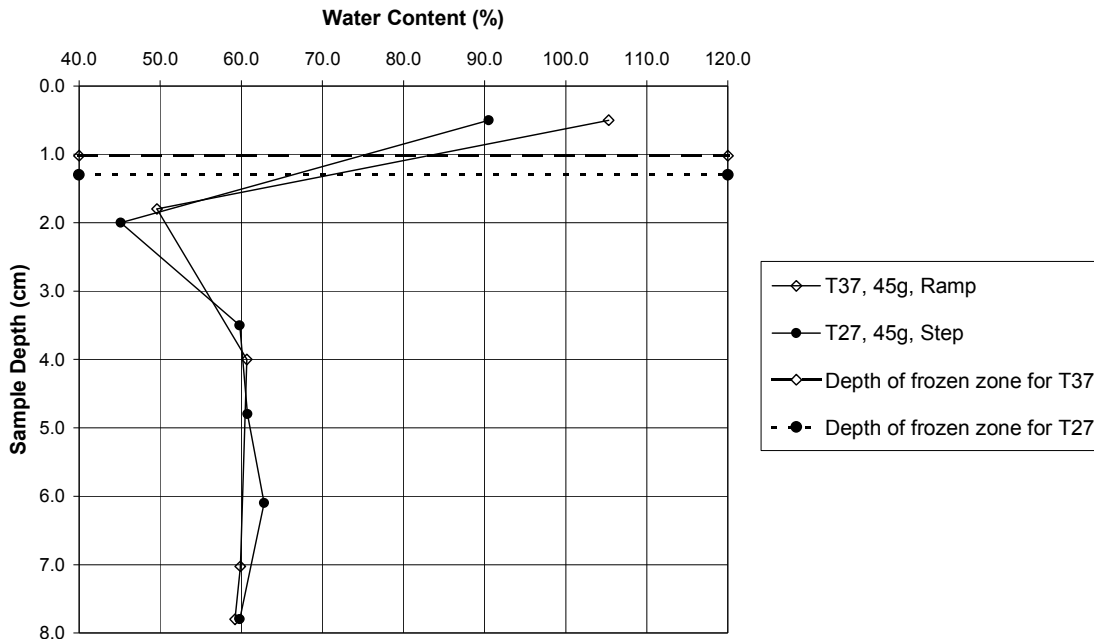
Figure 5. 18 Water content profile before and after freezing for 45g ramp and step

5.4.2 ONE STEP RAMP FREEZING VS TWO STEP RAMP FREEZING

As a means to examine freezing regime effects further, a second ramping scheme – temperature scheme 2 – was applied in a test, T51, on Ft Edwards clay for comparison to the response of a Ft.Edwards one step ramp test T38 (discussed earlier). Both models were prepared an initial moisture content of 45%. In the case of T51, the total of freezing degree days was greater than that applied in either the ramp or the step freezing tests, and the nature of the freezing sequence did not simulate anything likely to occur in nature. Nonetheless, freezing regime effects comparisons were possible.

The first ramp for the two step test, T51, involved an upper soil surface cooling rate of 3.3°C/hr (model scale) until -1.0˚C was reached. This temperature was held constant for 1.8 hours (model scale), followed by a second ramp with a cooling rate of 1.6°C/hr (model scale), to reach -3.0˚C; the soil surface was held constant at -3.0˚C for 2.5 hours (model time). This applied 600 freezing degree days (prototype equivalent) to the soil in T51. In contrast, the one step ramp model, T38, was cooled at 3.4 °C/hr (model scale) until -3.0˚C was reached, essentially the same rate as the first ramp of model T51, and then held constant for 1.76 hours (model time). This applied 340 freezing degree days to the soil.

Clearly the development of heave is very different in the two cases, and even when the number of freezing degree days applied is the same, the one step ramp test (T38) shows greater heave than the two step ramp test (T51). The heave plots magnify the different development in heave as shown in Figure 5.19.
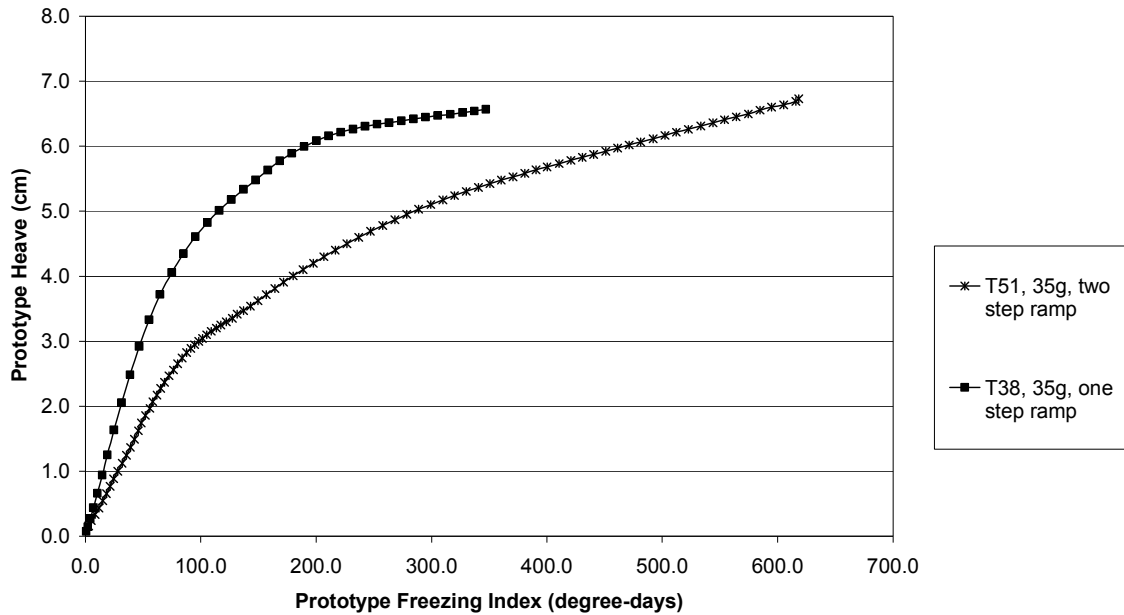
Figure 5. 19 Frost heave vs. Freezing Index for Ft.Edwards Clay (one step vs. two step ramp)

Figure 5.20 shows heave rate curves and the development of heave for both cases for model T38 and for model T51. Heave rates increase in a very similar pattern until the top temperature of the samples reaches -1.0 °C for both ramp schemes. When the temperature in the two step ramp test soil is held constant at -1.0 °C, the heave rate of the two step ramp model slackens. When the second ramp begins, the rate of heave increases again, and then reduces -- although not to zero -- when a new temperature plateau is reached at -3.0 °C. The one step ramp model shows much greater rate of heave developing, reaching its peak when the surface temperature reaches its plateau temperature of -3.0 °C, and then dropping almost as sharply, although rate of heave remains greater than zero. The maximum heave rates of two step ramp models are about one third times those of one step ramp model for both models.

Earlier comparison in Section 5.4 between heave developing when cooling is applied by the abrupt step cooling regime, v.s. the single ramp cooling regime indicated that ramped cooling led to greater heave. This would lead one to expect that even slower cooling, or smaller steps of ramped cooling, would cause even greater heave. This was not the case here. It appears that the rate of change in the external or surface temperature of a column of soil and the resulting rate of change in internal soil column temperature are both important in the development of heave. Surface measured heave is, of course, the net effect of water expansion during freezing, and simultaneous soil compression in the frozen fringe. It is possible that different freezing regimes lead to different expansion and compression effects. It is also possible that maximum heave is a function of the cooling regime as a function of soil permeability and compressibility. Further comment can only be made based on additional testing that was not possible to include in this experimental program.
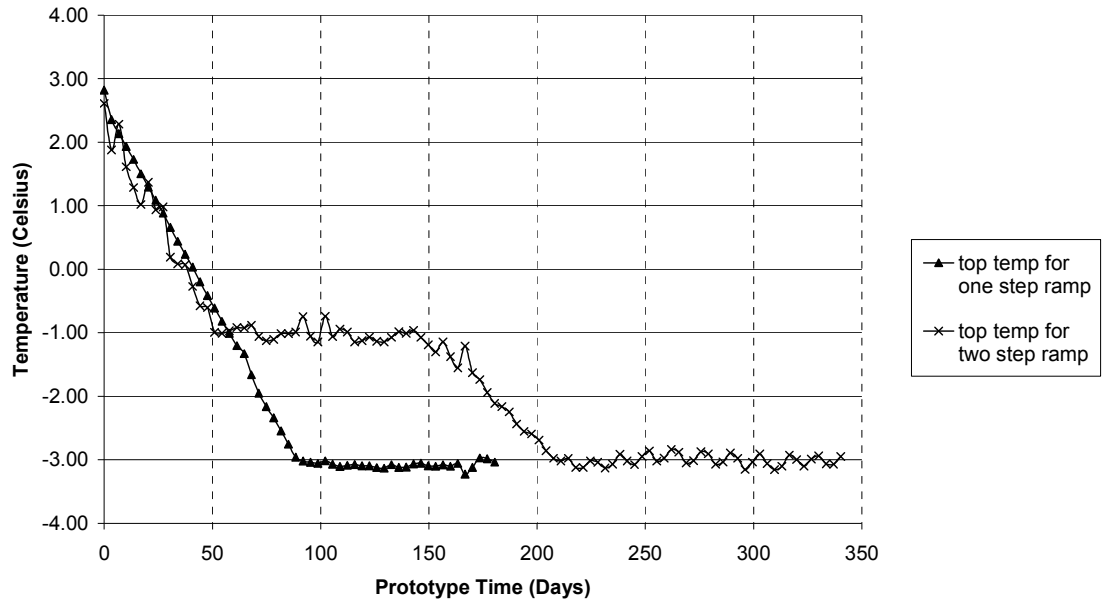
a
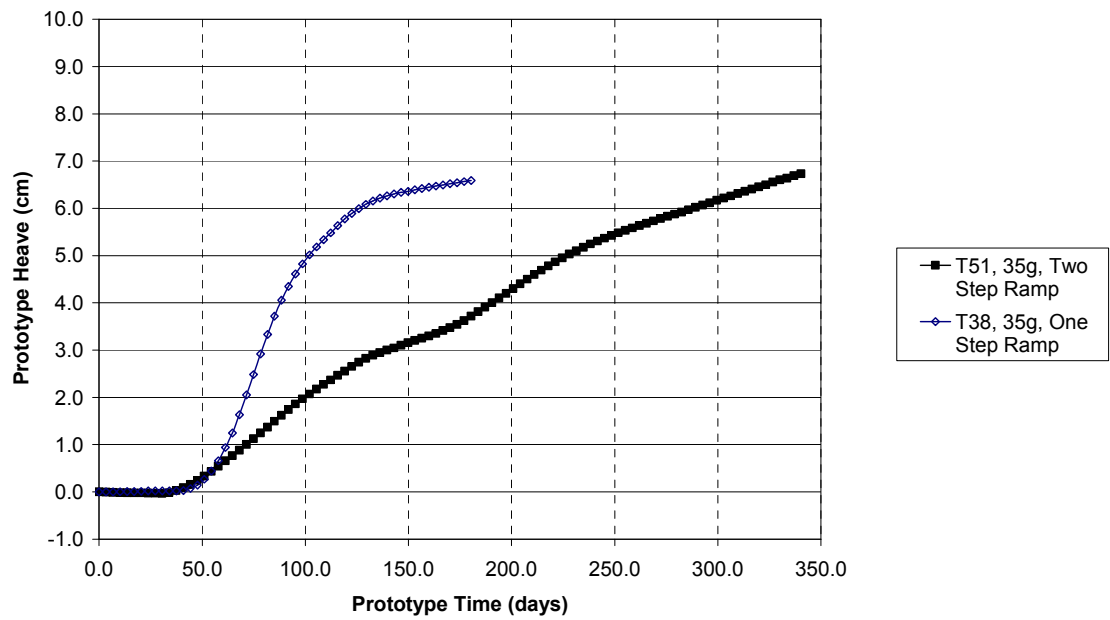
b
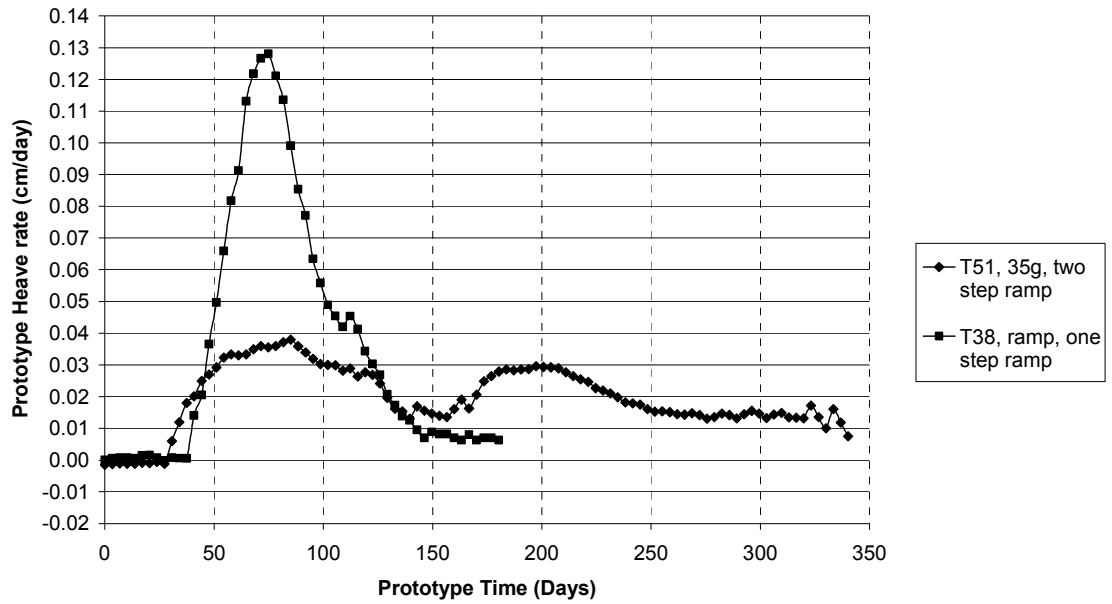
c

Figure 5. 20 one step and two step ramp for Ft.Edwards Clay
a: top temperature profile b: frost heave c: heave rate

A two step ramp test was also performed on a kaolin soil column. Since its water content was not equal to that of a kaolin soil column test performed with one step ramp cooling, the heave results are not presented. Nonetheless, it is noteworthy that the same relative behaviors were observed in those models.

5.5 WATER AVAILABILITY EFFECT

5.5.1 LOCATION OF PHREATIC SURFACE

Water availability in soil freezing strongly influences the magnitude of heave developing in the soil. This supply comes from immediately local, initial, unfrozen

pore water, and it is augmented by pore water drawn from unfrozen soil below the freezing front. The extent to which water comes from below the freezing front depends, in general, on several related factors, including: the permeability of the soil, its water content, the proximity of the phreatic surface, the height and degree of saturation of the continuous capillary rise, and the local temperature gradient and the rate at which the freezing front advances into the soil. Two tests were performed to assess effects on freezing response of the proximity of the phreatic surface to the soil surface in clay.

Model T41 was prepared and tested at 35g under conditions identical to the previous 35g model (T13), but with one exception. Whereas the phreatic surface in T13 was held at 1m prototype equivalent depth ($D_w = 0.25H_m$), the phreatic surface for T41 was held at 3m prototype equivalent depth ($D_w = 0.75H_m$). Both specimens were saturated throughout and had otherwise identical stress histories, leading to the same water content – w = 61% -- before freezing. Figure 5.21 shows the development of the frost heave and Figure 5.22 shows the corresponding water contents before and after freezing.

Development and magnitudes of heave were very similar in the two models, and so also were the end-of-test water content profiles. This indicates that water content in saturated clay appears to be far more important than the depth of the phreatic surface, when low permeability limits the amount of water that can migrate to the freezing front from other than the nearly immediate vicinity of freezing.

This conclusion is also supported by the results of a separate test in which dyed water was introduced to the bottom of a model soil column frozen on the centrifuge.

After the test was completed, and the model dissected, there was no evidence that the dyed water was drawn into the soil during the freezing process, reinforcing the conviction that little if any water is drawn from deep within the groundwater table. This occurred in spite of the fact that the system was an open system connected to two water reservoirs. Eigenbrod et al. (1996) arrived at the same conclusion in their tests on clayey silt.
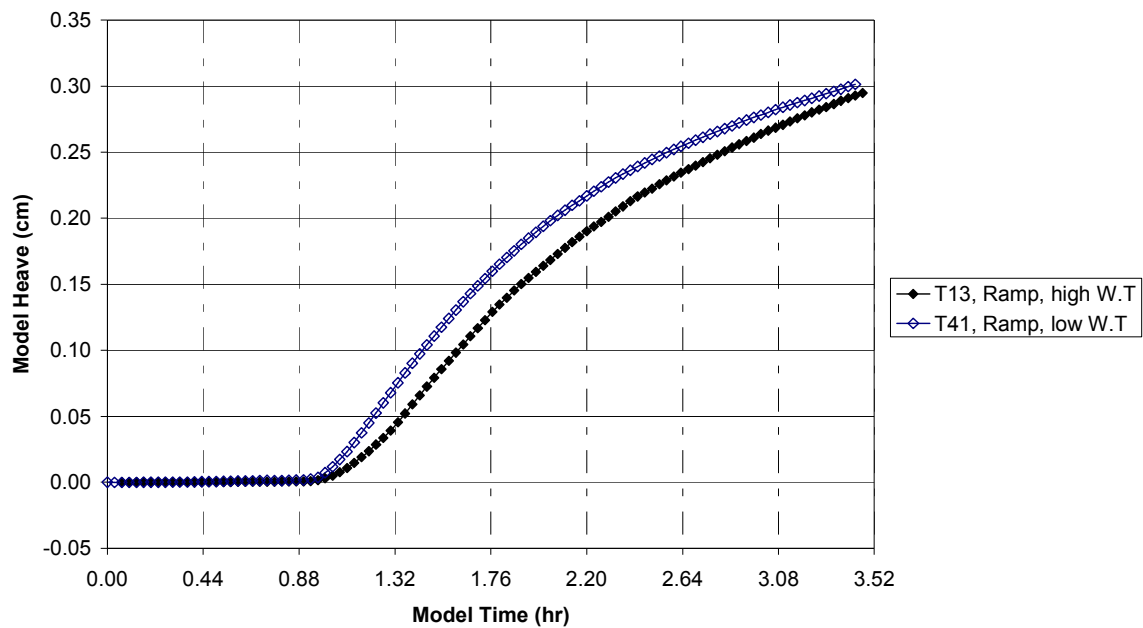
Figure 5. 21 Freezing Responses of Kaolin with two different location of water table
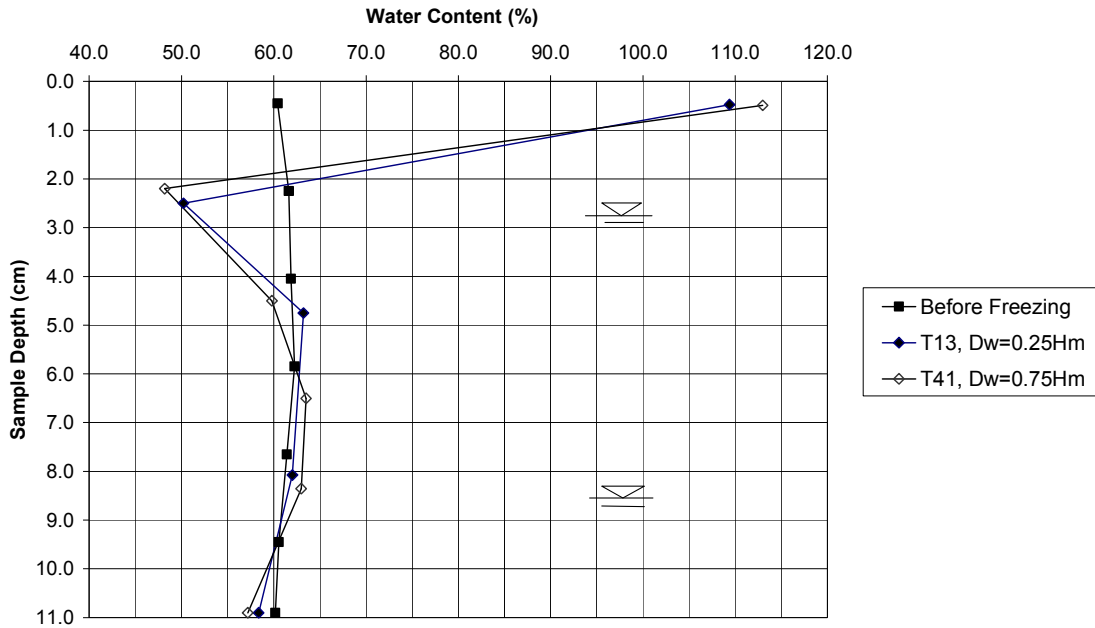
Figure 5. 22 Water content profiles of two different location of water table models before and after freezing

5.5.2 EFFECT OF INITIAL WATER CONTENT ON HEAVE

The evidence indicates that there is not significant water movement within these clay columns to the freezing front. This means that initial water content will be a critical factor in freezing response of clay, and more important to heave other than other factors such as proximity of the phreatic surface, soil density, or soil stress history, etc. To shed some light on this hypothesis, two sets of kaolin specimens were roughly compared: one set of kaolin specimens with initial water contents of $w_i =$ 61% were frozen under temperature scheme 1, and another set of specimens with initial water content of $w_i = 50\%$ were frozen under temperature scheme 2. Although these tests were not conducted for the purpose of investigating the effect of initial

water content on frost heave, they provided some small insight into the role of initial water content in freezing behavior of clays. Test results for the initial water content effects on frost heave were summarized in Table 5.4.

Table 5. 4 Summary of test results for initial water content effects on frost heave

Soil	Test No	Ng	Temperature Scheme	w_i %	Frost Heave cm	Depth of Freezing, cm	Heave/DOF
Kaolin	T13	35	1	61	0.29	1.5	0.24
	T47	35	2	50	0.24	1.8	0.15
	T37	45	1	61	0.26	1.0	0.24
	T46	45	2	50	0.20	1.5	0.15

As expected, the kaolin specimens with higher initial water contents developed larger ultimate heave and shallower depths of freezing than those kaolin models with lower initial water contents, regardless of the longer freezing involved in temperature scheme 2. Nixon (1991) commented that the effect of water content on heave in clayey soils was a function of how much greater initial water content was compared to the plastic limit of the soil, although he did not simulate full column response that includes the influence of water content on depth of freezing. The plastic limit for the kaolin was 34%. If the relevant ratio were: heave α $(w_1 - w_p)/ (w_2 - w_p)$, then the ratio for the kaolin tests would be $(61-34)/(50-34) = 1.7$, if temperature schemes were identical. Unfortunately, the difference in temperature regimes makes it difficult to comment further.

5.6 REPEATABILITY OF MODELS

Results of physical model tests conducted even under identical conditions will vary to some degree due to unavoidable internal and external variability. Konrad and

Seto (1994) attributed variability between freezing tests intended to be identical, to minor, local variation in void ratios that influence capillary tension. These effects, of course, are magnified in small specimens. Nonetheless, repeatability should be checked in any experimental program by examining the variation of test results from "identical" tests models, in order to have confidence in overall test results. This is particularly important in studies involving scale models where model results are multiplied by the scale of the model for application to full scale design.

In this study, three groups of identical models were repeated at intervals during the course of this experimental research. Each group simulated a different full scale prototype, so it is relevant only to compare results within a group. Table 5.5 summarizes the results of a univariate statistical analysis of the result of those three groups of models.

The data presented in that table show that the measured model heave had good consistency, with a range of coefficient of variation varying between 0.7% and 6.7 % among the three groups of models. The variation of ultimate model heave for the 35g models is larger than the other groups, but remains well below what is acceptable accuracy in engineering practice. The variation of DOF was very small with a maximum coefficient of variation of only 1.2%. Even the ranges of water contents are acceptable, with the largest variation being 6.8%. These results are well within recommended standard coefficient of variation for soil engineering tests. According to Lee, White, and Ingles (1983), typical geotechnical tests such as permeability, void ratio, and moisture content are considered to be acceptable if their coefficients of

116

variation are as large as 300%, 25%, and 15%, respectively. By these standards, these tests all easily meet reasonable expectations of reproducibility.

Billy Connor (personal communication, 2001) indicated that in frozen soil research, field results that are repeatable within 30%, or predictions that come within 30% of field results are considered to be acceptable in design. A good portion of that allowance is owing to unknowns, including details of soil conditions, phreatic surface location, purity of the water, and temperature regime, all of which are known, because they are controlled. These experimental results, however, fit both the liberal and the stricter standards.

Table 5. 5 Results of repeatability tests

Soil	Ng	Test No	[1]F.R	Ultimate model heave cm)	[2]DOF (cm)	[3]w_f (%)	[4]w_{ff} (%)
Kaolin	35	T13	1	0.29	1.21	110	54
	35	T14	1	0.26	1.24	105	53
	35	T31	1	0.27	1.23	120	54
	Mean			0.27	1.23	111.7	53.7
	Variance			0.0	0.0	58.3	0.3
	Standard deviation			0.02	0.02	7.64	0.58
	Coefficient of variation			6.7	1.2	6.8	1.1
	45	T37	1	0.25	1.04	120	52
	45	T17	1	0.24	1.05	107	54
	Mean			0.245	1.045	113.5	53
	Variance			0.0	0.0	84.5	2.0
	Standard deviation			0.01	0.01	9.19	1.41
	Coefficient of variation			0.7	0.7	8.1	2.7
	55	T45	2	0.19	0.91	71	44
	55	T52	2	0.18	0.92	73	45
	Mean			0.185	0.915	72	44.5
	Variance			0.0	0.0	2.0	0.5
	Standard deviation			0.01	0.01	1.41	0.71
	Coefficient of variation			3.8	0.8	2.0	1.6

Note: 1. F.R stands for freezing regime
2. DOF stands for depth of freezing
3. w_f = water content in frozen depth
4. w_{ff} = water content in frozen fringe

5.7 MODELING OF MODELS

5.7.1 KAOLIN CLAY

Modeling of models involves selecting a single hypothetical full scale prototype, constructing models of that prototype at different scales, testing them according to expected scaling laws, and then comparing their results for similarity in their predictions of behavior of that single full scale hypothetical prototype. If there is no unacceptable or identifiably scale dependent deviation in the predictions, then the method of modeling is considered to be confirmed. A better method is to have a perfectly documented full scale event which can be exactly duplicated in small models, and against which scale model results can be compared. In geotechnical engineering, this is seldom possible, and physical modelers routinely use this method; see for example R.N Taylor (1995). In the absence of a full scale event to model in this research, this method was used here.

Correctness of scaling laws in centrifuge modeling of soil freezing was investigated extensively by Yang and Goodings (1999). Their work provided convincing experimental evidence to support Miller and Miller's (1956) hypothesis that small scale modeling of frost response can be correctly modeled on a centrifuge. They tested this hypothesis for silt and silty clay using the modeling of models technique, testing over the range of scales of 1:20, 1:30; and 1:45. Although the main purpose of this research was to investigate the whole system response of freezing clay, and the assumption of the research was that the experimental results of Yang and Goodings provided the underlying support that modeling should be correct, it is reasonable also to check the validity of scaling laws in clay, in case the parameters

controlling freezing clay response were affected differently by the centrifuge model freezing conditions. The scales chosen for comparison were, 1:35 (tested at 35g), 1:45 (tested at 45g), and 1:55 (tested at 55g).

Three kaolin columns were frozen according to temperature scheme 1, and three according to temperature scheme 2, all with pre-freezing water contents of 61%. In addition six Ft Edwards clay models were prepared and subjected also to the same two temperature schemes, all with prefreezing water contents of 45%. Sample heights, freezing regimes, and data of model behavior are summarized in Table 5.6 and Table 5.7.

Table 5. 6 Results of modeling of model for one-step ramp

Soil	Test No	Ng	Model heave cm	Ultimate prototype heave cm	Maximum Prototype heave rate cm/day	Model DOF (cm)	Prototype DOF (cm)	Heave/ DOF
Kaolin	T13	35	0.29	10.2	0.14	1.21	43.4	0.24
	T37	45	0.25	11.3	0.14	1.05	47.3	0.24
	T55	55	0.12	6.6	0.08	0.58	32.0	0.21
Ft.Edwards	T38	35	0.19	6.7	0.13	1.31	45.9	0.15
	T43	45	0.10	4.6	0.08	0.90	40.5	0.11
	T48	55	0.06	3.3	0.05	0.64	35.2	0.09

To compare the frost heave between the models, all model results have been converted to prototype scale using the scaling relationships of $l_p = N * l_m$ (l = length = frost heave in this case) and $t_p = N^2 * t_m$. Figure 5.23 shows the development of surface heave plotted against time for the three kaolin single ramp freezing models at prototype scale, and Figure 5.24 shows the frost heave rates plotted against time for the same three models, converted to prototype scale. The internal temperature profiles in Figure 5.23 are shown fro the 55g kaolin model (T55). Although all models developed frost heave in a broadly similar pattern, the 55g model does not fall into

line with the 35g and 45g models in either plot. Those plots show that prototype magnitudes of heave and rates of heave are very similar in values for the 35g, and the 45g models, but not for the 55g model. The ultimate magnitudes of heave for the 1:35 and 1:45 scale models fall within 13.8 % of each other; depths of freezing are within 13.0 % of each other; and values of heave/DOF are equal to each other. The values of magnitudes of heave and depths of freezing for the 1:55 scale model point to different behavior, and that behavior is highlighted in Figure 5.24 which shows rates of heave. The maximum rate of heave for the 1:55 scale model was roughly half the rates shown for the 35g, and 45g models, and that maximum was achieved more slowly and was sustained for a shorter period of time, accounting for the marked difference in ultimate heave. Finally, post-freezing water contents are plotted in Figure 5.25 and while the three models show generally similar profiles, the effects of freezing on water content do not seem to have penetrated as far into the 1:55 scale model as for the other two.

There are two possible explanations for this difference in behavior for the 1:55 scale model. One possibility is that the cooling potential of the model apparatus was sufficient to allow correctly scaled and well controlled cooling at scales 1:35 and 1:45, but was not fast enough to simulate the same cooling rate for the 1:55 scale model. The apparatus was required to cool 1:55 scale models 1.5 times faster than 1:45 scale models, and 2.5 times faster than the 1:35 scale models. In fact, the behavior of the 1:55 scale model as represented in Figures 5.23, 5.24, and 5.25 is characteristic of a soil subjected to a more gradual ramped cooling regime than the other models.

The other possibility is that when time for ramped cooling in a model is reduced by a factor of N^2, a 1:55 scale model may effectively, although unintentionally, be subjected to the equivalent of step freezing, where the sudden application of cooling is too rapid for this soil with this low permeability to respond in the same way as the larger scale 1:35 and 1:45 scale models subjected to ramped freezing. Step freezing, discussed in Section 5.4, causes a specimen to respond with rapid but short lived development of heave, with an ultimate heave rate approaching zero. This situation was not observed here entirely, however, there may be some intermediate limiting rate effect being encountered. This limit may be a function of the relative values of the penetration rate (R_p) of the freezing front (affected by a combination of the temperature regime and the thermal conductivity of the saturated soil) and the permeability, k, of the soil changing over time.

A simplistic approach would be to estimate R_p as the average rate of penetration of the 0°C isotherm into the soil, to, for example, the mid-depth of the soil sample. And, then to compare R_p to unfrozen permeability, k. For these first three models, this ratio R_p/k equals roughly 27,000 for the 35g model; 34,000 for the 45g model, which predicted the same behavior as the 35g model; and 42,000 for the 55g model which under predicted heave.
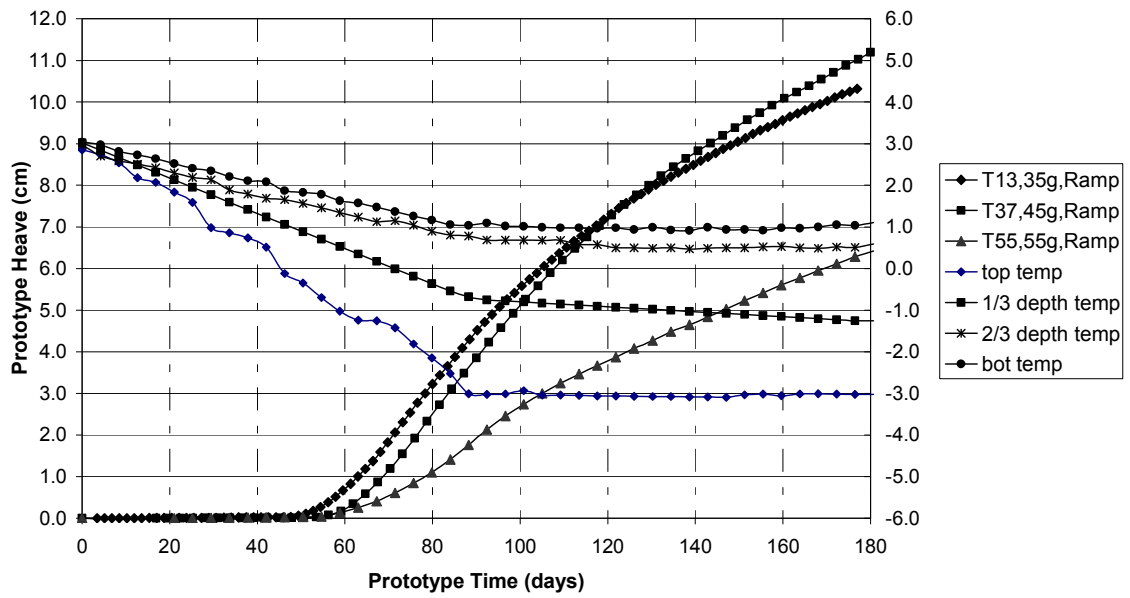
Figure 5. 23 Freezing Response of kaolin for one step ramp freezing at 35g, 45g, and 55g
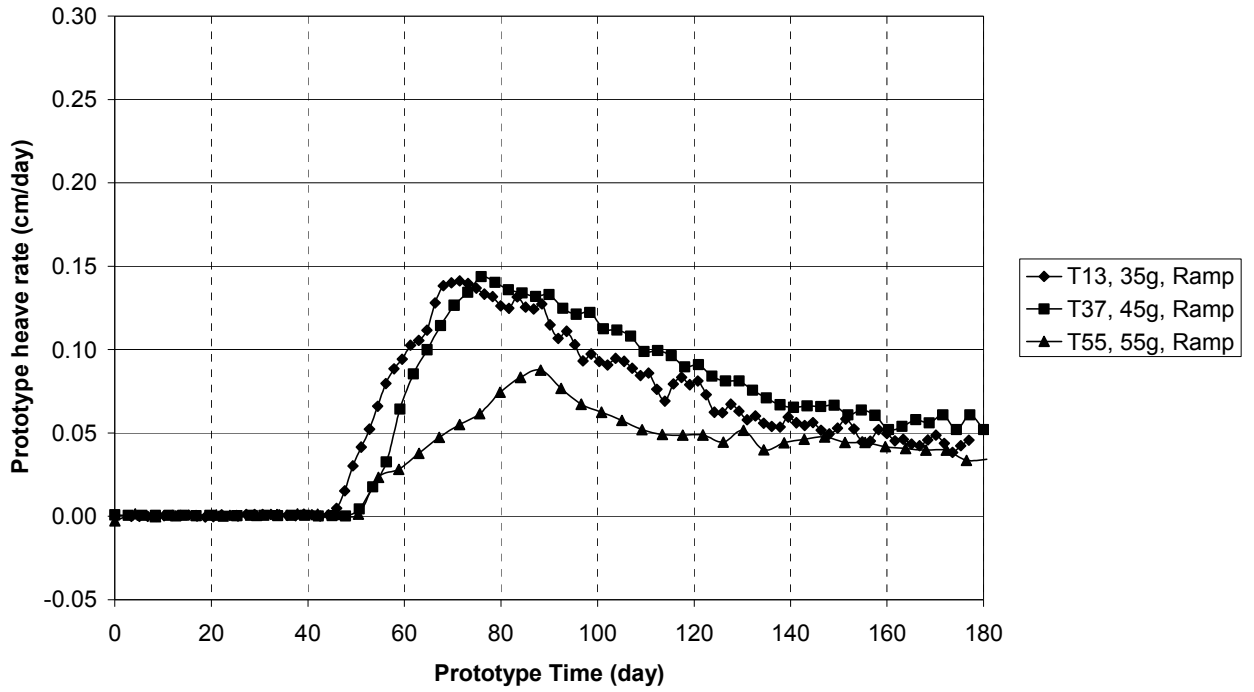
Figure 5. 24 Frost heave rate curve of kaolin for one step ramp freezing at 35g, 45g, and 55g
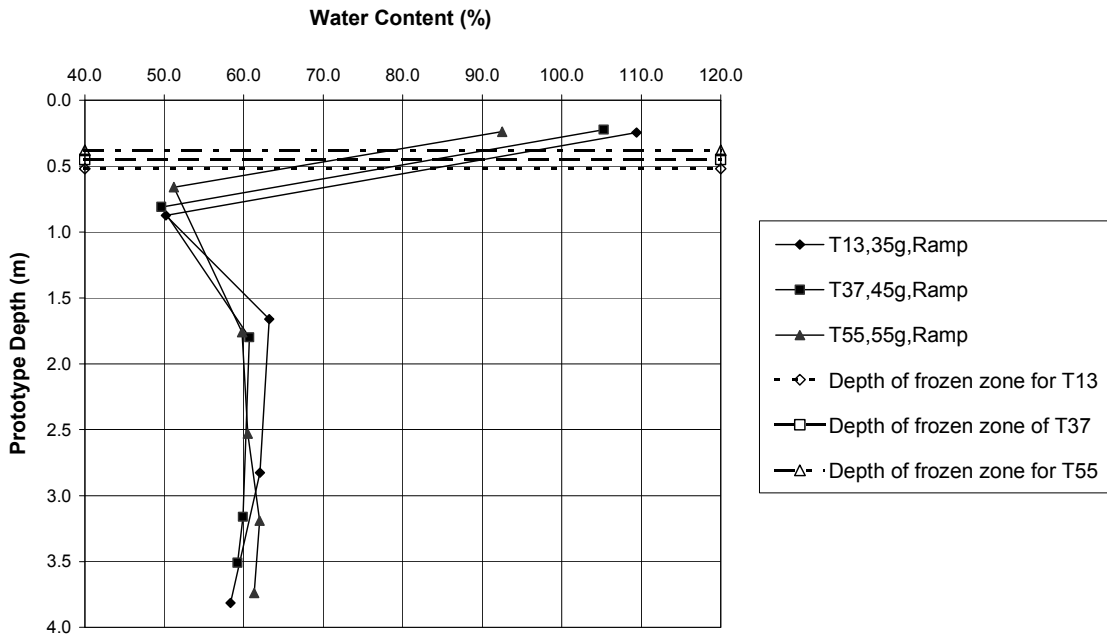
Figure 5. 25 Water content profile of kaolin for one step ramp freezing at 35g, 45g, and 55g

A second set of three kaolin models with the same range of scales was tested, with the same method of preparation, but with a slower, longer (340 day equivalent) two step cooling regime, designated in Section 5.1 as temperature scheme 2, and plotted in Figure 4.4; the freezing index was –600 freezing ºC-days. This allowed further investigation of rate effects, and modeling of models, although as noted previously, it does not simulate a likely, seasonally induced cooling cycle. Again each model simulated freezing in a full scale soil column 4m in height with its prototype phreatic surface at a depth of 1m. All results are plotted with time and magnitudes of heave converted to prototype scale. Table 5.6 summarizes the results of these model tests. Figure 5.26 shows surface heave elevation changes of the 35g, 45g, and 55g kaolin models throughout the freezing period. The internal temperature profile shown is that of the 35g model, although the 45g model, and the 55g model have a similar temperature profiles. Figure 5.27 shows the frost heave rate of these models throughout freezing.

Table 5. 7 Results of modeling of model for two-step ramp

Soil	Test No	Ng	Model heave cm	Ultimate prototype heave cm	Maximum prototype heave rate cm/hr	Model DOF (cm)	Prototype DOF (cm)	Heave/ DOF
Kaolin	T47	35	0.24	8.4	0.05	1.46	51.1	0.16
	T46	45	0.20	9.0	0.05	1.30	58.5	0.15
	T45	55	0.15	8.3	0.05	0.95	52.3	0.16
Ft.Edwards	T51	35	0.19	6.7	0.04	1.61	56.4	0.12
	T50	45	0.16	7.2	0.04	1.14	51.3	0.14
	T49	55	0.12	6.6	0.04	0.98	53.9	0.12

Model behaviors for all models in this set are shown in Figure 5.26 to be very similar in their patterns of heave development and close in actual values of heave. The average ultimate prototype frost heave was 8.6 cm, varying by less than ±11%

from the average. Depths of freezing (DOF) (= thickness of frozen soil minus heave) equaled 51.3 cm at full scale, varying less than 8% from that average, and, the ratios of heave/DOF differ little with an average of 0.15. Development of heave (Figure 5.26) indicates behavior in all models to be much closer than for the one step ramping, although the 1:55 scale model lagged slightly compared to the other two. Rates of heave (Figure 5.27) are very similar, and the underperformance of the 1:55 scale model in the first ramp of freezing, followed by the overperformance during the second ramp, suggests that requirements for precision of temperature control may be more stringent for small models, and more difficult for the model apparatus developed for these tests. Water contents after freezing (Figure 5.28) indicate very similar final conditions. Finally, estimates of R_p/k for these models were 10,000 for 35g; 12,500 for 45g; and 15,000 for 55g. These are all well below values of R_p/k identified for the more rapid ramp freezing. Overall, then, modeling of models is confirmed in this set of model tests, however results from the previous set of kaolin models suggest that there may be a limit to model correctness that is related to rate of cooling.
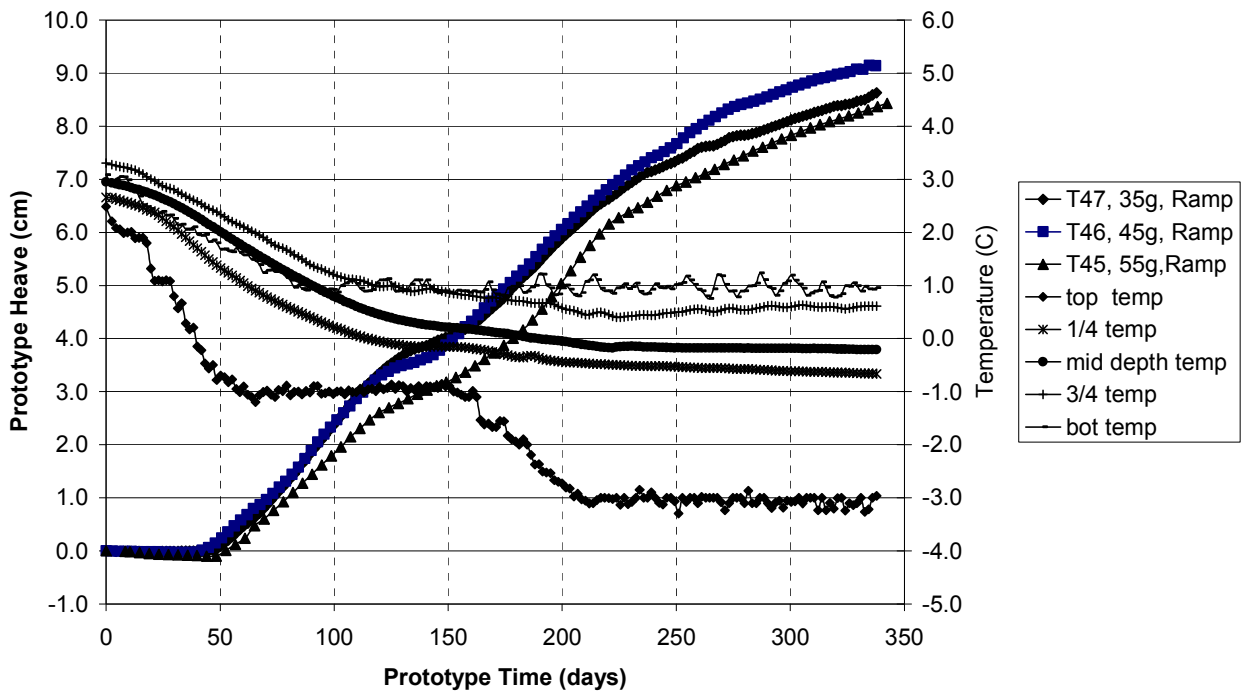
Figure 5. 26 Freezing Response of kaolin for two step ramping freezing at 35g, 45g, and 55g
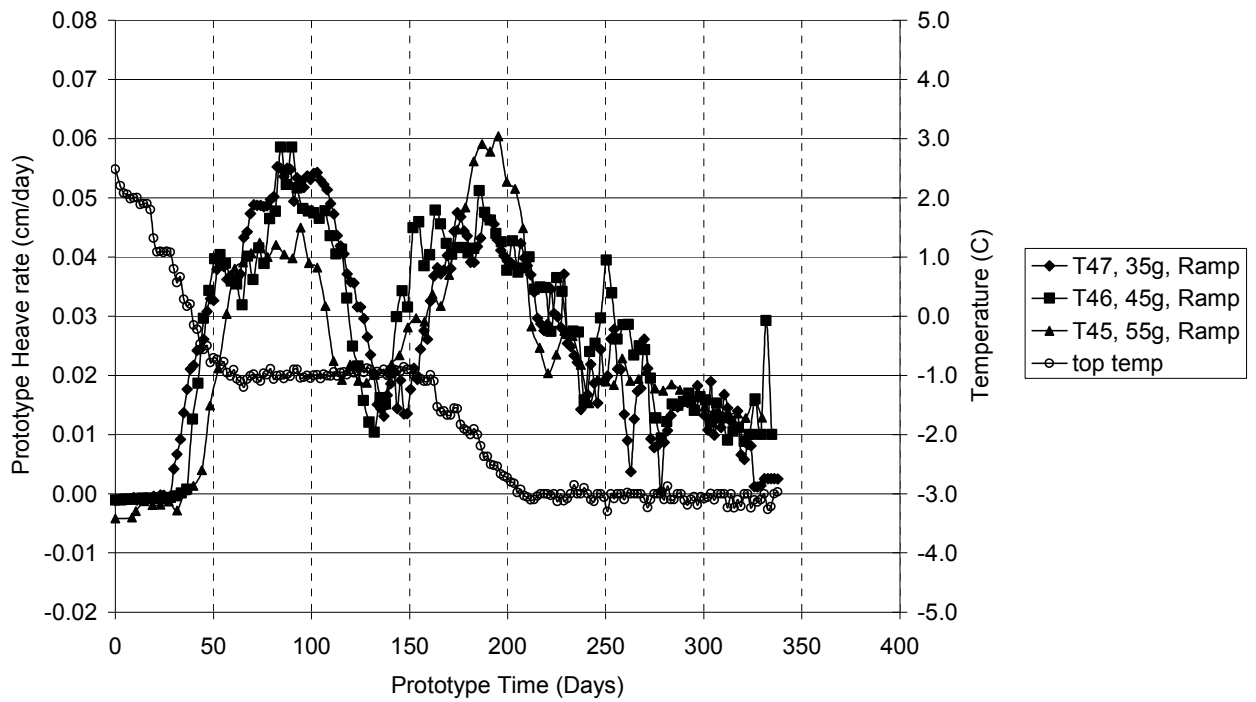
**Figure 5. 27 Frost heave rate of kaolin specimens for two step ramp freezing at 35g, 45g, and 55g ; top temperature is shown for the 35g model, but is representative of all two step models**
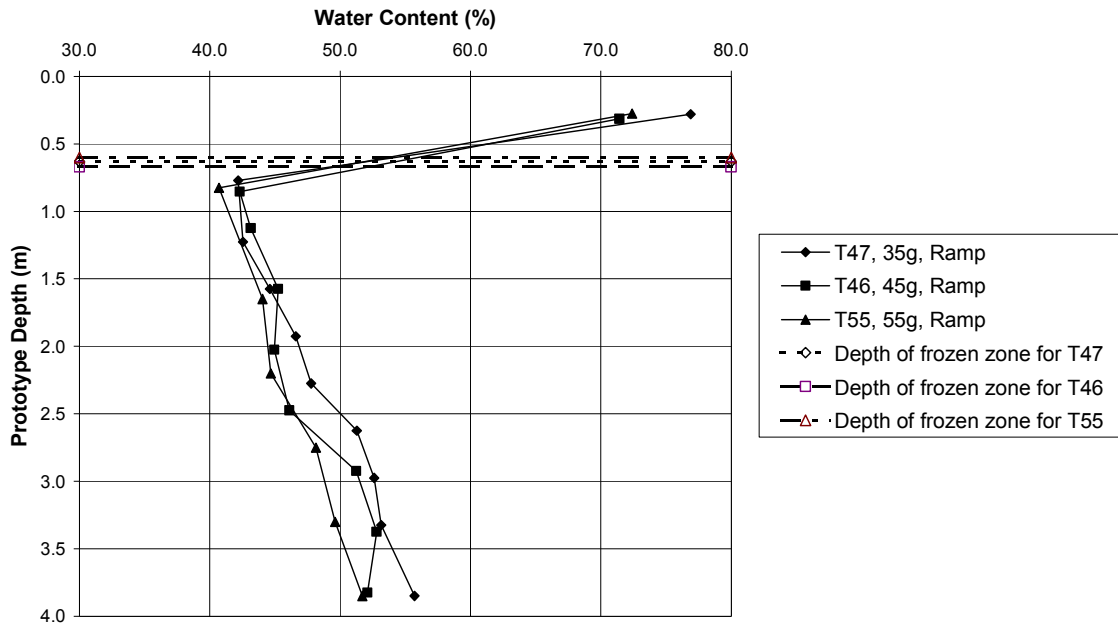
Figure 5. 28 Water Content Profile in kaolin after two step ramp freezing for 35g, 45g, and 55g models

5.7.2 FT.EDWARDS CLAY

Model results for Ft.Edwards clay tell a somewhat different story. Ft.Edwards clay has a permeability one-fourth that of the kaolin. Six Ft.Edwards clay models were prepared, each with water content of 45% immediately before freezing, and simulating full scale columns of the same soil 4 m in height. Three were subjected to temperature scheme 1, and three were subjected to the slower, longer freezing scheme 2.

Turning to the first three, Figure 5.29 shows the development of surface heave plotted against time, with both quantities converted to full scale equivalents. Although all the models had similar patterns of frost heave development, they are not predicting the same full scale behavior by any measure. Magnitudes of prototype ultimate heaves decreased as centrifugal acceleration increased and model scale

decreased. Depths of freezing (DOF) (= thickness of frozen soil minus heave) for the 35g, 45g, and 55g models at full scale equivalent were 45.8 cm at full scale; 40.5 cm; and 35.2 cm, respectively. The ratios of heave/DOF are 0.15, 0.11, and 0.09 for the 35g, 45g, and 55g models, confirming a pattern suggesting a scale effect, although there is little evidence of differences in the final water contents shown in Figure 5.31. Frost heave rates for these models are plotted in Figure 5.30. This figure highlights patterns established by the other measures of development of heave. Clearly, then, some sort of scale effect is present within this set of models. Values of R_p/k for these tests are estimated to be 94,000 for the 35g model; 121,000 for the 45g model; and 148,000 for the 55g model, all of which far exceed those calculated for any of the kaolin models described above.
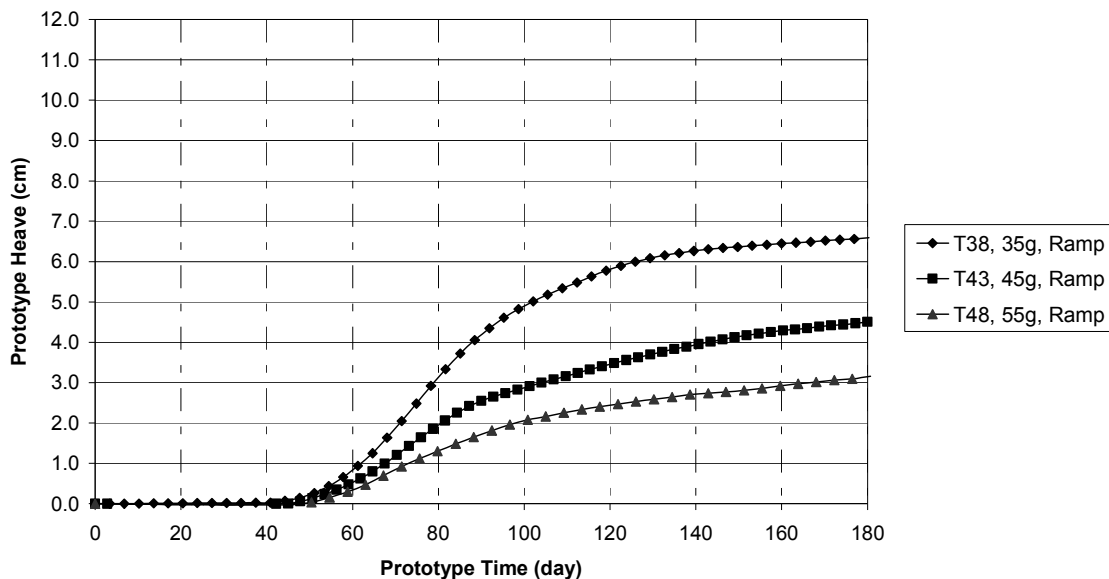
Figure 5. 29 Freezing Response of Ft.Edwards for one-step ramp freezing at 35g, 45g, and 55g

Figure 5. 30 Frost heave rate curve of Ft.Edwards for one step ramp freezing at 35g, 45g, and 55g

Figure 5. 31 Water content profile of Ft.Edwards for one step ramp freezing at 35g, 45g, and 55g

A second set of three Ft.Edwards clay columns was tested for scaling effects under the longer, more gradual freezing regime 2. Figure 5.32 shows surface heave elevation change of the 35g, 45g, and 55g models for Ft.Edwards clay. Unlike the previous set, heave had not begun to approach an asymptotic value by the end of the test, but, more significantly, all three models predict, essentially, the same full scale behavior. Depths of freezing (DOF) (= thickness of frozen soil minus heave) at full scale was for the 35g model was 56.3 cm; 51.3 cm in the 45g model; and 53.9 cm at 55g for an average of 53.8 cm, with no connection apparent between model scale and full scale prediction. Values of heave/DOF were very similar: 0.12 for the 35g model and the 55g model, and 0.14 for the 45g model. The frost heave rate curves for these models are shown in Figure 5.33 to have a self-similar pattern.

Finally, values of R_p/k for these model tests were roughly 34,000 for the 1:35 scale model; 44,000 for the 1:45 scale model; and 54,000 for the 1:55 scale model. These values are all substantially less than values in the previous set of three Ft Edwards single ramp cooling, for which rate effects were identified, although they exceed the values for the first set of kaolin models that showed a divergence of behavior for the one step ramp 1:55 scale model test. This indicates that this ratio is not adequate on its own as a threshold indicator of scale effects. Nonetheless, these results together point to the fact that models at different scales can predict the same full scale event, provided the rate of penetration (R_p) of the freezing front does not exceed the rate that water can be delivered to the frost front. When that occurs, different scale models will predict different full scale freezing effects.

Figure 5. 32 Freezing Response of Ft.Edwards for two step ramp freezing at 35g, 45g, and 55g
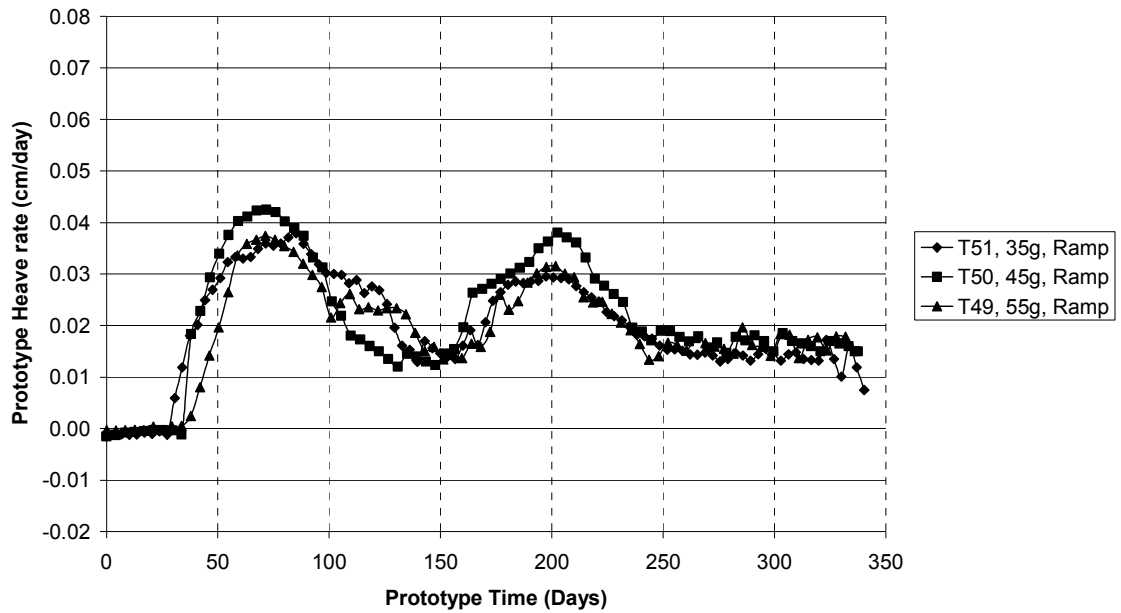
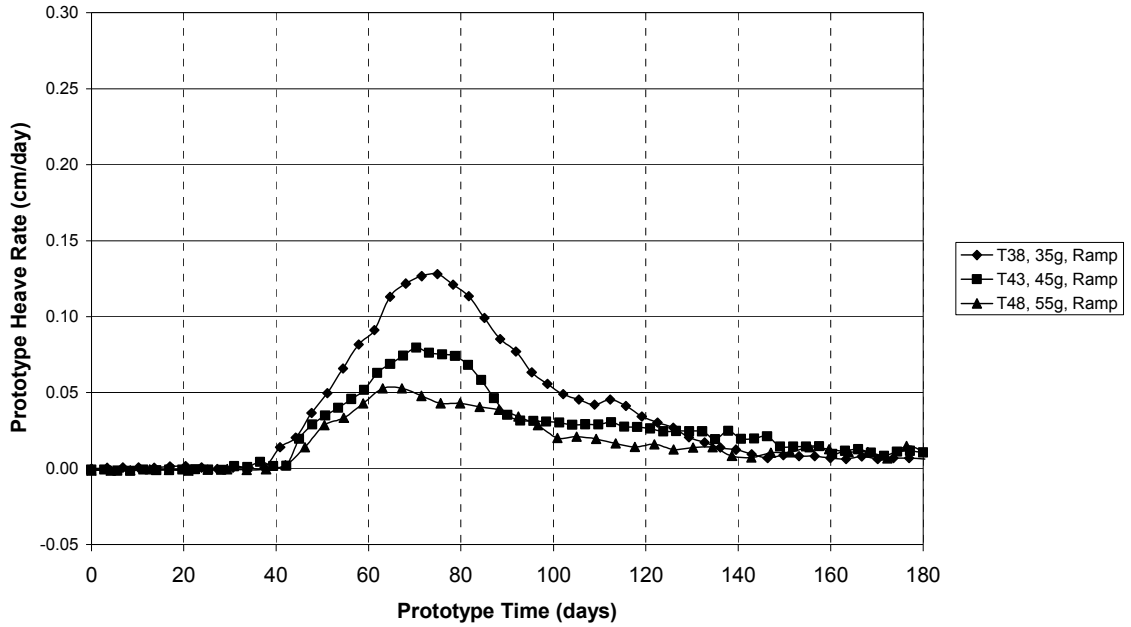**Figure 5. 33 Frost heave rate curve of Ft.Edwards for two step ramp freezing at 35g, 45g, and 55g**
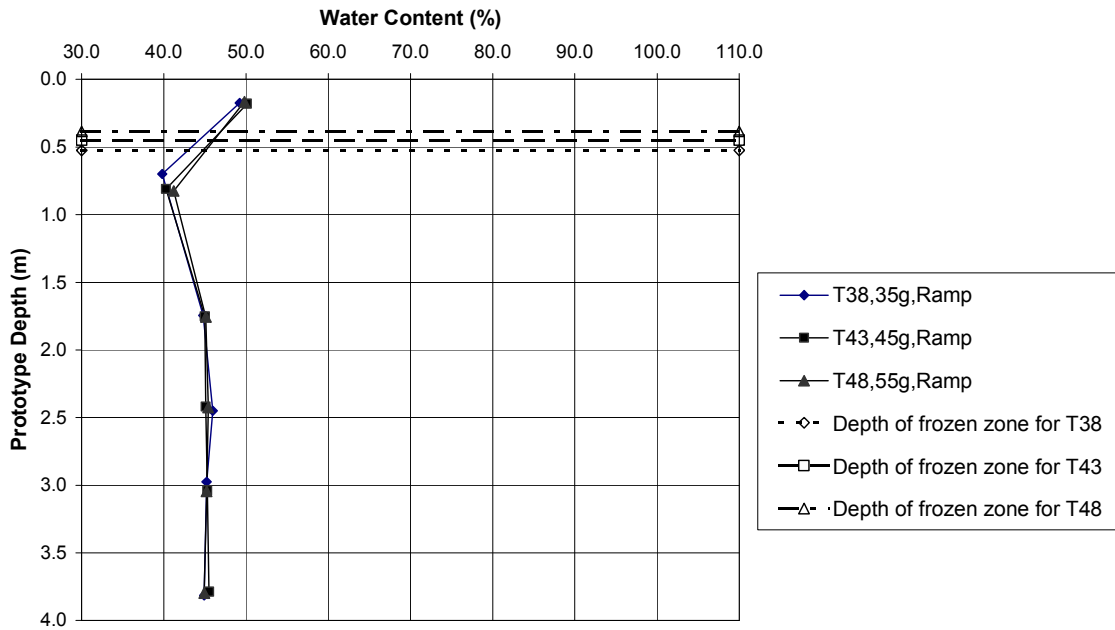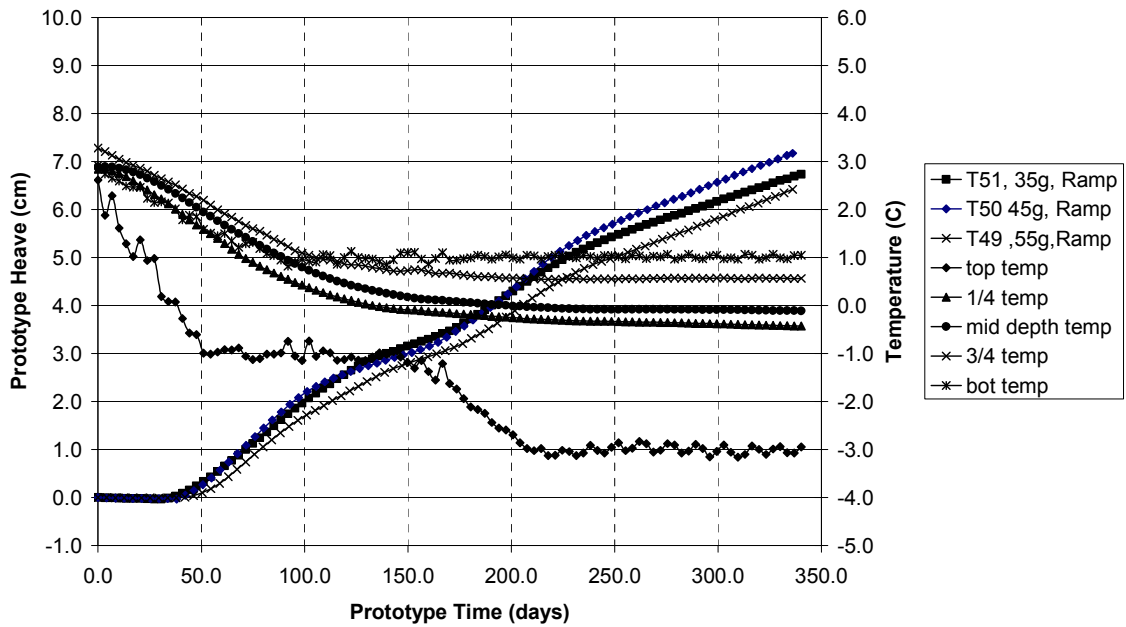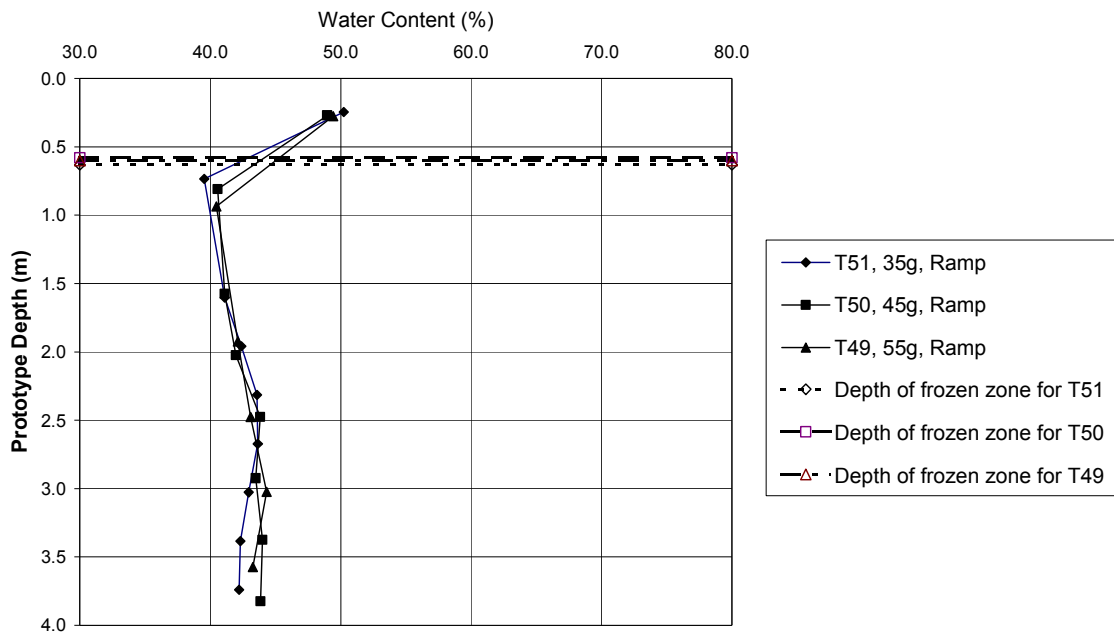
Figure 5. 34 Water Content Profile of Ft.Edwards for two step ramp freezing for 35g, 45g, and 55g models

CHAPTER 6: ANALYSYS OF FROST HEAVE IN CLAY

Chapter 5 examined experimental results to understand development of frost heave in clay. It also explored the validity of using reduced scale centrifuge modeling to measure response of clay to freezing, for purposes of extrapolating physical model response of a full soil column to full scale, field conditions. A conclusion of Section 5.3.4 is that small columns of soil frozen at 1g did not provide data that could be directly extrapolated to full scale conditions. In contrast, most centrifuge models tested at different scales showed behavior that predicted very similar full scale behavior, and this is considered to support the validity of the centrifuge modeling method for modeling clay freezing response. A limit may exist on the scale at which models may usefully be tested: when models are very small, and/or rate of frost penetration is rapid, water migration that feeds the development of heave may not occur quickly enough to preserve the scaling relationships. The question of equipment limitations was also examined. Nonetheless, the overwhelming majority of models that did support the modeling of models exercise provide useful insights into soil response that can and should be used to understand response of clays to freezing.

This chapter examines information on frost heave revealed by those physical models. This information is an excellent complement to the few laboratory tests conducted on isolated elements of soil, such as those reported by Konrad and Morgenstern (1980).

In this section, frost heave is examined quantitatively to develop an understanding of heave in clay. Data of the measured final thicknesses of the frozen

zone and the frozen fringe, the water contents before and after freezing in both the frozen zone and the frozen fringe, and the final magnitudes of frost heave were used to examine development of heave between t = 0 and the end of several freezing tests.

6.1 MODEL DEVELOPMENT

Frost heave requires: sustained freezing conditions; pore water; and frost susceptible soil. The presence of pore water and the migration of water that occurs during cooling are essential components in heave. When cooling is introduced at the top of a soil specimen, pore water flows towards the freezing front. Konrad and Seto (1993) noted that this water is coming from three distinct sources; 1) immediately local pore water; 2) water from unfrozen soil entering the specimen from below the freezing front; and 3) water freed from within the unfrozen the frozen fringe as a result of consolidation of the fringe.

Figure 6.1 shows the generalized profile of a frozen soil column. In any soil models that were dissected after freezing, it was not possible to distinguish between the active ice lens layer and the frozen zone at the end of freezing, however, when the models were dissected, three zones were evident: an uppermost frozen zone, an intermediate frozen fringe, and a lower unfrozen zone.

The uppermost zone was identifiable by its clearly visible ice lenses. This was accompanied by a pronounced increase in water content (frozen + unfrozen) above the pre-cooling water content. This increase is a result of water drawn into the frozen zone from the soil immediately below. The amount of water drawn from below the unfrozen soil and into the developing active ice lens zone depends on the balance

135

between the rate at which the frost front penetrates into the soil, compared to the rate at which unfrozen pore water can be delivered to that freezing front. The low permeability (k) of clay means that while substantial cooling induced suction (i) can develop, the resulting water movement is slow (v = ki). In clay, then, freezing must be very slow if the significant water migration that leads to substantial heave is to develop. Even then the depth of unfrozen soil from which water is drawn to the active ice lenses is expected to be shallow, when compared to silt, due to the lower permeability of clay.

Three pieces of experimental evidence confirm that the depth of soil from which water migrates in clay is shallow. First, dyed water introduced to the bottom of model soil columns frozen on the centrifuge was not drawn into the soil during the freezing process, indicating that no detectable water was drawn from outside the specimens. This occurred in spite of the fact that the system was an open system connected to two water reservoirs. Second, immediately below the frozen zone, there was a marked depression in water content when compared to the pre-freezing water content, and the depression in water content tapered off with depth to the pre-freezing water content. Since there was no evidence that water was drawn from the reservoirs, this further supports that the "open" system behaved, instead, as a closed system. And third, the increased water content in the frozen zone appears to be accounted for, approximately, by the decreased water content in the soil immediately below the frozen zone. Note that a reduction in water content would also be accompanied by local freezing consolidation if saturation or near saturation is maintained. This development is confirmed by over-consolidation characteristics identified in Figure

5.8. In effect, then, the low permeability of clay makes freezing response essentially a closed system, and prediction of net heave simpler than in silt.
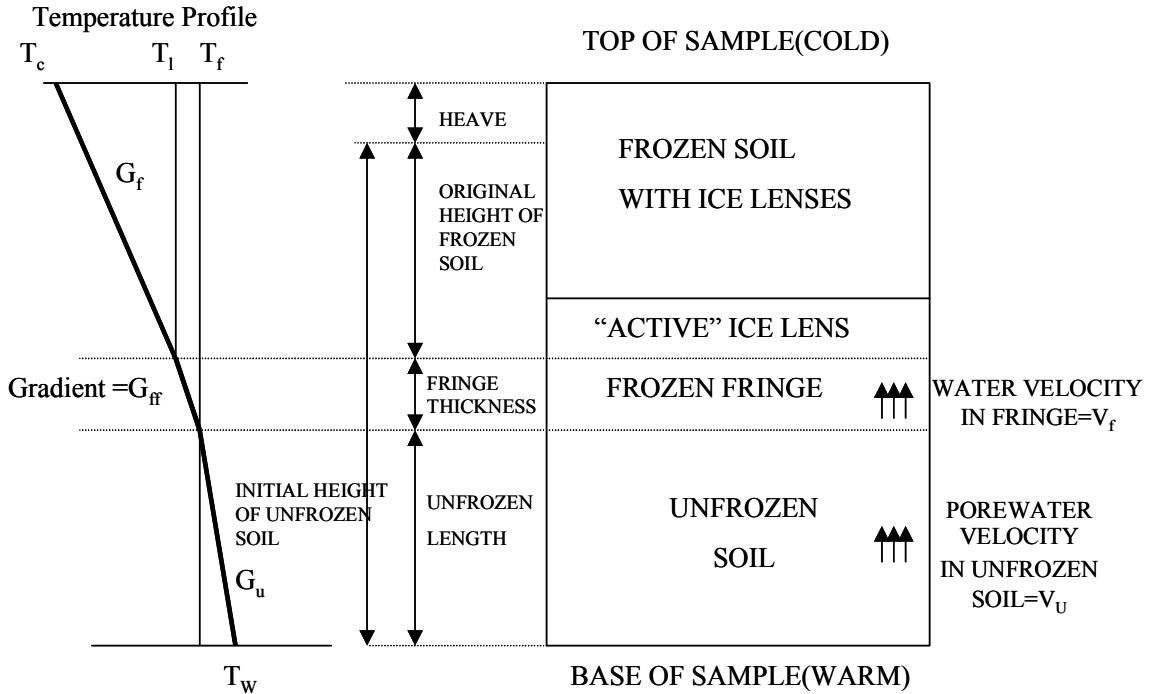
Figure 6. 1 Frost Heave in an idealized one-dimensional soil column (After Nixon, 1992)

The thickness of the depressed water content zone is not constant, but was influenced by the duration of freezing and how slowly the cooling was applied. In models frozen under temperature scheme 2, when cooling was applied slowly and over a long period, the thickness of that depressed water content zone was greater than in models frozen under temperature scheme 1, where ramped cooling was applied somewhat more quickly and freezing duration was shorter, even for models tested at the same scales. Finally, in a step freezing model test where temperature change was applied abruptly, frost heave was very small and the thickness of soil undergoing water content depression was small.

Assuming, then, that the water system in freezing clay is essentially closed, the components of heave, settlement, and net heave are described in the following equations. Net heave in all cases is a result of frost heave due to expansion of voids in the frozen soil, minus consolidation settlement or contraction in the frozen fringe that has given up some portion of its original water content to become ice in the frozen soil. All water in the frozen soil is assumed to have frozen, for simplicity's sake, although it is likely that unfrozen water may remain at these temperatures in clay. If unfrozen water remains, then predicted heave will exceed actual heave by some small amount.

These equations assume initial (i.e. prefreezing) full saturation of the clay which was the condition in these models, however, three cases are developed assuming different final degrees of saturation (by water and ice) in the frozen soil and in the frozen fringe.

Although heave in frozen soil has typically been assumed by other researchers to develop only under saturated conditions, that is, voids are completely filled by some combination of water and ice, with no accompanying air, the degree of saturation after freezing, in both the frozen zone and in the frozen fringe is unknown here, and becomes uncertain. It stands to reason that development of ice lenses in the frozen zone may easily be accompanied by the creation of some air voids in the process. The development of air voids created would seem to depend on the size and shape of individual ice lens, associated with freezing rate, overburden pressure, soil stresses, and initial degree of saturation, for example. Also along these lines, Shoop and Bigl (1997) made a convincing case based on results from their full scale, long

term, laboratory experiments that full saturation cannot be assumed to be the case in the frozen, heaving soil. They reported average saturation of the frozen soil in their experiments to be 87%. Unfortunately, the degree of saturation of the frozen zone in this research could not be measured because the University of Maryland does not possess the appropriate apparatus.

It is also possible that some air voids may develop in the frozen fringe, as water is being drawn up into the frozen zone by the suction created by temperature gradient. This case seems unlikely, as freeze consolidation, created in response to suction in the frozen fringe pore water, would be less likely if saturation fell much below 100%. Loss of saturation in this zone would be more likely to occur if a phreatic surface is far below the freezing front. This last scenario (denoted as Case 2) is explored below for completeness, but was not investigated using data from experiments.

The simple consolidation settlement equation, $\Delta H = \left(\dfrac{H_f \, \Delta e}{1 + e_o} \right)$, is the beginning of the model of equations that explain frost heave. The challenge is to predict or explain changes in void ratios – expansion in the frozen zone and compression in the frozen fringe zone immediately below -- and degree of saturation (or development of air voids) as well as thicknesses of those two zones. The equations developed below use experimental data to explain response and to shed light on the magnitude of these parameters.

Case 1: Full saturation is assumed to be maintained throughout freezing.

Consider, first, the frozen soil layer that undergoes expansion. Expansion is dependent on the combined effect of drawing water from the soil below the frozen zone, and the freezing of that "new" water, as well as the pore water already existing

139

in that zone. When no air voids are assumed to develop anywhere in the soil as a

result of soil water freezing, the expansion can be explained through the changes in

void ratios:

$$\text{Frost heave} = \left(\frac{1.09 \times e_f - e_i}{1 + 1.09 \times e_f} \right) \times H_f, \quad \text{............................. Equ'n 6.1}$$

The water drawn from below the frozen soil layer will lead to compression of that

affected layer, and that settlement can be explained as:

$$\text{Settlement} = \left(\frac{e_f - e_i}{1 + 1.09 \times e_f} \right) \times H_f \quad \text{... Equ'n 6.2}$$

$$\text{Net Heave= Frost Heave} - \text{Settlement} = \left(\frac{0.09 \times e_f}{1 + 1.09 \times e_f} \right) \times H_f \text{ .... Equ'n 6.3}$$

To balance the water equation for the self-creating closed system, the thickness of the

frozen fringe is predicted to be:

$$\text{Thickness of the Frozen Fringe} = \left(e_f - e_i \right) \times \left(\frac{1 + e_{ff}}{e_i - e_{ff}} \right) \times \frac{1}{1 + 1.09 \times e_f} \times H_f . \text{ Equ'n 6.4}$$

Here, e_i = initial void ratio of the sample, e_f = final void ratio in the frozen zone, e_{ff} =

final void ratio in the frozen fringe, H_f = depth of freezing including frost heave

(measuring from the frozen soil surface to the bottom of the frozen soil layer), S_{rf} =

degree of saturation in the frozen zone, S_{rff} = degree of saturation in the frozen fringe.

Note that e (void ratio) is calculated from the water content using the equation of

$S*e=w*Gs$; therefore, when S_r = 100%, e = w G_s.

Case 2. Full saturation is assumed to be maintained in the frozen zone, but partial saturation develops in the frozen fringe

The following equations apply, first to the expansion in the frozen soil:

$$\text{Frost heave} = \left(\frac{1.09 \times e_f - e_i}{1 + 1.09 \times e_f} \right) \times H_f, \quad \dots\dots\dots\dots\dots\dots\dots\dots\dots\dots\dots \quad \text{Equ'n 6.5}$$

The equation for compression or settlement in the frozen fringe:

$$\text{Adjusted Settlement} = \left(\frac{e_i - e_{ff}}{e_i - S_{rf} \times e_{ff}} \right) \times \left(\frac{e_f - e_i}{1 + 1.09 \times e_f} \right) \times H_f \quad \dots\dots\dots\dots \quad \text{Equ'n 6.6}$$

The net heave is calculated as:

Adjusted Net Heave = Frost Heave – Adjusted Settlement

Adjusted thickness of Frozen Fringe

$$= \left(e_f - e_i \right) \times \left(\frac{1 + e_{ff}}{e_i - S_{rf} \times e_{ff}} \right) \times \frac{1}{1 + 1.09 \times e_f} \times H_f \quad \dots\dots\text{Equ'n 6.7}$$

Case 3. Partial saturation is assumed to develop in the frozen zone, but full saturation is maintained in the frozen fringe,

The following equations apply, first to the expansion in the frozen soil:

Fig 6.2 shows the phase diagrams for Case 3.

$$\text{Adjusted Frost Heave} = \left(\frac{1.09 \times e_f - S_{rf} \times e_i}{S_{rf} + 1.09 \times e_f} \right) \times H_f, \quad \dots\dots\dots\dots\dots\dots\dots \quad \text{Equ'n 6.8}$$

The equation for compression or settlement in the frozen fringe:

$$\text{Settlement} = \left(\frac{e_f - e_i}{1 + 1.09 \times e_f} \right) \times H_f \quad \dots\dots\dots\dots\dots\dots\dots\dots\dots\dots\dots \quad \text{Equ'n 6.9}$$

The net heave is calculated as:

Adjusted Net Heave = Adjusted Frost Heave – Settlement

Adjusted thickness of Frozen Fringe

$$= \left(e_f - e_i\right) \times \left(\frac{1 + e_{ff}}{e_i - e_{ff}}\right) \times \frac{1}{1 + 1.09 \times e_f} \times H_f \dots \text{ Equ'n 6.10}$$

A	Frozen Zone
B	Frozen Fringe
C	Unfrozen Zone

A:

B:
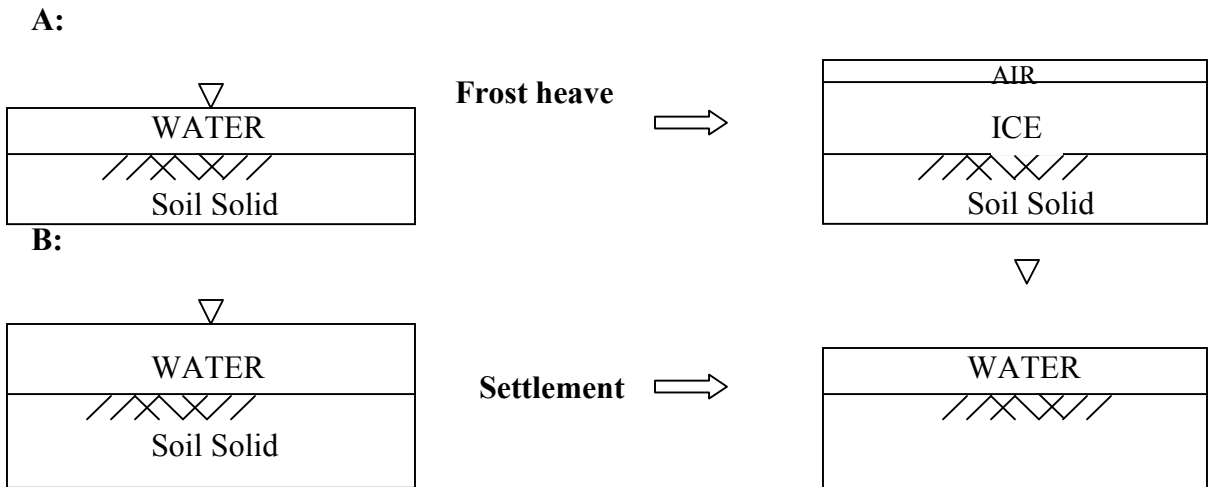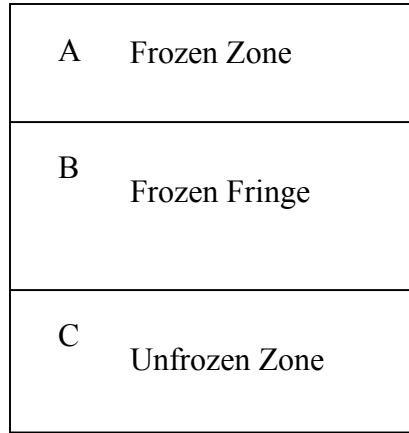
Figure 6. 2 Phase Diagram Concepts for Case 3

6.2 MODEL APPLIED TO EXPERIMENTAL RESULTS

Data from the physical models were input to the equations to compare predictions to observations, and from that to develop an appreciation of the overall system mechanics.

For Case 1, full saturation was assumed throughout the system and throughout the duration of the freezing. Input to equations 6.1, 6.2, and 6.3 included initial and final water contents in the frozen soil, and thickness of the frozen zone. Output was predicted heave and thickness of the frozen fringe. Table 6.1 shows the resulting predictions.

The magnitudes of net heaves predicted using the Case 1 assumptions are much smaller than all the measured values of heave except for two step-frozen model results, model test numbers T22 and T27. In fact, no predicted heave for Case 1 is greater than 40% of the measured heave except the two step frozen models that two values are close each other. A sensitivity analysis indicates, too, that predicted values using these Case 1 equations for net heave are sensitive only to the depth of freezing. Even accounting for experimental inaccuracy in measurement of that depth, the predictions are not considered adequate.

Case 3 equations were then tested against the data. In the Case 1 exercise, equations were used to predict heave, which was compared to experimentally measured heave. In this second test, net heave was also input to the Case 3 equations, along with all other experimentally measured values input in the previous Case 1 test. The degree of saturation in the frozen zone was then back-calculated to make the calculated and measured values of heave equal, and from that to assess both the

sensitivity of the solution to degree of saturation and the reasonableness of back-calculated values. Table 6.2 shows the summary of results of all the models in this research. The results of these back calculated values are discussed by the test target categories. These categories are organized based on the centrifugal accelerations, freezing mode, temperature scheme, and etc. Degrees of saturation are average values through the depth of freezing.

First, for the tests grouped to examine centrifugal acceleration effect on frost heave, the degree of saturation back-calculated in the frozen zone in 1g models was marginally but consistently larger than that back-calculated in Ng models by 0.01 to 0.02. This modest difference is attributed to the smaller overburden pressure applied during freezing in the 1g models, compared to the otherwise identical Ng models. The degrees of saturation calculated for Ft.Edwards clay models are greater than those for kaolin models. This is attributed to the lower permeability and the lower initial water content and void ratio of Ft.Edwards clay models.

In models grouped to explore the effects of freezing regime on frost heave, the degree of saturation in step frozen models is very close to 1. This means that fully saturated condition in specimens before freezing appears to have persisted throughout the freezing duration due to the abrupt cooling of step freezing mode, and the absence of conditions that promote the development of ice lenses. For ramp frozen models, in contrast, freezing is slow, ice lenses develop, and air voids appear to develop, judging from the back-calculated values of degree of saturation.

Table 6. 1 Results of Predictive Model Application for Case 1

Soil	Ng	Test No	‡F.R	w_{EOC}[1] %	w_F[3] %	w_{FF}[4] %	H_f[5] cm	Δh_f[6] cm	Predicted Heave, cm	S_{rf}[7]
Effect of gravitational acceleration										
K	1(35)	T11	1	61	90	51	2.0	0.42	0.12	1.0
	35	T13	1	61	110	49	1.5	0.29	0.09	1.0
	1(45)	T39	1	61	92	52	1.3	0.32	0.08	1.0
	45	T37	1	61	105	50	1.0	0.25	0.06	1.0
E	1(35)	T54	1	45	49	40	1.6	0.23	0.08	1.0
	35	T38	1	45	48	41	1.5	0.19	0.07	1.0
Freezing regime effects										
K	35	†T22	1	61	85	45	1.5	0.10	0.08	1.0
	45	†T27	1	61	90	45	1.3	0.09	0.07	1.0
Water table effects										
K	35	T41	1	61	115	49	1.5	0.31	0.09	1.0
Repeatability										
K	35	T14	1	61	109	48	1.5	0.29	0.09	1.0
	35	T31	1	61	103	49	1.5	0.28	0.10	1.0
	45	T17	1	61	107	51	1.3	0.25	0.08	1.0
	55	T52	2	50	74	42	1.0	0.18	0.09	1.0
Modeling of models: one-step ramp										
K	35	(T13)	1	61	110	49	1.5	0.29	0.09	1.0
	45	(T37)	1	61	105	50	1.0	0.25	0.06	1.0
	55	T55	1	61	92	51	0.7	0.12	0.04	1.0
E	35	(T38)	1	45	50	42	1.5	0.19	0.07	1.0
	45	T43	1	45	50	42	1.0	0.10	0.05	1.0
	55	T48	1	45	50	42	0.7	0.06	0.03	1.0
Modeling of models: two-step ramp, longer freezing, milder freezing rate										
K	35	T47	2	50	76	42	1.8	0.24	0.10	1.0
	45	T46	2	50	72	42	1.5	0.20	0.08	1.0
	55	T45	2	50	73	41	1.1	0.15	0.06	1.0
E	35	T51	2	45	50	39	1.8	0.19	0.09	1.0
	45	T50	2	45	49	41	1.3	0.16	0.06	1.0
	55	T49	2	45	49	41	1.1	0.12	0.05	1.0

Note: [1] w_{EOC} = water content at the end of consolidation, but before freezing

[2] N = centrifuge acceleration

[3] W_F = water content in the frozen zone after freezing (measured)

[4] W_{FF} = water content in the frozen fringe after freezing (measured)

[5] H_f = depth of freezing (measured)

[6] Δh_f = net heave (measured)

[7] S_{rf} = degree of saturation in the frozen zone (assumed to be 100%)

‡ = Freezing Regime

† = Step Freezing, all other model are ramp freezing

( ) = the duplicate test for grouping purpose

In the models grouped to examine modeling of models, the models for one-step ramp freezing have somewhat larger degrees of saturation than those for two step ramp freezing models. Three observations are relevant.

- First of all, within the one-step ramp freezing models, the 55g model of kaolin, and the 45g, and the 55g model of Ft.Edwards clay have larger back calculated degrees of saturation than the 35g model of each soil. Those models, discussed in Section 5.6, were judged to face issues of scaling effects, in which model rate of freezing was too fast for the rate of delivery of water to the freezing soil – that is, the clay permeability was too small to keep up with the demand for water. These models, then, were behaving somewhat as if they were step frozen, and consistent with findings for step frozen models, degree of saturation remained high.

- Secondly, within the second step ramp freezing models, models of freezing of Ft.Edwards clay which has lower initial water content and permeability, again have greater degrees of saturation than kaolin.

- Thirdly, comparison of responses of kaolin models between one step ramp freezing and two step ramp freezing indicates that degree of saturation in the frozen zone appears to increase as freezing duration becomes longer and rate becomes slower. This can be generalized to conclude that soil with larger ratios of heave/DOF had smaller final average degrees of saturation

Below the last ice lens in the "frozen zone", is the frozen fringe. The division between this frozen layer and the frozen fringe is identified by the last visible ice lens. The thickness of frozen fringe itself, in contrast, is somewhat difficult to measure

because the transition from the frozen fringe to the unfrozen layer is less clearly marked. However, its distinguishing features include its obviously denser condition, the absence of visible ice lenses, and its depressed water content. The thicknesses of the frozen fringe in models were also calculated by the simple predictive model based on the assumption that all water content increase in the frozen zone was due to the flow of water from the frozen fringe. The measured values of thickness of the frozen fringe are in the range of 4 cm to 5 cm for kaolin, and 2 cm to 3 cm for Ft.Edwards clay- only considered to be approximate due to the difficulty in measuring this thickness mentioned earlier- which are found to be reasonable when compared to calculated values of thickness.

In comparing the experimental values of the final magnitude of heave to those calculated by the predictive model, the Case 3 condition that allowed for a reduction in saturation as heave develops, produced the "best" fit. In this context, "best" refers to a simple model of heave that fits with measurable experimental data, and the conclusions of previous researchers – Shoop and Bigl (1997) – who also sought to compare numerical predictions of heave with full scale experimental data of frost heave development. Further testing of this approach is clearly required, applying it to a broad range of soil conditions. Freezing response of unsaturated clay must also be the subject of further study.

Table 6. 2 Results of Predictive Model Application for Case 3

Soil	Ng	Test No	‡F.R	w_{EOC}[1] %	w_F[3] %	w_{FF}[4] %	H_f[5] cm	Δh_f[6] cm	Thickness of FF[7], cm	S_{rf}[8]
Effect of gravitational acceleration										
K	1(35)	T11	1	61	90	51	2.0	0.42	4.8	0.86
	35	T13	1	61	110	49	1.5	0.29	5.3	0.88
	1(45)	T39	1	61	92	52	1.3	0.32	4.7	0.86
	45	T37	1	61	105	50	1.0	0.25	4.9	0.87
E	1(35)	T54	1	45	49	40	1.6	0.23	3.0	0.92
	35	T38	1	45	48	41	1.5	0.19	2.0	0.93
Freezing regime effects										
K	35	†T22	1	61	85	45	1.5	0.10	3.6	0.99
	35	(T13)	1	61	110	49	1.5	0.29	5.3	0.88
	45	†T27	1	61	90	45	1.3	0.09	3.6	0.98
	45	(T37)	1	61	105	50	1.0	0.25	4.9	0.87
Water table effects										
K	35	T41	1	61	115	49	1.5	0.31	5.4	0.85
	35	(T13)	1	61	110	49	1.5	0.29	5.3	0.88
Repeatability										
K	35	T14	1	61	109	48	1.5	0.29	5.2	0.88
	35	T31	1	61	103	49	1.5	0.28	5.9	0.87
	45	T17	1	61	107	51	1.3	0.25	5.1	0.86
	55	T52	2	50	74	42	1.0	0.18	3.3	0.89
Modeling of models: one-step ramp										
K	35	(T13)	1	61	110	49	1.5	0.29	5.2	0.86
	45	(T37)	1	61	105	50	1.0	0.25	5.1	0.85
	55	T55	1	61	92	51	0.7	0.12	2.3	0.89
E	35	(T38)	1	45	50	42	1.5	0.19	2.2	0.93
	45	T43	1	45	50	42	1.0	0.10	1.4	0.95
	55	T48	1	45	50	42	0.7	0.06	1.0	0.97
Modeling of models: two-step ramp, longer freezing, milder freezing rate										
K	35	T47	2	50	76	42	1.8	0.24	4.8	0.91
	45	T46	2	50	72	42	1.5	0.20	3.8	0.92
	55	T45	2	50	73	41	1.1	0.15	2.9	0.92
E	35	T51	2	45	50	39	1.8	0.19	2.6	0.94
	45	T50	2	45	49	41	1.3	0.16	2.3	0.93
	55	T49	2	45	49	41	1.1	0.12	2.0	0.94

Note: [7] FF = The thickness of the Frozen fringe (predicted)

[8] S_{rf} = degree of saturation in the frozen zone (back-calculated)

† = Step Freezing, all other model are ramp freezing

( ) = the duplicate test for grouping purpose

The physical models also provide data for analysis of the development of heave over time. The final depth of freezing, identified at the end of tests during model dissection by measuring the location of the deepest ice lens, coincided with the −1.2ºC isotherm, and not the 0ºC isotherm, which is usually too warm for ice to form in fine grained soils with very small pores. The −1.2ºC isotherm was therefore assumed to represent the ongoing depth of freezing for this exercise.

Model T11 was a 1g one step ramp frozen kaolin model. Figure 6.3 shows the penetration depths of the 0ºC isotherm and the −1.2ºC isotherm. Figure 6.4 shows the same data replotted as penetration rate of the 0ºC and the −1.2ºC isotherms of 1g model during freezing, and accompanying Figure 6.5 shows the measured development of frost heave plotted as rate of heave. The figures show that patterns of the penetration rates of these freezing temperatures agree well with the rates of measured frost heave. The 0ºC isotherm starts to penetrate into the clay at t = 0.90 hr, and its penetration rate steadily increases until t = 1.32 hr, which coincides with the time of maximum frost heave rate. The −1.2ºC isotherm starts to penetrate into clay specimen at t = 1.20 hr, a little later than the 0ºC isotherm. It reaches its maximum penetration rate at the same time as the 0ºC isotherm. It is worth noting that maximum rate of frost heave, and freezing temperature penetration both occurred when the soil surface reached −2ºC, and before it reached the colder ultimate boundary temperature of −3ºC. This indicates that local, transient temperature gradients are likely to be more important than overall averaged temperature gradients in development of heave.

Plots of development of heave from the physical models allow an additional check on the usefulness of the predictive models, well beyond comparison of ultimate values of heave alone. A prediction of development of heave through the duration of freezing, then, was computed by inputting the known, continuous penetration of the depth of freezing -- which was tracked from the internal temperature profiles in the models – into the Case 3 method of predicting heave. As noted previously, there was evidence that the $-1.2ºC$ isotherm was the critical freezing isotherm, so this was assumed to represent the ongoing depth of freezing for this exercise.
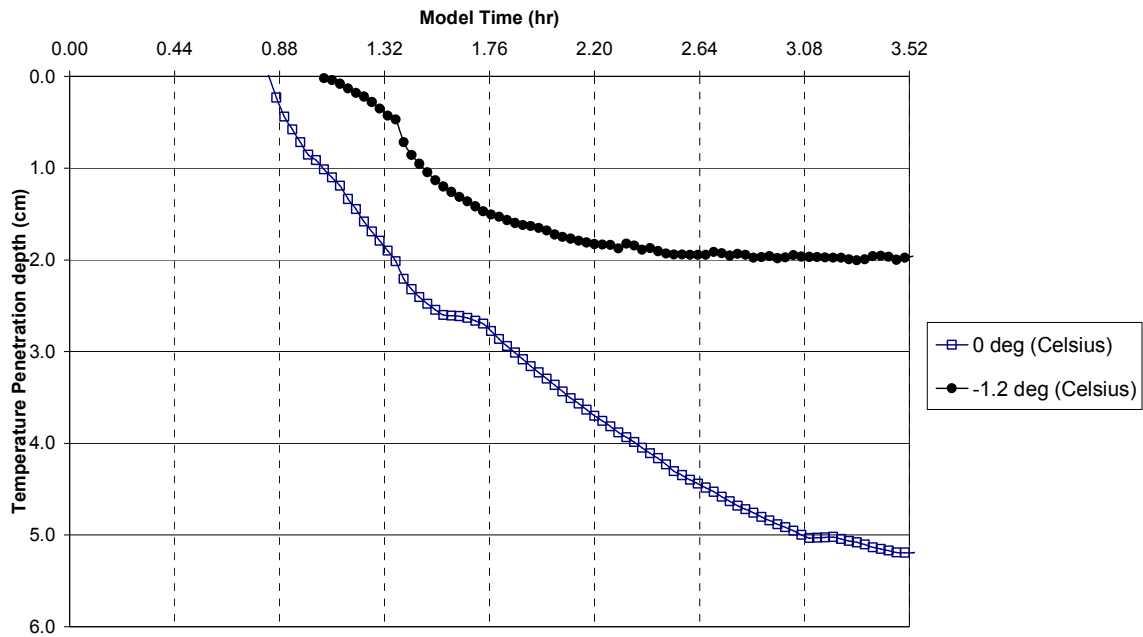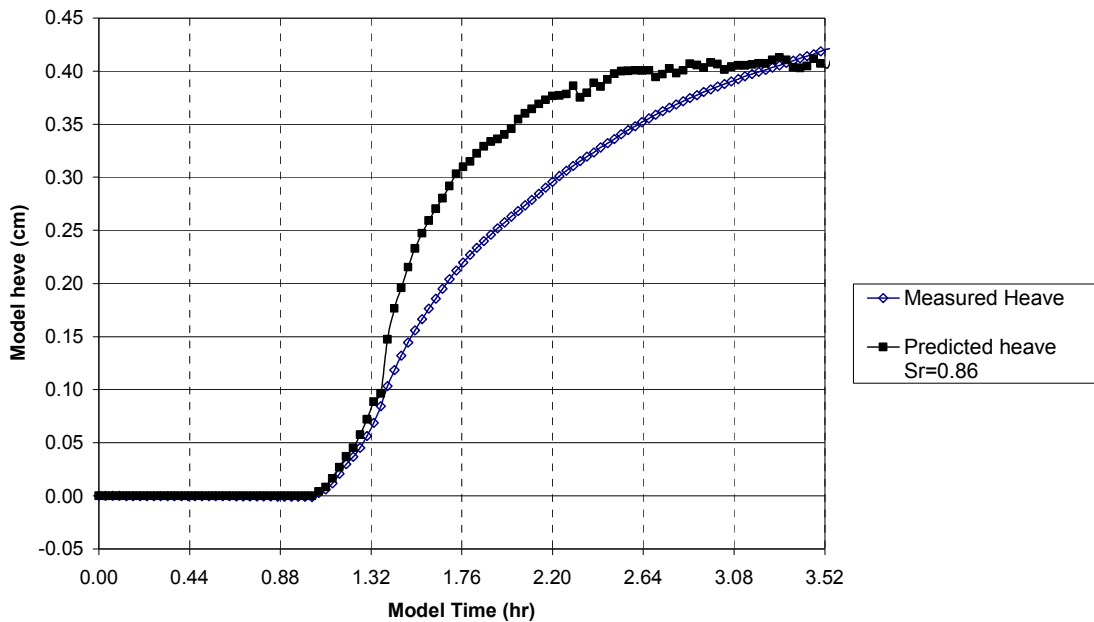

Figure 6. 3 Temperature penetration depth vs. Time for kaolin model of one step ramp freezing at 1g (T11)
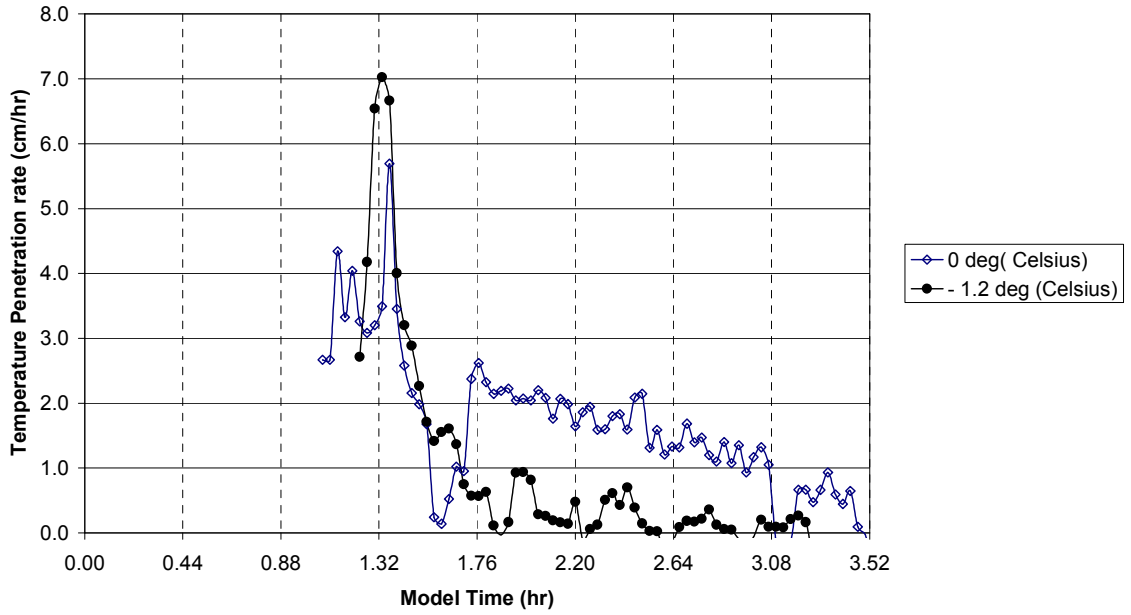
Figure 6. 4 Temperature penetration rate vs. Time for kaolin model of one step ramp freezing at 1g (T11)
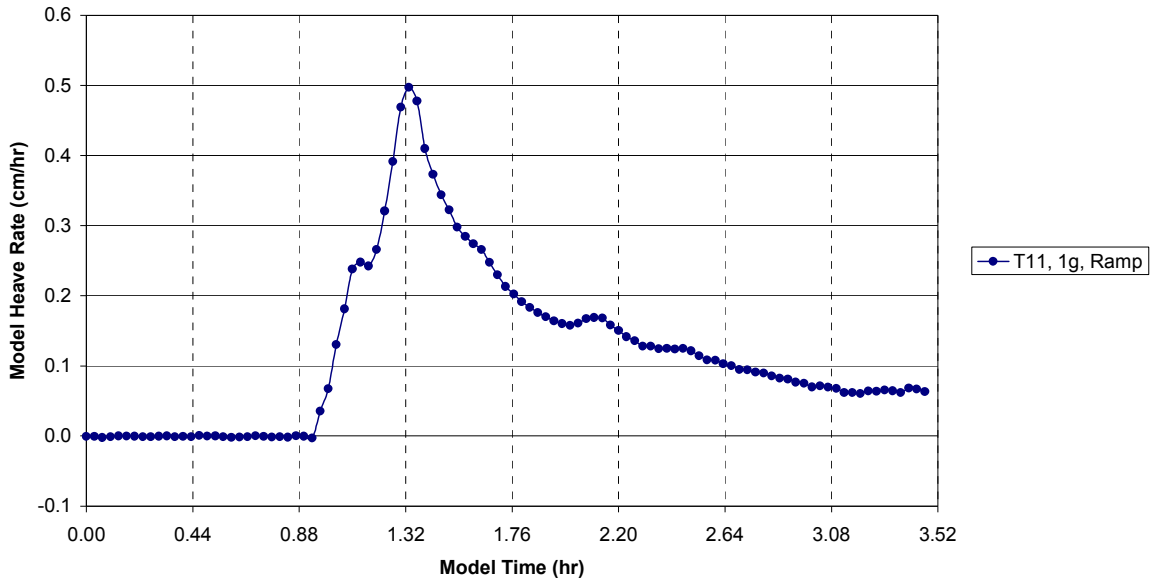

Figure 6. 5 Frost heave rate curve for kaolin model of one step ramp freezing at 1g

Figure 6. 6 Measured Heave vs. Predicted Heave for kaolin model of one step ramp freezing at 1g (T11)

Figure 6.6 shows a plot of predicted heave and measured heave for physical model T11, which was a kaolin model frozen at 1g in response to one step ramping. Case 3 assumptions of behavior were used in the calculations. Degree of saturation, which was back calculated to average 86% at the conclusion of the freezing test, was assumed to be constant and take effect as soon as heaving began in this calculation. This led to predicted heave that is larger than measured heave throughout freezing period, with values converging only at the end of freezing. A sudden change in degree of saturation from 100% to 86% which then persists throughout the freezing period is unlikely, however. It is more likely that the degree of saturation would decrease gradually from 100% to its final value over the duration of the test, ultimately reaching some asymptotic value, although that final "value" might not have been achieved during the period of this testing, since heave continued to develop, even

though the internal temperatures had stabilized. In order to test this hypothesis, the period between the initiation of heave and the end of the test was divided into six evenly spaced intervals, and the degrees of saturation were back-calculated to cause the predicted heave to equal the measured heave. This change in the degree of saturation over freezing period is plotted in Figure 6.7, and is clearly reasonable. This is considered to strengthen confidence in this method of frost heave prediction.
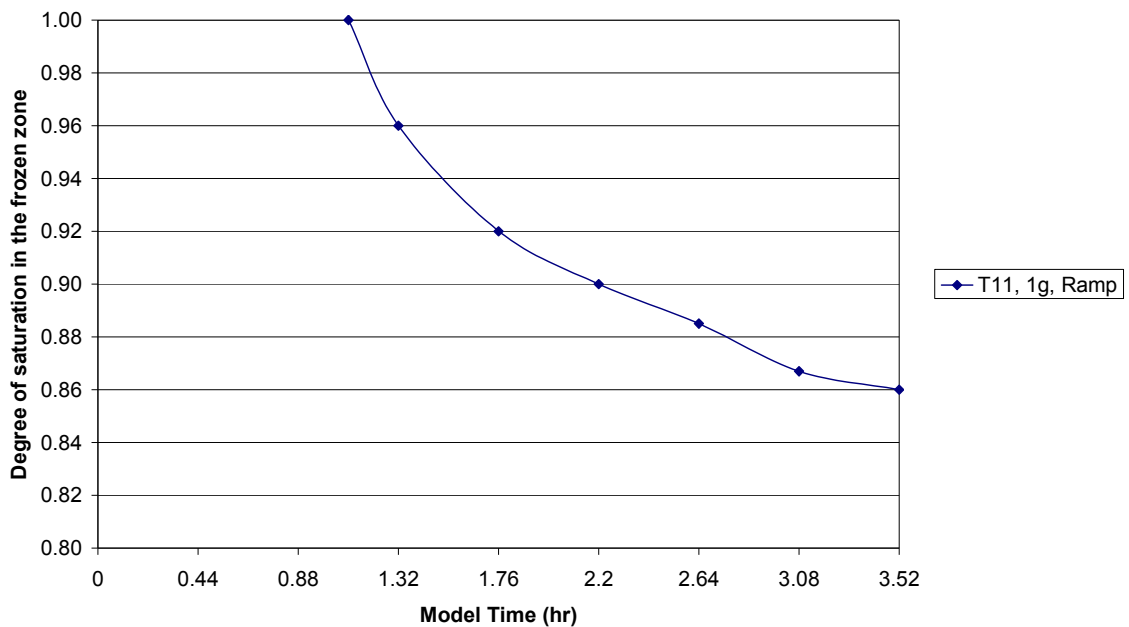
Figure 6. 7 Degree of saturation vs. Time for kaolin model of one step ramp freezing at 1g (T11) using Case 3 assumptions

The same process was then repeated for a step frozen kaolin model at 35g (T22). Its final degree of saturation, based on Case 3 analysis, was 99%. The 0ºC, and the −1.2 ºC isotherms for this model are shown in Figure 6.8. In Figure 6.9, these temperatures are also plotted as penetration rate. As in the case of the previous model, temperature penetration rates are greatest at the beginning of freezing, and steadily decrease. The changing depths of the 0°C isotherm, and the −1.2°C isotherm were

input to the Case 3 equation to predict heave. The predicted value and measured values are shown in Figure 6.10 and agreement is good without tuning degree of saturation throughout, since final degree of saturation was only marginally less than the initial condition of 100% saturation.
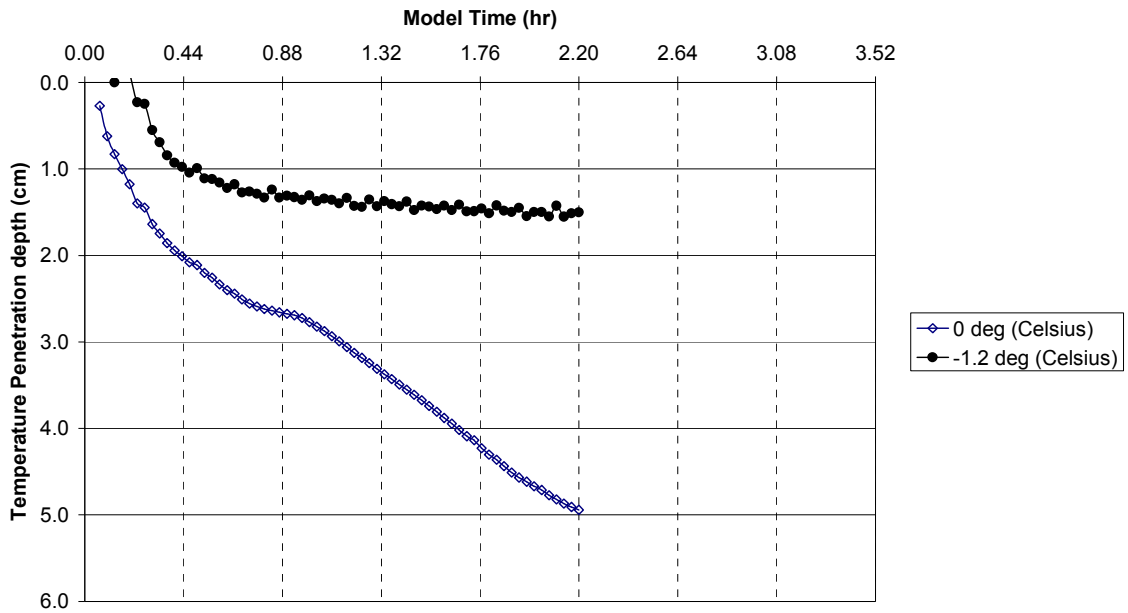
Figure 6. 8 Temperature penetration depth vs. Time for step frozen kaolin model at 35g (T22)
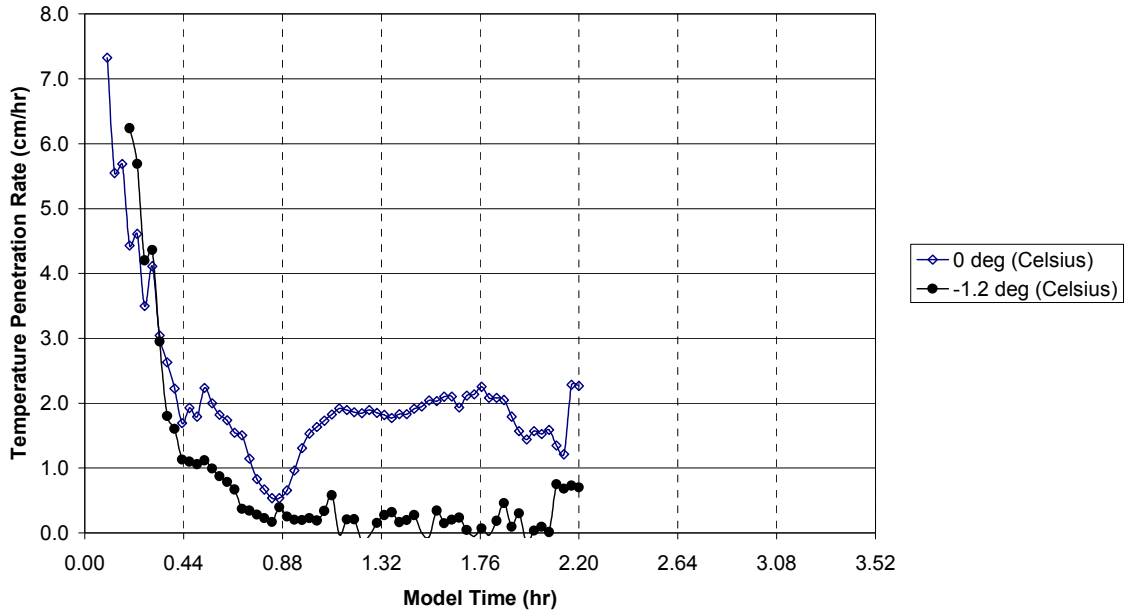
Figure 6. 9 Temperature penetration rate vs. Time for step frozen kaolin model at 35g(T22)
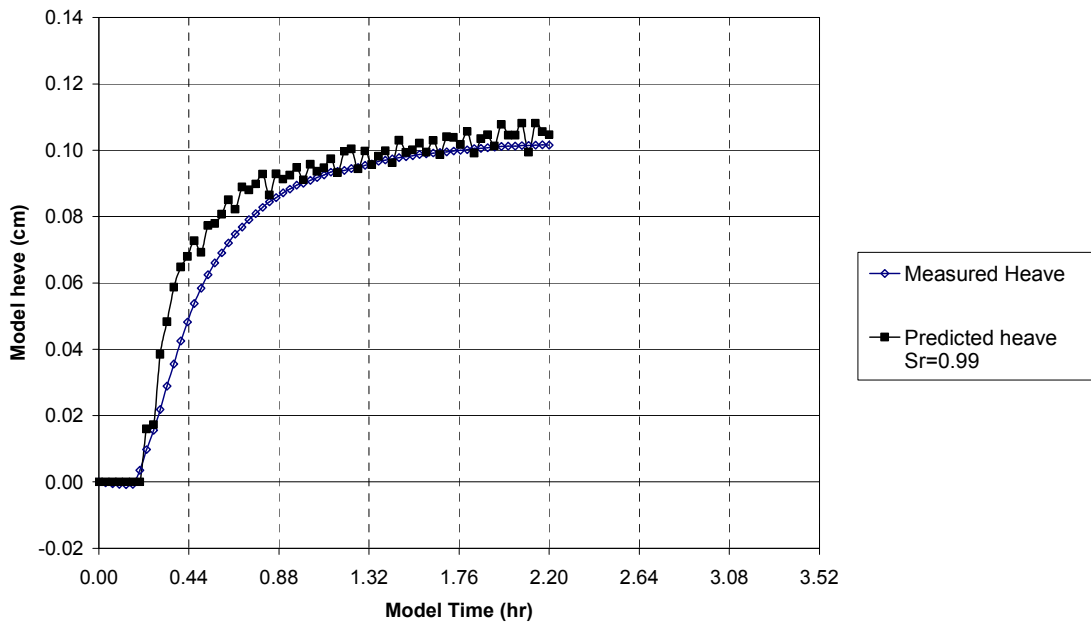
Figure 6. 10 Measured Heave vs. Predicted Heave for step frozen kaolin model at 35g (T22)

155

Development of heave for the 35g, two step ramp-frozen kaolin model T47 was predicted following the same procedure. Final degree of saturation for this model was 91%. The penetration of the 0ºC isotherm, and the −1.5 ºC isotherm are shown in Figure 6.11. For this model, the final depth of freezing, identified at the end of tests during model dissection by the location of the deepest ice lens, coincided with the − 1.5ºC isotherm, which was very slightly less than in than previous models by 0.3ºC. The reasons for this difference can be one of following causes or combinations: 1) there might easily be measurement errors in terms of temperature and frozen depth; 2) all the internal temperatures were not +3.0ºC at the beginning of freezing; 3) this model was frozen under freezing regime that applies slower cooling rate and longer duration.

In Figure 6.12, temperature penetration rates are also plotted. The fact that the temperature regime involved two ramps to reach the ultimate temperature, and the total freezing period was longer than in other regimes allows a more demanding test of the predictive model. As for the previous cases, the penetration rate change of the 0ºC isotherm and −1.5ºC isotherm again coincide with the timing for the two peaks in frost heave rate as shown in Figure 6.13. When the final degree of saturation (91%) is assumed to apply throughout the heaving period, there are periods when measured heave exceeds predicted heave, as shown in Figure 6.14. Again, dividing the period between the initiation of heaving and the completion of the of the test into six intervals and back-calculating degrees of saturation, leads to a gradual decrease in degree of saturation to the final value of 91% as shown in Figure 6.15.
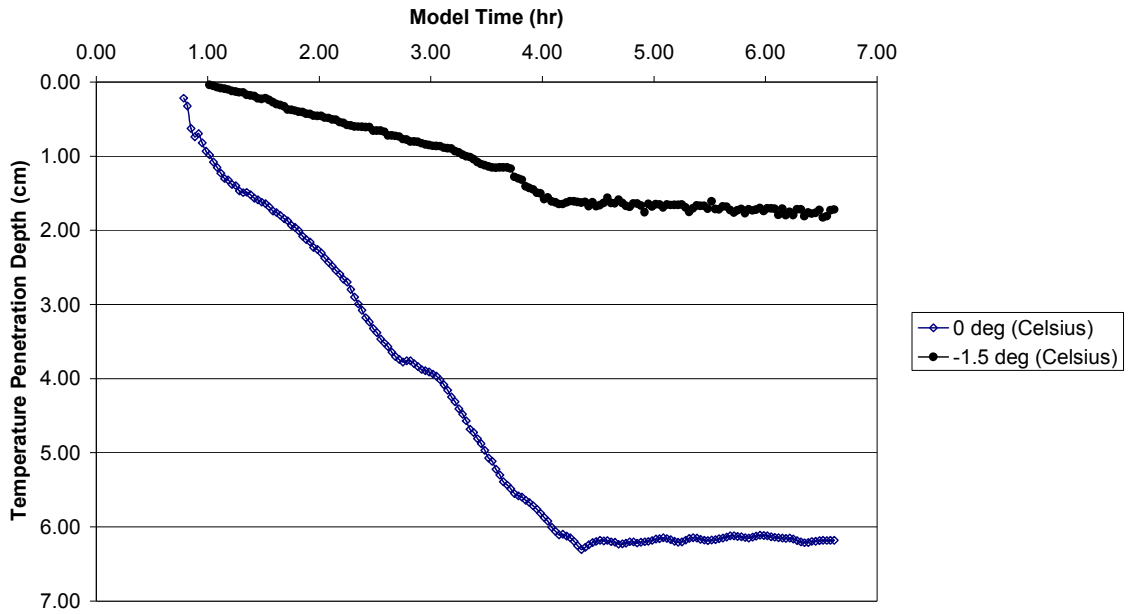
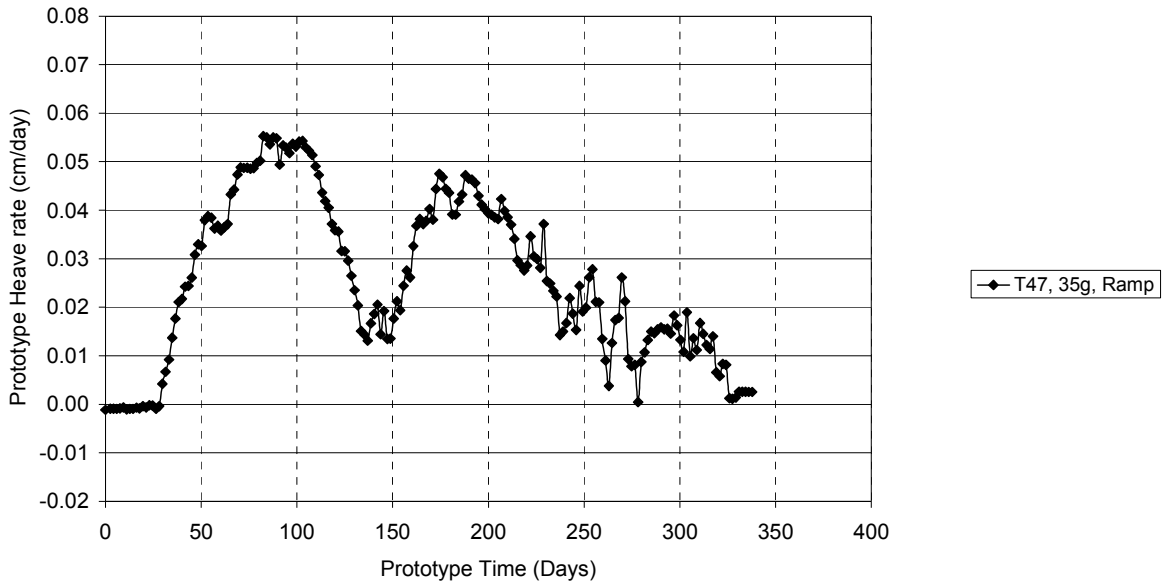**Figure 6. 11 Temperature penetration depth vs. Time for kaolin model of two step ramp freezing at 35g (T47)**
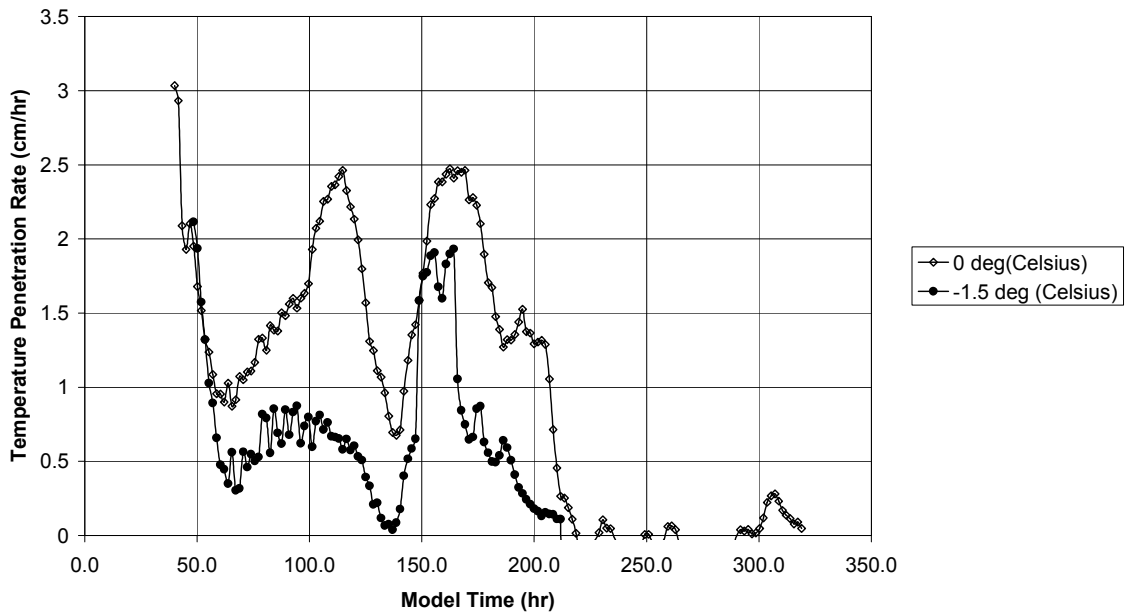
Figure 6. 12 Temperature penetration rate vs. Time for kaolin model of two step ramp freezing at 35g (T47)

Figure 6. 13 Frost heave rate for kaolin model of two step ramp freezing at 35g
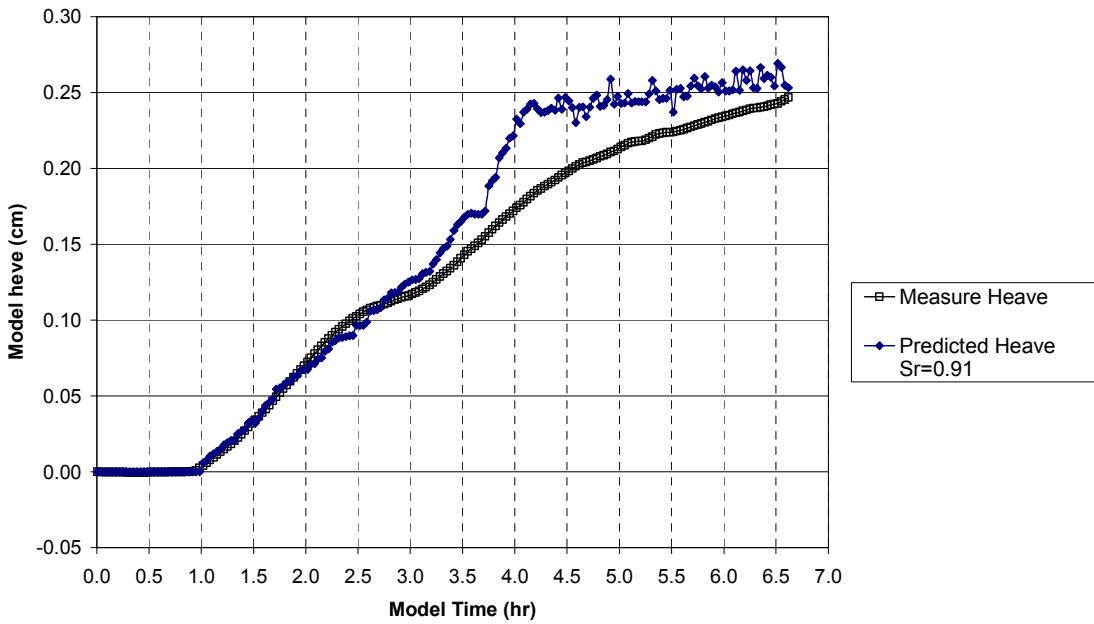
Figure 6. 14 Measured Heave vs. Predicted Heave for kaolin model of two step ramp freezing at 35g using Case 3 assumptions (T47)
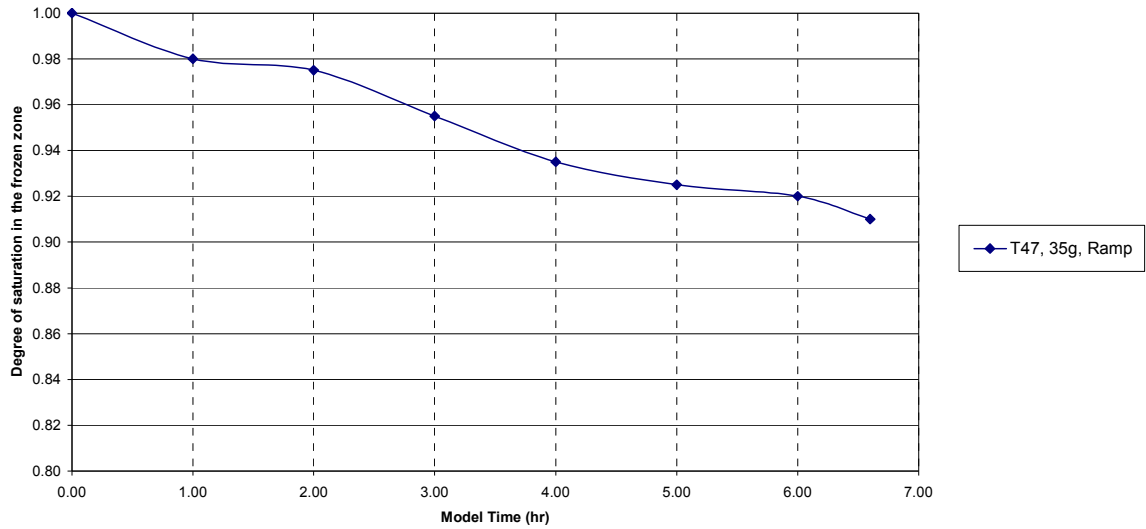
Figure 6. 15 Degree of saturation vs. Time for kaolin model of two step ramp freezing at 35g

Lastly, the same process was then repeated for a one step ramp-frozen Ft.Edwards clay model T38. Its final degree of saturation, based on Case 3 analysis, was 93%. For this model, the final depth of freezing, identified at the end of tests during model dissection by the location of the deepest ice lens, coincided with the -1.2°C isotherm, which is the same as that for one step ramp frozen kaolin models. The penetration rate of the 0°C isotherm, and the -1.2 °C isotherm are shown in Figure 6.17.

Figure 6.18 shows a plot of predicted heave and measured heave for physical model T38. Case 3 assumptions of behavior were again used in the calculations. Degree of saturation, which was computed to average 93% at the conclusion of the freezing test, was assumed to be constant and take effect as soon as heaving began in this calculation. This led to predicted heave that is larger than measured heave throughout freezing period, with values converging only at the end of freezing.

Again, the period between the initiation of heave and the end of the test was divided into six evenly spaced intervals, and the degrees of saturation were back-calculated to cause the predicted heave to equal the measured heave. This change in the degree of saturation over freezing period is plotted in Figure 6.19.

Figure 6. 16 Temperature penetration depth vs. Time for Ft.Edwards clay model of one step ramp freezing at 35g (T38)

**Figure 6. 17 Temperature penetration rate vs. Time for Ft.Edwards clay model of one step ramp freezing at 35g (T38)**
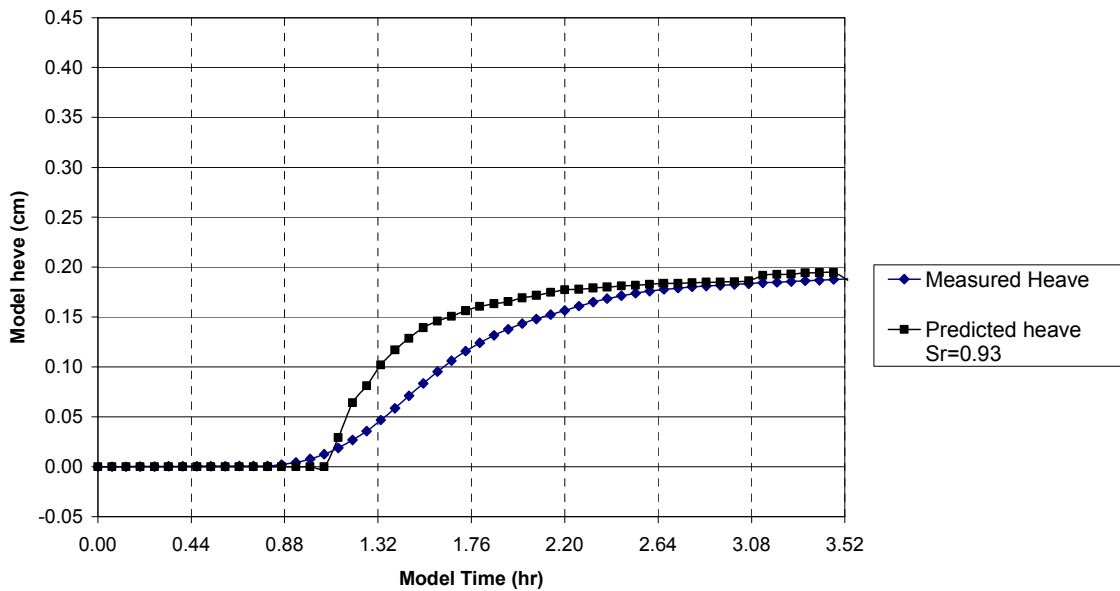
Figure 6. 18 Measured Heave vs. Predicted Heave for Ft.Edwards clay model of one step ramp freezing at 35g using Case 3 assumptions (T38)
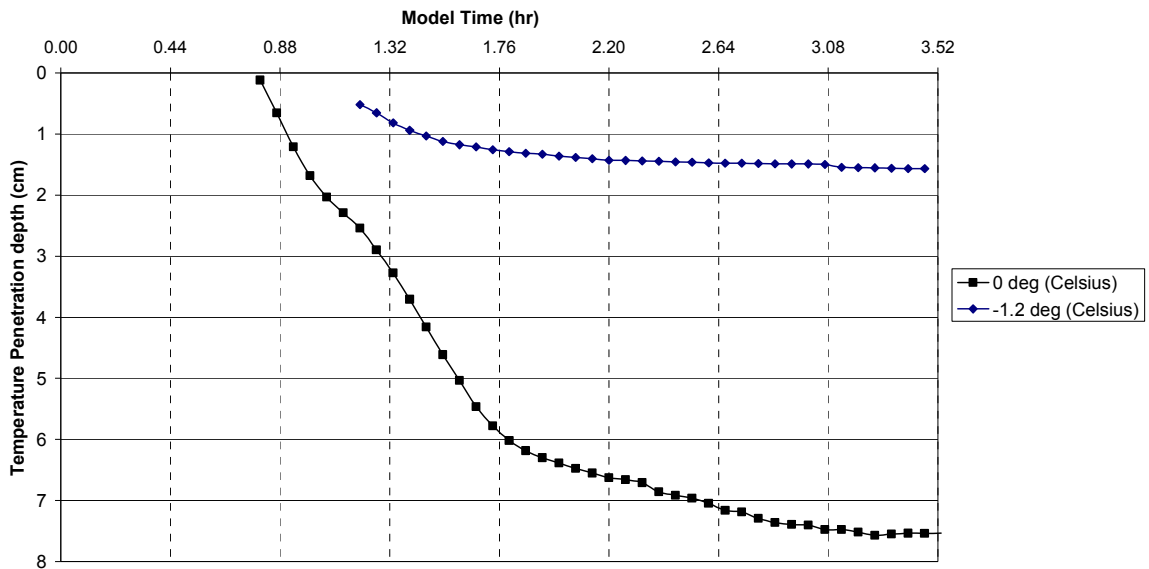
161

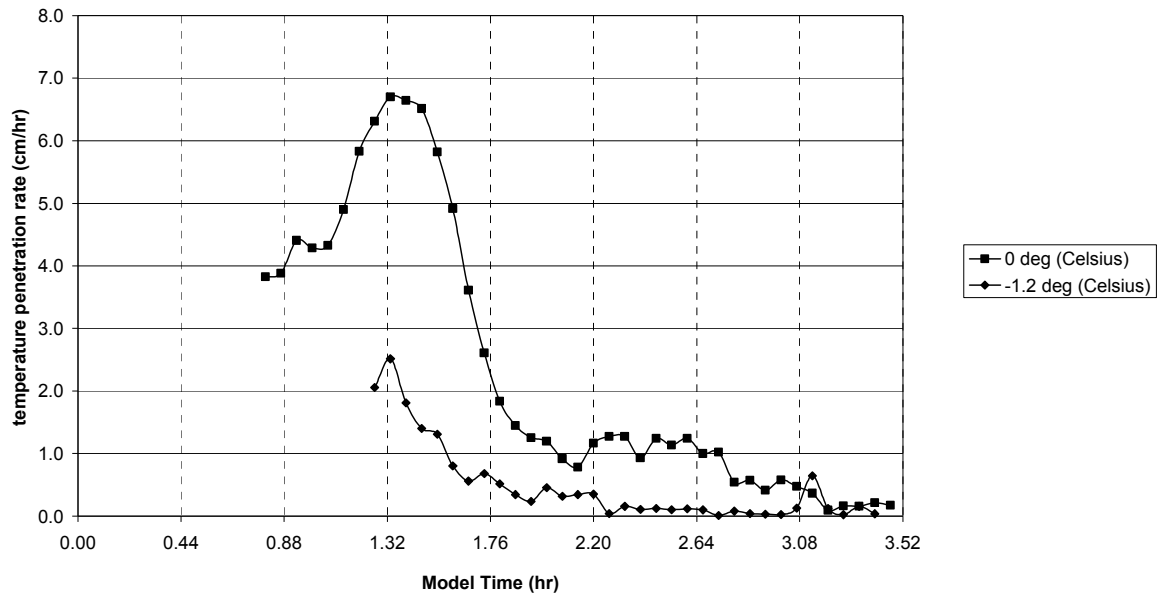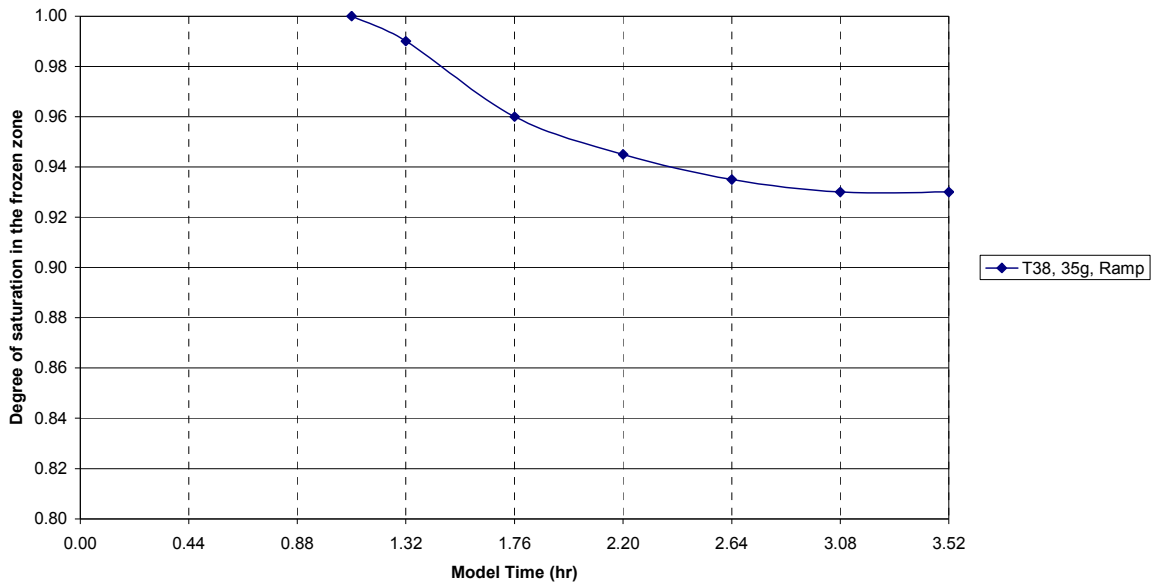**Figure 6. 19 Degree of saturation vs. Time for Ft.Edwards clay model of one step ramp freezing at 35g (T38)**

An analytical model has been developed that explains heaving in clay, supporting the speculation that clay heave behaves as a closed system because of its low permeability. Analysis of the internal temperatures in models and of likely degrees of saturation also suggest the following:

1. In these clays, penetration of an isotherm colder than 0°C appeared to provide a better indicator of development of heave. In these models, this isotherm was between -1.2°C and -1.5°C. This is to be expected in clays in which small pore sizes are shown to be associated with depressed freezing temperatures, however, trace impurities in the water in the models may also bear some responsibility for this freezing point depression. Soil temperatures and temperature gradients in the vicinity of the freezing, are considered to be more

important than more distant boundary temperatures, although, of course, internal temperatures are a result of external and more remote cooling.

2. Degree of saturation of the clays appears to fall to less than 100% during freezing and remains after freezing is complete, in the frozen soil. Degree of saturation seems to be affected by freezing regime (slower freezing leads to more air in the frozen soil); by permeability and void ratio (slower permeability and lower void ratio lead to maintenance of a higher degree of saturation); total stress at the depth undergoing freezing (loss of saturation is more pronounced in soil at lower total stress – this is the case in 1g models, and in Ng models for initial freezing closer to the soil surface. In these models, degree of saturation was back calculated to fall to in the order of 90%, assuming 100% initial, unfrozen saturation; that reduction occurred most quickly in the early stages of freezing, reaching some asymptotic value before the end of the freezing tests conducted in this experimental series.

6.3 RECOMMENDATION FOR EXTENDING THE ANALYTICAL MODEL TO FULL SCALE FIELD CONDITIONS

One desirable goal is to develop a simple analytical model that can both explain, and predict the development of heave in saturated clay. Such a model should be based on verifiable physical events that develop when soil is subjected to freezing conditions, yet it should be simple enough to be practical in terms of its input. Along those lines, Konrad and Morgenstern (1980) emphasized that "… any theory requiring local measurements of high accuracy such as temperature, unfrozen water

content, or permeability of frozen soil cannot result in a theory that will yield practical results."

Data of development of frost heave in saturated clay were gathered in physical models in these experiments. Conditions were well controlled, and stress correct, full system response was measured in the small models. The simple analytical model developed from those external observations can be said to explain full system response in those models to a very acceptable accuracy.

Since internal details of small model response during development of frost heave were impractical to collect, confidence in a broader application of the model to predict heave for many different clay and saturation conditions subjected to a wide range of possible temperature conditions at full scale remains to be developed. Nonetheless, the modeling of models provides support to the assertion that full scale freezing of a soil column with all conditions, including initial degree of saturation and temperature regime, similar to those in these models but N times larger, would be similar to those in these models. That is: depth of freezing, thickness of the frozen fringe, and magnitude of heave would all be N times greater; duration of any events would take N^2 times longer; and model water contents would be similar in similar zones of the soil profile.[1]There is also reason to expect that degree of saturation of an initially saturated clay may fall below 100% in the frozen zone as freezing and heave develop, depending on soil properties and conditions (for example, water content and

---

[1] It is important to note that not all model scales were found to be acceptable predictors of a single full scale equivalent freezing event. This is considered to be an important indicator of the interrelated effects of permeability and rate of freezing on the development of heave that is relevant to full scale conditions. It is also considered to provide a caution that certain model scales may be acceptable for certain freezing regime and soil conditions, whereas progressively smaller models may encounter unacceptable scale effects. This means that scaling correctness should always be checked in soil freezing modeling.

permeability); and freezing regime, including temperature, duration, and temperature-time change gradients.

Unfortunately there is a distinct absence of data in the literature of full scale freezing of clay against which to test this model. This is attributed to the fact that heave in clays has typically been assumed to be negligible. The results of this research, and that of Konrad and Seto (1994) working in Champlain Sea Clay, confirm that clay with large water content, subjected to prolonged, gradual freezing conditions can well produce heave, although those same large water contents will inhibit deep frost penetration. This simple model, then, should be viewed as a first step toward some eventual, practical analytical model of frost heave in clay.

CHAPTER 7: CONCLUSIONS AND RECOMMENDATIONS

7.1 CONCLUSIONS

This research was initiated to investigate the freezing mechanisms of clay, and to make a contribution to the development of a simple analytical model that can characterize frost heave in clay. It was also undertaken to examine the correctness of modeling full scale frost heave in small models cooled on the geotechnical centrifuge to simulate full scale stress conditions.

These objectives were fulfilled by conducting a total of twenty-three model tests, including three 1g freezing tests, and twenty centrifuge tests. The model tests included two clays: a manufactured pure kaolin clay, and a naturally occurring clay provided by the US Army Corps of Engineers Cold Regions Research Engineering Laboratory, Ft.Edwards clay. Models were tested at three different scales of 1:35, 1:45 and 1:55. They were tested under three different cooling regimes: step freezing; single step ramp freezing; and two step ramp freezing. Elevation of the phreatic surface was varied to assess its effect. Models results were checked for repeatability. All model tests were analyzed measuring water content profiles, frost heave rate, and cooling rate. These observations provided the foundation to develop the analytical model. The following conclusions were drawn from the results of the physical models.

1. Centrifugal acceleration was found to influence the magnitude and the development of frost heave compared to freezing of similarly sized models frozen at 1g. The soil columns ramp frozen at 1g developed more heave than the

otherwise identical specimen frozen at Ng sample. Early rates of heave in 1g models clearly exceeded early rates of heave in centrifuge models, but longer term rates were similar. Depths of freezing were greater in 1g models than in centrifuge models. Unexpectedly, ratios of (heave/depth of freezing) were similar in 1g and centrifuge models, when soil and cooling regimes were the same.

Water contents in the frozen zone, that is through the depth of freezing (DOF) where ice lenses are observable, were greater in Ng models than in corresponding 1g models. This is attributed to two effects. First, the decrease in freezing temperature that occurs at higher stress, permits water to continue to flow to the freezing zone longer and at cooler temperatures. Second, the fact that magnitude of heave at 1g was greater than in corresponding Ng models, even though water contents were similar or less, suggests degree of saturation falls below 100%, and is less in 1g models than in Ng models.

Ice lenses developed in all models, but were too small and too variable in size to identify differences between 1g and Ng models.

These effects were noted in both the kaolin models and the Ft Edwards clay models, and were more pronounced in the kaolin models in which permeability and water contents were larger.

2. Freezing consolidation that was observed to occur in freezing clay by many researchers was verified indirectly by conducting the consolidation test on the frozen sample. This indicated an overconsolidation effect of 60 kPa, for an overconsolidation ratio of 3 for the kaolin samples tested from the frozen fringe.

3. Water availability was found to be an important factor in development of heave in terms of moisture content at the point of freezing. Initial high moisture content in the soil undergoing freezing led to greater heave and acted to: reduce the depth of freezing; increase the immediately accessible supply of pore water available for freezing; and allow suction pressures to be sustained in the zone preceding the freezing front. The position of the phreatic surface did not appear to affect the development and magnitude of heave, unlike the case of silt.

4. Although water appears not to migrate far in freezing clay, local permeability (both before freezing, and changing during freezing) appears to have an important effect on development of heave, and its effect is strongly linked to the rate of cooling. Characterization of a test program using freezing degree days alone is confirmed to be wholly inadequate.

Step freezing leads to rapid plugging of pores with ice and development of heave quickly trails off. Ramp cooling leads to more heave. However, there appears to be some optimum balance between rate of cooling and permeability of the soil that could not be pinpointed in these tests. Although this does affect the permissible range of model scales that can be successfully tested to simulate a given full scale cooling regime, it also has relevance to cooling effects in full scale conditions. The fact that silt can exhibit a great deal of heave is a result of the balance between cooling rate, and both permeability and capillary rise. It is not surprising, then, that these are linked in clays also. This linkage deserves further investigation by other researchers interested in heave in clay. In the

context of centrifuge model research of frost heave, this finding indicates that freezing rate should be selected with care for correct centrifuge model tests.

6. Attention to repeatability between models was checked during the experimental program. The results indicate a largest coefficient of variation of less than 7%, which easily meets experimental standards.

7. The analytical model that was developed from this research explained, rather than predicted, frost heave at this point. A simple model that predicts heave will be the subject of other research. Depth of freezing and thickness of the frozen fringe are key elements of the analytical model. These were measured, rather than predicted, at this stage. The model assumed, based on the experimental results, that water migration was modest, and that the system behaves almost as a closed system.

The analytical model was satisfactory in characterizing magnitudes of heave, both ultimate heave and during development of heave, when the model included the assumption that heave can and does occur even when soil is not saturated, and the soil may, in fact, transition from a prefreezing saturated condition to an unsaturated frozen condition. This idea of heave in the absence of full saturation has been asserted by other researchers. This loss of prefreezing saturation is expected to be influenced by the freezing mode, the permeability of the soil, and the initial water content, and possibly by other factors.

This analytical model shows promise but requires further development for use as a predictive model. Further development should continue to place emphasis on ease of use and ease of measuring input parameters, if the model is to be used in engineering practice.

7.2 RECOMMENDATIONS FOR FURTHER RESEARCH

1. The overall difference of freezing behavior between clay and silt or cohesionless soil was investigated from the series of tests in this research. The next step is to expand this series of tests to investigate further the freezing mechanism peculiar to clay by changing the boundary temperatures, the soil's permeability, the initial water contents, and introducing cycles of freezing and thawing, among other variations.

2. Even though freezing induced consolidation is an important occurrence in clay, its settlement could not be measured due to lack of appropriate, sophisticated instrumentation that can record water pressure during freezing, yet does not interfere with freezing and water flow.

3. In a practical sense, the condition of soil after thawing is more important than that after freezing. Investigation of thawing processes in clays should be conducted utilizing a proper drainage system that allows the melted water to drain in a way similar to that that exists in the field. In addition, the attempt to monitor changes in soil strength due to freezing by means of the cone penetration test in flight was not successful. Measuring changes in soil properties will remain a problem in small models, in which soil samples will necessarily be small.

5. The samples made in this research were fully saturated at the time of freezing in order to make repeatable samples, however, the degree of saturation of soils in field conditions is normally less than 1, which will affect the freezing behavior significantly in terms of freezing response. Testing samples with partially saturated condition is necessary to understand the freezing mechanism of clays

170

better in their natural field condition. Understanding and characterizing heave of unsaturated soil will also improve the analytical model developed in this research.

6. Data from field freezing tests of clay are seldom reported because clay has historically received less attention from researchers, and from field engineers. Any physical or analytical model should be checked from time to time against field conditions to confirm their correctness. Construction work involving ground freezing for temporary ground stabilization, is one possible source for data

REFERENCES

Akagawa, S. (1990). Evaluation of the X-ray radiography efficiency for heaving and consolidation observation. In Proceedings of the 5th International Symposium on Ground Freezing, July 26-28. Balkema, Rotterdam, pp. 23-28.

Andersland, O.B., Ladanyi, B. (1994). "An Introduction to Frozen Ground Engineering" Chapman & Hall, N.Y., 352pp.

Arakawa, K. (1966). Theoretical studies of ice segregation in soil. Journal of Claciology, Vol. 6, No.44, pp.225-260.

Arulanandan, K., Thompson, P.Y., Kutter, B.L., Meegods, N.J., Muraleetharan, K.K. and Yogachandran, C. (1988) Centrifuge modeling of transport processes for pollutants in soil. J.Geotech. Eng., ASCE, 114(2), pp.185-205.

Banin, A. Anderson, D.M.(1974). Effects of salt concentration changes during freezing on the unfrozen water content of porous materials. Water Resour Res, 10, 1, pp124-126.

Benson, C.H., Othman, M.A. (1993). Hydraulic conductivity of compacted clay frozen and thawed in-situ. Journal of Geotechnical Engineering, ASCE, 119(2), pp.276-294.

Burt, T.P, and William S, P.J. (1976). Hydraulic conductivity in frozen soils. Earth surface Processes, Vol.1, 3, pp349-360.

Chamberlain, E.J. (1981). Overconsolidation effect of ground freezing. Eng. Geol. V. 18, pp.97-110.

Chamberlain, E.J., and Gow, A.J. (1979). Effect of freezing and thawing on the permeability and structure of soils. Engineering Geology, Vol.13, pp.73-92.

Chen, X.B., Wang, Y.Q. (1988). Frost heave prediction for clayey soils. Cold region Science and Technology, 15(3), s. pp.233-238.

Duquennoi, C., Fremond, M., Levy, M. (1989). Modelling of thermal soil behavior. VTT Symposium 95. s. pp. 895-915.

Eigenbrod, K.D. (1996). Effect of cyclic freezing and thawing on volume changes and permeabilities of soft fine-grained soils. Can Geotechnical Journal, Vol. 33, pp.529-537.

Everett, D.H. (1961). "Thermodynamics of damage to porous solids". Transportation Faraday Society, Vol.57, pp.1541-51.

Foriero, A, and Ravonison, N. (1998). "Frost Heave: FEM Modeling with the abaqus software report. Report by University LAVAL for the U.S. Army Cold Regions Research and Engineering Laboratory.

Fremond, M. and Mikkola, M., (1991). Thermodynamical modeling of freezing soil. International Symposium on Ground Freezing 91, pp. 17-24.

Fukuda, M. (1982). Experimental studies of coupled heat and moisture transfer in soils during freezing. Contribution no. 2528 from the Institute of Low temperature Science, Hokkaido University, Sapporo, Japan, pp. 35-91.

Gilpin, R.R. (1980). A model for the prediction of ice lensing and frost heave in soils, Water Resour. Res. 16, pp. 918-930.

Gold, L. (1957). " A possible force mechanism associated with the freezing of water in porous material". Highway Research Board Bulletin, Vol. 168, pp. 65-71.

Graham, J., and Au, V.C.S. (1985). Effects of freeze-thaw and softening on a natural clay at low stresses. Canadian Geotechnical Journal, Vol. 22, pp.69-78.

Guymon, G.L., Berg, R.L. and Hromadka, T.V. (1993). Mathematical model of frost heave and thaw settlement in pavements. U.S. Army CRREL Report 93-2.

Hamilton, A.B. (1966). Freezing Shrinkage in Compacted Clays. Can Geotechnical Journal, Vol. 3, No.1, pp.1-77.

Harlan, R.L. (1973). Analysis of coupled heat-fluid transport in partially frozen soil. Water Resources. Res. 9, pp.1314-1322.

Harris, J.S. (1995). "Ground Freezing in Practice" Thomas Telford, London, 264pp.

Hopke, S.W. (1980). A model for frost heave including overburde, Cold Reg. Scie. Tech Vol. 14, pp.13-22.

Jansson, P-E., Haldin, S. (1979). Model for the annual water and energy flow in a layered soil. Society for Ecological Modeling Copenhage, pp.145-163.

Jessberg, H.L. (1989). Opening address. Ground Freezing '88, Vol.2, pp. 407-411. Balkema, Rotterdam.

Jones R.H & Baba H.U (1997), Suction characteristics and frost heave of cohesive soils. pp. 235 - 240. Ground Freezing 97, 1997 Balkema, Rotterdam.

Konrad J.-M, (1980). A mechanistic theory of ice lens formation in fine-grained soils. Can. Geotech. J., 17, pp. 473-486.

Konrad J.-M, (1988). Influence of freezing mode on frost heave characteristics Cold Regions Science and Technology 15 pp.161-175.

Konrad, J.-M. (1994). "Frost heave in soils: concepts and engineering'". 16th Canadian Geotechnical Colloquium, Canadian Geotechnical Journal, Vol. 31, No.2, pp.223-45.
Konrad, J.-M., and Morgenstern, N.R. (1980). Effects of applied pressure on freezing soil. Can. Geotech. J., 19(4), 494-505.

Konrad, J.-M., and Morgenstern, N.R. (1981). The Segregation Potential of a freezing soil. Can. Geotech. J., 18, pp. 482-491.

Konrad, J.-M, J.T.C Seto (1994). Frost heave characteristics of undisturbed sensitive Champlain Sea Clay. Can. Geotech. J., 31, pp.285-298.

Knutsson, A. (1973). Frost action on roads OECD Symposium, Paris.

Knutson, S., Domaschuk, L., Chandler, N. (1985). Analysis of large-scale laboratory and in situ frost heave tests. In Proceedings, 4th international Symposium on Ground Freezing, 5-7 August, Sapporo, Japan.

Kujala K (1997), Estimation of frost heave and thaw weakening by statistical analyses and physical models. Ground Freezing 97, 1997 Balkema, Rotterdam.

Loch, J.P., and Kay, B.D. (1978) Water redistribution in partially frozen, saturated silt under several temperature gradients and overburden loads. Soil Science Society of America, Journal, Vol. 42, No. 3, pp. 400-406.

Lock, J.P., Miller, R.D. (1975). Tests of the concept of secondary frost heaving. Soil Science Society of America Journal. Vol.39 (6), pp.1036-1041.

Lovell, M.S. and Schofield, A.N. (1986) Centrifuge modeling of sea ice. Proc., 1st International Conference on Ice Technology, pp.105-113.

Miller, R.D. (1972). "Freezing and heaving of saturated and unsaturated soils". Highway Research Record, Vol. 393. pp 1-11.

Miller, R.D. (1977). Lens initiation in secondary heaving. Proceedings, International Symposium on Frost Action in Soils, University of Lulea, Sweden, Vol.1, pp.68-74.

Nixon, J.F. (1982). Field frost heave predictions using the segregation potential concept, Can. Geotech. J. Vol. 19, pp. 526-529.

Ohrai, T., Yamamoto, H. (1985). Growth and migratin of ice lenses in partially frozen soil. Proceedings of the Fourth International Symposium on Ground Freezing, Sapporo, Japan, vol.1. pp.79-84. Rotterdam:Balkerma.

O'Neill, K., Miller, R.D. (1982). Numerical solutions for a rigid-ice model of secondary frost heave, U.S. Army cold Reg. Res. Engg. Lab. Rep. 82-13, Hanover, NH, 11pp.

O'Neill, K., Miller, R.D. (1985). Exploration of a rigid-ice model of frost heave, Water Resource. Res. 21, pp.281-296.

Palmer, A.C., Schofield, A.N., Vinson, T.S., and Wadhams, P. (1985) Centrifuge modeling of underwater permafrost and sea ice. Pro. 4th International Offshore Mechanics and Arctic Engineering Symposium, Vol.2, pp.65-69.

Penner, E. (1957). "Soil moisture tension and ice segreation". Highway Research Bulletin, Vol. 168, pp. 50-64.

Penner, E. (1967). Heaving pressure in soils during unidirectional freezing. Canadian Geotechnical Journal. Vol.4, pp.398-408.

Penner, E. (1969). Frost Heaving Forces in Leda Clay. Can Geotechnical Journal, Vol. 7, pp.8-16.

Penner, E., Goodrich, L.E. (1980). Location of segregated ice in frost susceptible soil. Proc. 2nd International Symposium on Ground Freezing, Trondheim, 1, pp.626-639.

Phukan-Morgenstern-Shannon (1979) Development of a frost heave soil classification system. Revised interim report. Prepared for Eluor Northwest, Inc,. Fairbanks, Alaska, pp. 81.

Ravaska. O & Kujala K (1997), Freeze-thaw effect on soil-bentonite mixture. pp. 147 - 152.Ground Freezing 97, 1997 Balkema, Rotterdam.

Saarelainen, S., (1992) Modelling frost heaving and frost penetration in soils at some observation sites in Finland. VTT Publications 95. Espoo. 120p. + app. 1p.

Savvidou, C. (1988) Centrifuge modeling of heat transfer in soil. Proc. Int. conf. Geotechnical Centrifuge Modeling, Paris, pp. 583-591. Balkem, Rotterdam.

Shen, M., Ladanyi, B. (1987). Modeling of coupled heat, moisture and stress field in freezing soil. Cold Region Science and Technology, Vol.14, pp.237-246.

Sheng, D. (1994). Thermodynamics of freezing soils. Theory and application. Doctoral Thesis. Lulea university of Technology.

Sheppard, M., Kay, B., Loch, J. (1978). Development and testing of a computer model for heat and mass flow in freezing soils. Proc. Vol. 1, 3rd International Conference on Permafrost, Edmonton, Alberta, Canada, pp.76-81.

Shoop, A.S., Bigl, R.S. (1997). Moisture migration during freeze and thaw of unsaturated soils: modeling and large scale experiments. Cold Region Science and Technology, Vol.25, pp.33-45.

Smith, C.C. (1992) Thaw Induced Settlement of Pipelines in Centrifuge Model Test. Ph.D. Thesis, University of Cambrige.

Straub, N.A. (1999). Centrifuge modeling of Boulder Jacking by Frost Heave. M.S thesis, University of Maryland.

Taber, S. (1929). Frost heaving. Journal of Geology, Vol. 37, pp.428-461.

Tasaki, T., Yamamoto, H., Ohrai, T., Masuda, M (1978). Effect of penetration rate of freezing and confining stress on the frost heave ratio of soil. 3rd Int. Permafrost Conf., pp. 737-742.

Tsytovich, N.A. (1975). The mechanics of frozen ground. McGraw Hill, New York.

Yang, D. (1996). Investigation of the scaling law for centrifuge modeling of frost heave. Ph.D. Thesis, University of Maryland.

Yang, D., Goodings,D.J.(1998). Climatic soil Freezing modeled in Centrifuge. Journal of Geotechnical and Geoenvironmental Engineering. Vol.124. No.12. pp.1186-1194.

Yong, R.N., Boonsinsuk, P., Tucker, A.E. (1984). A Study of Frost-Heave Mechanics of High-Clay Content Soils. Pro. 3rd International Offshore Mechanics and Arctic Engineering Symposium, Vol.106, pp.502-508.

Washburn, A.L. (1980). "Geocrylogy". John Wiley & sons, N.Y., 406pp.

Wong, L.C., Haug, M.D. (1991). Cyclical closed-system freeze-thaw permeability testing of soil liner and cover materials. Canadian Geotechnical Journal, Vol. 28, pp.784-793.

Zhang, S., Zhu, Q. (1983). A study of the calculation of frost heaving. Proc. Fourth International Conference on Permafrost. Fairbanks, Alaska, pp.1479-1483.